Investigating the localization and function of the *C. elegans* HAM-1 protein

by

Khang L.D. Hua

B.Sc., University of Ottawa, 2010

Thesis Submitted in Partial Fulfillment of the
Requirements for the Degree of
Master of Science

in the
Department of Molecular Biology and Biochemistry
Faculty of Science

SIMON FRASER UNIVERSITY

Fall 2014

Approval

Name: **Khang L.D. Hua**

Degree: **Master of Science**

Title: ***Investigating the localization and function of the C. elegans HAM-1 protein***

Examining Committee: **Chair: Dr. Esther Verheyen**
Professor

Dr. Nancy Hawkins
Senior Supervisor
Associate Professor _____

Dr. Nicholas Harden
Supervisor
Professor _____

Dr. Harald Hutter
Supervisor
Professor _____

Dr. Michel Leroux
Internal Examiner
Professor
Molecular Biology and Biochemistry _____

Date Defended/Approved: December 2nd, 2014 _____

Partial Copyright Licence

Abstract

In *C. elegans*, HAM-1 is an asymmetrically localized protein that regulates several asymmetric neuroblast divisions. Although the protein contains a putative DNA binding domain, nuclear localization of HAM-1 has never been observed through immunostaining of embryos with anti-HAM-1 antibodies. However, a GFP::HAM-1 fusion protein has been detected in the nucleus of transgenic animals under direct fluorescence microscopy. Through a biochemical subcellular fractionation of embryonic extracts, I determined that endogenous HAM-1 is primarily a nuclear protein. I have also examined HAM-1 localization in different *ham-1* mutant embryos. This analysis has revealed several key residues in the N-terminus and a region in the C-terminus that are required for proper cortical localization of HAM-1. Finally, I have shown that Tyrosine residue 369 is crucial for HAM-1 function. Thus, my work has lent insight into HAM-1 sequences that contribute to function and localization of the protein.

Keywords: *C. elegans*; asymmetric cell division; HAM-1

Dedication

To my family

Acknowledgement

I would first and foremost like to thank my supervisor, Dr. Nancy Hawkins, for giving me the opportunity to be a part of a wonderful lab. I greatly appreciated the guidance and support she provided to help me improve my lab techniques and writing skills. I have learned a tremendous amount from her and I truly admire her passion for research.

I would like to thank my committee members, Dr. Harald Hutter and Dr. Nicholas Harden for all their helpful suggestions and advice.

Thank you to Dr. Christopher Beh for all of your great suggestions for improving my presentations as well as the troubleshooting for my experiments.

Sincere thanks to my fellow labmates and in the Hawkins lab and the Beh lab for all their support and encouragement: Kyla Hingwing, Hamida Safi, Jesper Johansen, Evan Quon and Vidhya Ramanathan. Thank you to Kyla Hingwing for all of her help with genetics and worm work when I first started. Thank you to Evan and Jesper for all of their advice and suggestions when it came to troubleshooting. Thank you to all of the Molecular Biology and Biochemistry Department staff and professors.

I would like to thank Tyler Daniels for generating the phosphonull *gfp::ham-1(Y369F)* construct and Ziwei Ding for generating the phosphomimetic *gfp::ham-1(Y369E)* construct used for this study.

Special thank you go out to my wonderful girlfriend Shannan May-McNally for supporting me and keeping me positive through tough times. I greatly appreciate all of your advice for troubleshooting experiments and presentations. You have been a large part of my thesis in many ways through all of the editing and suggestions on improving my writing. I truly admire your passion for research and fish.

Support for this study was provided by Natural Sciences and Engineering Research Council of Canada grants awarded to Dr. Nancy Hawkins and the Department of Molecular Biology and Biochemistry Graduate Fellowship.

Table of Contents

Approval ii
Partial Copyright Licence iii
Abstract iv
Dedication v
Acknowledgement vi
Table of Contents vii
List of Tables ix
List of Figures x

Chapter 1. Introduction 1
1.1 Mechanisms of asymmetric cell division 1
1.2 Asymmetric division in the *Drosophila melanogaster* nervous system 3
1.2.1 Neuroblast divisions in the CNS 4
1.2.2. SOP divisions in the PNS 6
1.3 Asymmetric cell division in *Caenorhabditis elegans* 8
1.3.1 Role of Wnt Signalling in *C. elegans* EMS division 9
1.3.2 Intrinsic mechanisms regulate asymmetric division of the zygote 12
1.4 HAM-1 is a key regulator of asymmetric neuroblast divisions in *C. elegans* 14
1.5 HAM-1 sequence homology 23
1.6 Regions of HAM-1 required for function and localization 24
1.7 Models of HAM-1 function 27
1.8 Research objectives 28

Chapter 2. Material and Methods 30
2.1 Strains 30
2.2 Generation of transgenic animals 30
2.3 Genetic crosses 31
2.4 Worm lysis for PCR reaction 32
2.5 Subcloning of *src-1* into L4440 RNAi vector 32
2.6 RNAi knockdown of *src-1* by feeding 34
2.7 RNAi knockdown of *src-1* by microinjection 35
2.8 Embryo isolation by hypochlorite treatment 36
2.9 Preparation of embryonic protein extracts 36
2.10 Immunohistological Methods 37
2.11 Microscopy 38
2.12 Nuclear-cytoplasmic fractionation and Western blotting 38
2.12 Large SDS-PAGE and Western blotting 40
2.13 Bioinformatics analyses 40
2.14 Quantification of GFP::HAM-1, GFP::HAM-1(Y369F) and GFP::HAM-1(Y369E). 41

Chapter 3. Results 42
3.1 Function and localization analysis of the phospho-null GFP::HAM-1(Y369F) 42
3.2 Function and localization analysis of the phospho-mimetic GFP::HAM-1(Y369E) 48
3.3 RNAi knockdown of *src-1* tyrosine kinase did not result in loss of PLM neurons 50
3.4 A *ptp-2* mutant does not cause a loss of PLM neurons 53
3.5 Endogenous HAM-1 is primarily localized to the nucleus 55
3.6 Further identifying residues required for membrane localization 58
3.7 Identifying residues required for the closely migrating doublet observed on Western blot 63

Chapter 4. Discussion 67
4.1 A potential nuclear role for HAM-1 67
4.2 The N-terminus and the C-terminus of HAM-1 are required for membrane localization 70
4.3 Residues within the N-terminus of HAM-1 contribute to the closely migrating doublet observed on a Western blot 73
4.4 Tyrosine residue 369 is crucial for the function and localization of HAM-1 75
4.5 SRC-1 kinase knockdown by RNAi does not affect PLM/ALN production 77
4.6 PTP-2 tyrosine phosphatase is not required for PLM/ALN neuroblast asymmetric division 79
4.7 Future Directions 79

Chapter 5. Conclusion 82

References 83

Appendix. 92

List of Tables

Table 3.1 Knock down of *src-1* using RNAi by feeding. 52
Table 3.2 *src-1* RNAi by microinjection. 54
Table 3.3 PLM neuron in *ptp-2(op194)* mutants. 56

List of Figures

Figure 1.1 Intrinsic and extrinsic mechanisms of asymmetric cell division. 2

Figure 1.2 Asymmetric division of the *Drosophila* CNS neuroblast. 5

Figure 1.3 Asymmetric division of a sensory organ precursor (SOP) in the *Drosophila* peripheral nervous system. 7

Figure 1.4 Wnt signalling regulates asymmetric division of the EMS blastomere. 11

Figure 1.5 Asymmetric division of the *C. elegans* one cell zygote. 13

Figure 1.6 Amino acid sequence and schematic of domains within HAM-1. 16

Figure 1.7 Immunostaining of HAM-1 in wild-type embryos. 17

Figure 1.8 Divisions of the HSN/PHB neuroblast. 18

Figure 1.9 Divisions of PLM/ALN neuroblast during embryonic development. 20

Figure 1.10 Divisions of the Q neuroblast during L1 larval development. 22

Figure 1.11 GFP::HAM-1 localization. 26

Figure 3.1 Visualization of PLM neurons using the *zdIs5(mec-4::GFP)* reporter. 44

Figure 3.2 GFP::HAM-1(Y369F) is unable to rescue *ham-1(gm279)* PLM defects. 45

Figure 3.3 Localization of GFP::HAM-1, GFP::HAM-1(Y369F) and GFP::HAM-1(Y369E) 47

Figure 3.4 GFP::HAM-1(Y369E) is unable to rescue *ham-1(gm279)* PLM defects. 49

Figure 3.5 Western blot analysis of HAM-1 subcellular distribution. 59

Figure 3.6 Schematic of various *ham-1* mutant alleles. 61

Figure 3.7 Localization of HAM-1 in wild type and *ham-1* mutant embryos 62

Chapter 1.

Introduction

1.1 Mechanisms of asymmetric cell division

Development from a zygote into a multicellular organism requires the generation of multiple cell types. Asymmetric cell division is an essential process for generating the required cellular diversity during development (Horvitz and Herskowitz, 1992). This process is defined as a division in which a mother cell divides to give rise to two daughter cells each with a distinct cell fate (reviewed in Hawkins and Garriga, 1998; Knoblich, 2008). Asymmetric division also has a crucial role in the maintenance of stem cell fates by allowing stem cells to self-renew and generate daughter cells that are committed to lineage-specific differentiation (reviewed in Knoblich, 2008; Neumüller and Knoblich, 2009). Defects in asymmetric cell division may result in developmental abnormalities as well as cancer (reviewed in Knoblich, 2010; Neumüller and Knoblich, 2009). A defining feature of any stem cell is its ability to generate both self-renewing and differentiating daughters which can be accomplished through asymmetric cell division. Defects in asymmetric cell division can result in the production of only self-renewing daughters which will lead to tumorigenesis (reviewed in Knoblich, 2010). Further studies looking into mechanisms regulating asymmetric cell division can therefore improve our understanding of development, cancer biology and stem cell biology.

There are both intrinsic and extrinsic mechanisms which contribute to asymmetric cell division. Intrinsic mechanisms involve an asymmetric distribution of cell fate determinants within the dividing mother cell (Figure 1.1).

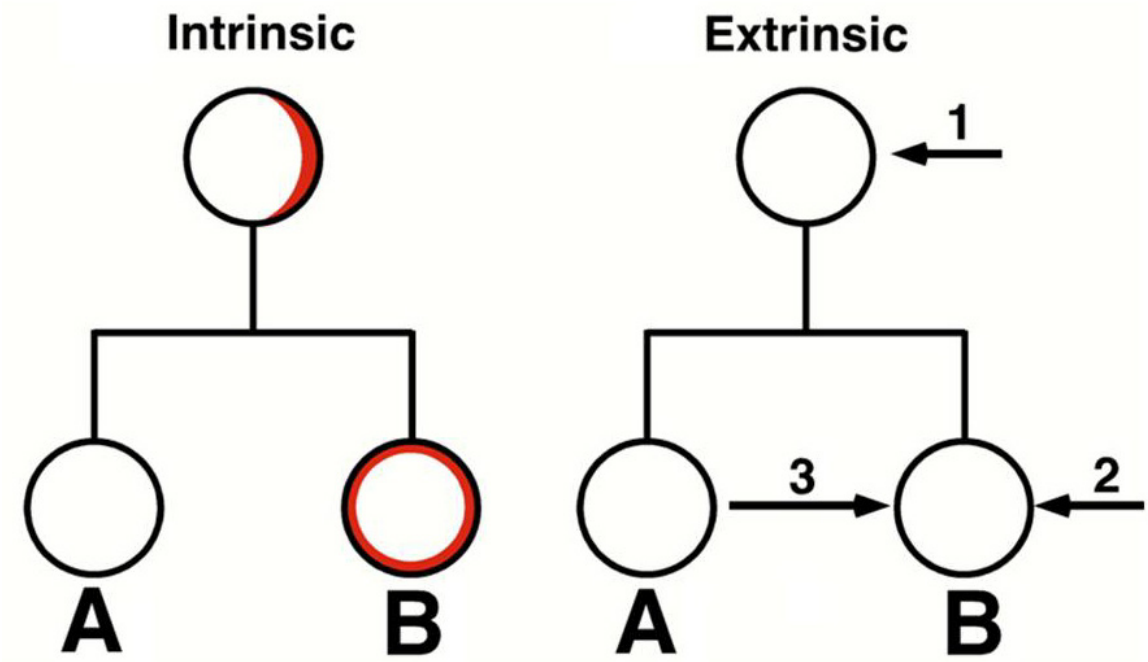

Figure 1.1 Intrinsic and extrinsic mechanisms of asymmetric cell division.

Intrinsic mechanisms require the asymmetric distribution of intrinsic factors within the dividing mother cell as shown in red. Following division, only one daughter cell (B) inherits these intrinsic factors resulting in two daughter cells with different fates. Extrinsic mechanisms involve cell signalling between surrounding cells and the mother cell (1), the surrounding cells and one of the daughter cells (2) or between the two daughter cells (3) (Hawkins and Garriga, 1998).

During mitosis, the position of the mitotic spindle is also asymmetrically biased which allows for unequal segregation of cell fate determinants into only one of the two daughter cells (reviewed in Hawkins and Garriga, 1998; reviewed in Knoblich, 2008).

Since cells within developing multicellular organisms do not divide in isolation, asymmetric cell division can also be influenced by cell signalling. The mother cell can receive extrinsic signals from surrounding cells instructing it to divide asymmetrically and give rise to daughter cells with distinct cell fates. The daughter cells may also receive signals from surrounding cells to induce differential cell fates (Figure 1.1). Intrinsic and extrinsic mechanisms, however, are not acting independently of each other and a combination of both mechanisms can contribute to the regulation of asymmetric cell division (reviewed in Hawkins and Garriga, 1998; Knoblich, 2008).

1.2 Asymmetric division in the *Drosophila melanogaster* nervous system

Detailed studies regarding the mechanisms underlying asymmetric cell division have been primarily undertaken in the common fruit fly (*Drosophila melanogaster*) through analyses of sensory organ precursors (SOPs) in the peripheral nervous system (PNS) and neuroblasts in the central nervous system (CNS). The SOPs of the PNS and neuroblasts of the CNS provide great examples of intrinsic mechanisms regulating asymmetric cell division. During development, asymmetric division of these cells is required to generate neuronal diversity in the *Drosophila* nervous system (reviewed in Hawkins and Garriga, 1998; Knoblich, 2008).

1.2.1 Neuroblast divisions in the CNS

Neurons in the *Drosophila* CNS arise from neuroblasts that undergo stem cell-like divisions. During each division the neuroblast divides asymmetrically along the apical-basal axis to produce a larger apical daughter cell and a smaller basal daughter cell. The larger daughter will maintain a stem cell fate while the smaller daughter, called the ganglion mother cell (GMC) will divide to generate two differentiating neurons (Figure 1.2) (reviewed in Knoblich, 2008). For asymmetric division to occur, an apical-basal polarity must be established within the neuroblast. The establishment of this apical-basal polarity requires an asymmetric distribution of an evolutionarily conserved PAR-3/6 complex which consists of Bazooka (PAR-3), DmPAR-6 (PAR-6), and aPKC (PKC-3) to the apical cortex of the neuroblast (Rolls et al., 2003; Wodarz et al., 2000). An adaptor protein Inscuteable (Insc) is also localized to the apical cortex and associates with the PAR-3/6 complex via direct interaction with Bazooka. Inscuteable (Insc) in turn recruits a complex consisting of a heterotrimeric G-protein α subunit (Gαi), Partner of Inscuteable (Pins) and a NuMA-related Dynein-binding protein (Mud) by binding to Partner of Inscuteable (Pins) (Figure 1.2). These complexes function to displace the mitotic spindle towards the basal end, resulting in the generation of a larger apical daughter cell and a smaller basal daughter cell (Figure 1.2) (reviewed in Betschinger and Knoblich, 2004; Goldstein and Macara, 2010).

Following the establishment of cell polarity, cell fate determinants are asymmetrically distributed and inherited by daughter cells. An important asymmetrically distributed cell-fate determinant is the homeodomain transcription factor Prospero (Doe et al., 1991). Prospero is localized to the basal cortex of the neuroblast during mitosis and is inherited by the GMC. Miranda is an important tethering protein responsible for the basal localization of Prospero through direct physical interaction with Prospero. Miranda also localizes Staufen, an RNA binding protein, to the basal cortex of the cell prior to division (Matsuzaki et al., 1998; Shen et al., 1998).

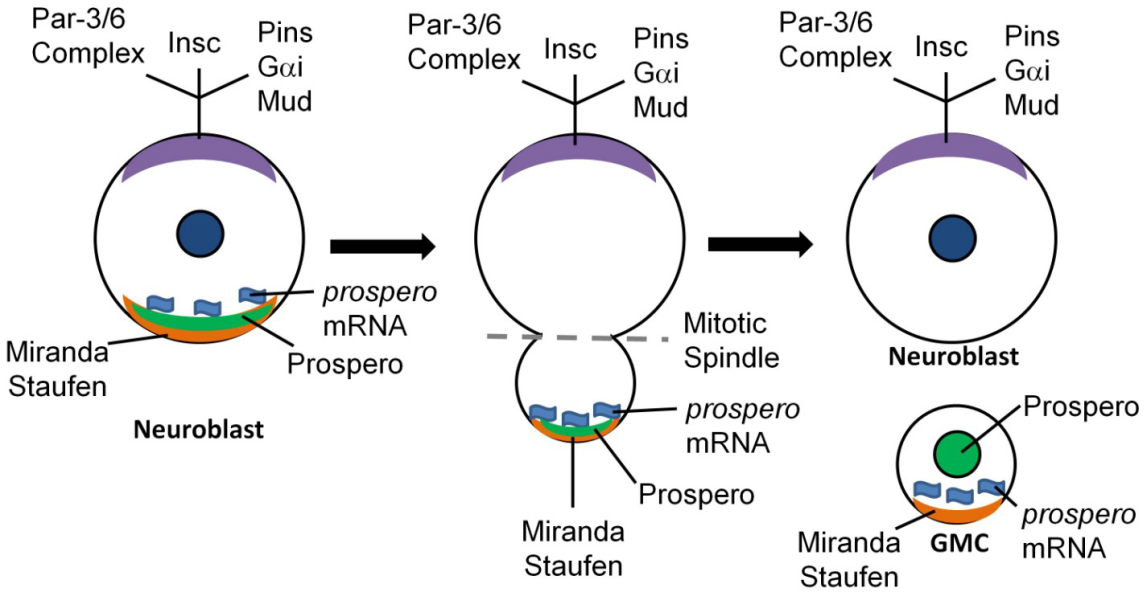

Figure 1.2 Asymmetric division of the *Drosophila* CNS neuroblast.

The neuroblast divides asymmetrically along its apical-basal axis to generate a larger apical neuroblast and a smaller basal ganglion mother cell (GMC). Bazooka (PAR-3), DmPAR-6 (PAR-6), and aPKC (PKC-3) form a Par-3/6 complex which localizes to the apical cortex of the neuroblast. The Par-3/6 complex recruits the adaptor protein Inscuteable (Insc) which in turn recruits a complex consisting of a heterotrimeric G-protein α subunit (Gαi), Partner of Inscuteable (Pins) and a NuMA-related Dynein-binding protein (Mud). These complexes are responsible for displacing the mitotic spindle. The tethering protein Miranda recruits Prospero and Staufen carrying *prospero* mRNA to the basal cortex of the neuroblast. Following division, Prospero translocates to the nucleus to specify GMC fate (reviewed in Knoblich, 2008).

Staufen specifically binds to *prospero* mRNA to localize and segregate it asymmetrically to the basal daughter cell. Following division, these factors are inherited exclusively by the GMC (Hirata et al., 1995; Li et al., 1997). Once Prospero is within the GMC, it dissociates from Miranda and translocates into the nucleus (Figure 1.2). Prospero could then specify the GMC fate by activating GMC specific genes while repressing neuroblast specific genes (reviewed in Knoblich, 2008).

1.2.2. SOP divisions in the PNS

In the *Drosophila* PNS, the external sensory organs arise from SOP cells which divide asymmetrically. The SOP divides to produce a pIIa cell and a pIIb cell. The pIIa cell divides asymmetrically to produce a socket cell and a hair cell. The pIIb cell divides asymmetrically to produce a glial cell that undergoes apoptosis and a pIIIb cell which divides asymmetrically again to produce a sheath cell and a neuron cell (Figure 1.3). In the SOP, Bazooka (PAR-3), DmPAR-6 (PAR-6), and aPKC (PKC-3) are localized posteriorly which sets up the polarity of the cell to direct asymmetric distribution of cell fate determinants (reviewed in Neumüller and Knoblich, 2009).

One key cell fate determinant is the membrane-associated protein Numb. In *numb* mutants, the SOP divides symmetrically to produce two pIIa cells which results in the production of four outer support cells and no neurons or sheath (Rhyu et al., 1994). The membrane association of Numb is regulated by aPKC phosphorylation. When Numb is phosphorylated, its affinity for the plasma membrane is decreased. A non-phosphorylatable form of Numb is cortical; however it is not asymmetrically localized. Thus, the posterior localization of aPKC is responsible for concentrating Numb at the anterior cell cortex (Figure 1.3) (Smith et al., 2007). Numb is then inherited only by the pIIb daughter where it can specify the cell fate through inhibition of the Notch/Delta pathway. Loss of Notch function results in the opposite phenotype of *numb* mutants.

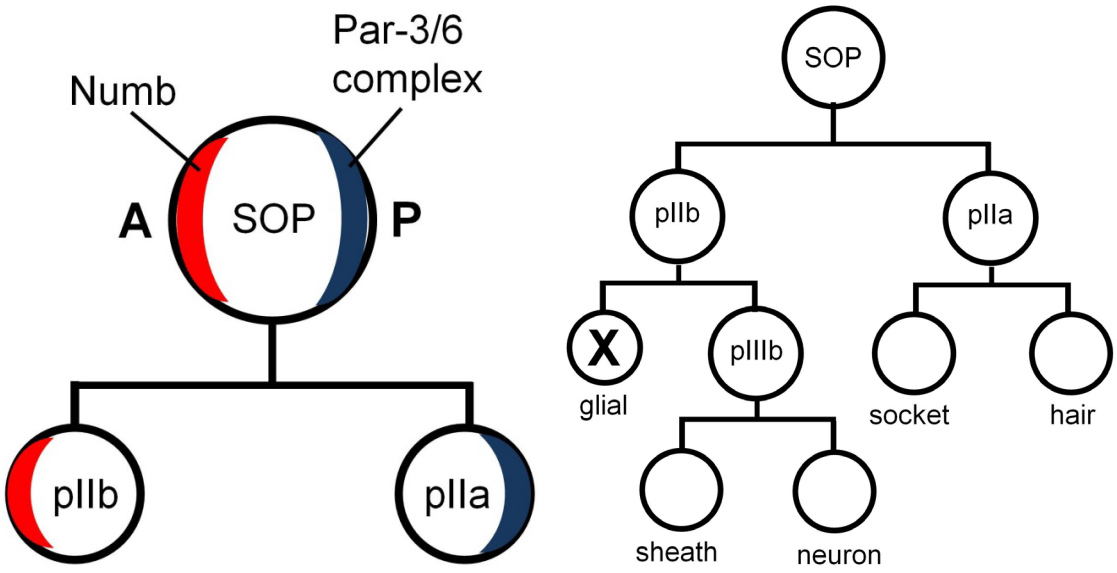

Figure 1.3 Asymmetric division of a sensory organ precursor (SOP) in the *Drosophila* peripheral nervous system.

The left panel illustrates the localization of the Par-3/6 complex to the posterior (P) cortex of the cell. The Par-3/6 complex inhibits Numb from associating with the membrane at the posterior end of the cell. This results in Numb concentrating at the anterior (A) cortex of the cell. Only the pIIb daughter will inherit Numb which will specify the pIIb fate. The right panel shows the divisions in the SOP lineage tree. The SOP generates the socket, hair, sheath and neuron cells of the sense organs (reviewed in Neumüller and Knoblich, 2009).

The SOP divides symmetrically to produce two pIIb daughters rather than two pIIa daughters (Guo et al., 1996; Rhyu et al., 1994). Numb can regulate the Notch/Delta pathway at the early endocytic step through interaction with the endocytic adaptor protein α-adaptin and the Notch receptor (Berdnik et al., 2002; McGill et al., 2009; Santolini et al., 2000). Numb also interacts with Sanpodo which is a transmembrane protein required for Notch signalling. Thus, Numb could inhibit Notch signalling by translocating Sanpodo to endocytic vesicles where it cannot signal downstream effectors of Notch signalling (Hutterer and Knoblich, 2005; O'Connor-Giles and Skeath, 2003). This pathway exemplifies the importance of both intrinsic and extrinsic mechanisms for the proper regulation of asymmetric cell division.

1.3 Asymmetric cell division in *Caenorhabditis elegans*

Along with *Drosophila*, the nematode *Caenorhabditis elegans* (*C. elegans*) is an ideal model organism to elucidate the mechanisms regulating asymmetric cell division. *C. elegans* is simple to maintain in the lab, has a short life cycle, well-developed genetics and there are a wealth of molecular tools available. Perhaps the greatest strength of this system however, is its fully described cellular development from a single-cell embryo to mature adult. This makes *C. elegans* a powerful genetic model to investigate the role of asymmetric cell division during neurogenesis. From the complete lineage it is known that 807 of the 949 nongonadal divisions are derived from asymmetric divisions (Sulston and Horvitz, 1977). In addition, all 302 neurons are generated through asymmetric cell division (Sulston et al., 1983). Thus in *C. elegans*, asymmetric cell division can be studied at the resolution of single cells.

1.3.1 Role of Wnt Signalling in *C. elegans* EMS division

A great example of an extrinsic mechanism regulating asymmetric cell division at several stages of development is the Wnt signalling pathway. This pathway has been the paradigm for asymmetric cell division in *C. elegans*. The canonical Wnt pathway is dependent on the transcriptional co-activator β-catenin. In the absence of a Wnt signal, non-junctional β-catenin is degraded by a destruction complex composed of glycogen synthase kinase (GSK) 3β, the tumor suppressor adenomatous polyposis coli (APC), and the Axin scaffolding protein. In the presence of a Wnt signal, the Wnt ligand binds to the Frizzled receptor which recruits the scaffolding folding protein Dishevelled. This inhibits the destruction complex which allows for the stabilization and accumulation of cytoplasmic β-catenin resulting in the nuclear translocation of β-catenin. Inside the nucleus, β-catenin can interact with the LEF/TCF family of transcription factors to activate transcription of target genes (reviewed in MacDonald et al., 2009). In *C. elegans*, the canonical pathway functions mainly post-embryonically for regulating cell migration and cell fate specifications by utilizing the *C. elegans* β-catenin BAR-1 (reviewed in Sawa and Korswagen, 2013).

Asymmetric cell divisions in *C. elegans* utilize a Wnt/β-catenin asymmetry pathway which differs slightly from the canonical pathway and is responsible for the regulation of most asymmetric divisions from the four-cell stage embryo through to larval development. The Wnt/β-catenin asymmetry pathway utilizes components of the canonical pathway including the β-catenins WRM-1 and SYS-1 but this pathway is categorized as a divergent pathway because of its unique regulation which involves the asymmetric localization of signalling components. The regulation of the asymmetry pathway is dependent on the accumulation of β-catenin as well as the decrease in the nuclear TCF transcription factor, POP-1. In divisions controlled by the Wnt/β-catenin asymmetry pathway, nuclear POP-1 is lowered in the actively signalled daughter and remains high in the unsignalled daughter (reviewed in Phillips and Kimble, 2009; Sawa and Korswagen, 2013).

The decrease in nuclear TCF has been shown to be required for derepression of target genes since high levels of TCF represses target gene expression (Calvo et al., 2001).

The lowering of nuclear TCF was first observed in the EMS division during early embryogenesis. At the four-cell stage the EMS blastomere receives a MOM-2/Wnt signal from the neighbouring P2 cell instructing it to divide asymmetrically along its anterior-posterior axis (reviewed in Korswagen, 2002; Lin et al., 1998). EMS divides to produce an anterior daughter, the MS cell and a posterior daughter the E cell. The MS is the progenitor of the pharyngeal and body wall muscle cells while the E cell will form the intestine (Sulston and Horvitz, 1977; Sulston et al., 1983). The fate difference between MS and E is specified by POP-1. Nuclear POP-1 level remains high in the MS cell while nuclear POP-1 level is lowered in the E cell (Figure 1.4). POP-1 is a repressor of endoderm specific genes. Thus, the lower POP-1 level results in the induction of endoderm development (Calvo et al., 2001; Lin et al., 1995, 1998). Instead of converting POP-1/TCF into a transcriptional activator as in the canonical pathway, the asymmetry pathway, when activated by MOM-2/Wnt, blocks the repressive function of POP-1 by exporting it out of the nucleus (reviewed in Korswagen, 2002). This is done in conjunction with a MAPK pathway involving LIT-1/NLK and MOM-4/TAK-1. Upon activation by MOM-4/TAK-1, LIT-1/NLK and WRM-1/β-catenin form a stable complex and phosphorylates POP-1 to export it out of the nucleus (Rocheleau et al., 1999; Shin et al., 1999).

Similar to the canonical Wnt pathway, the Wnt/β-catenin asymmetry pathway also depends on the stabilization and accumulation of the β-catenin-like protein SYS-1 (Huang et al., 2007; Phillips et al., 2007). SYS-1 level is high in the posterior daughter cell and low in the anterior daughter cell. Within the posterior daughter cell, where POP-1 levels are low, SYS-1 acts as a transcriptional co-activator (Figure 1.4). Regulation of the Wnt/β-catenin asymmetry pathway is focused on the asymmetry and ratio of POP-1 and SYS-1 rather than their absolute protein levels (Kidd et al., 2005).

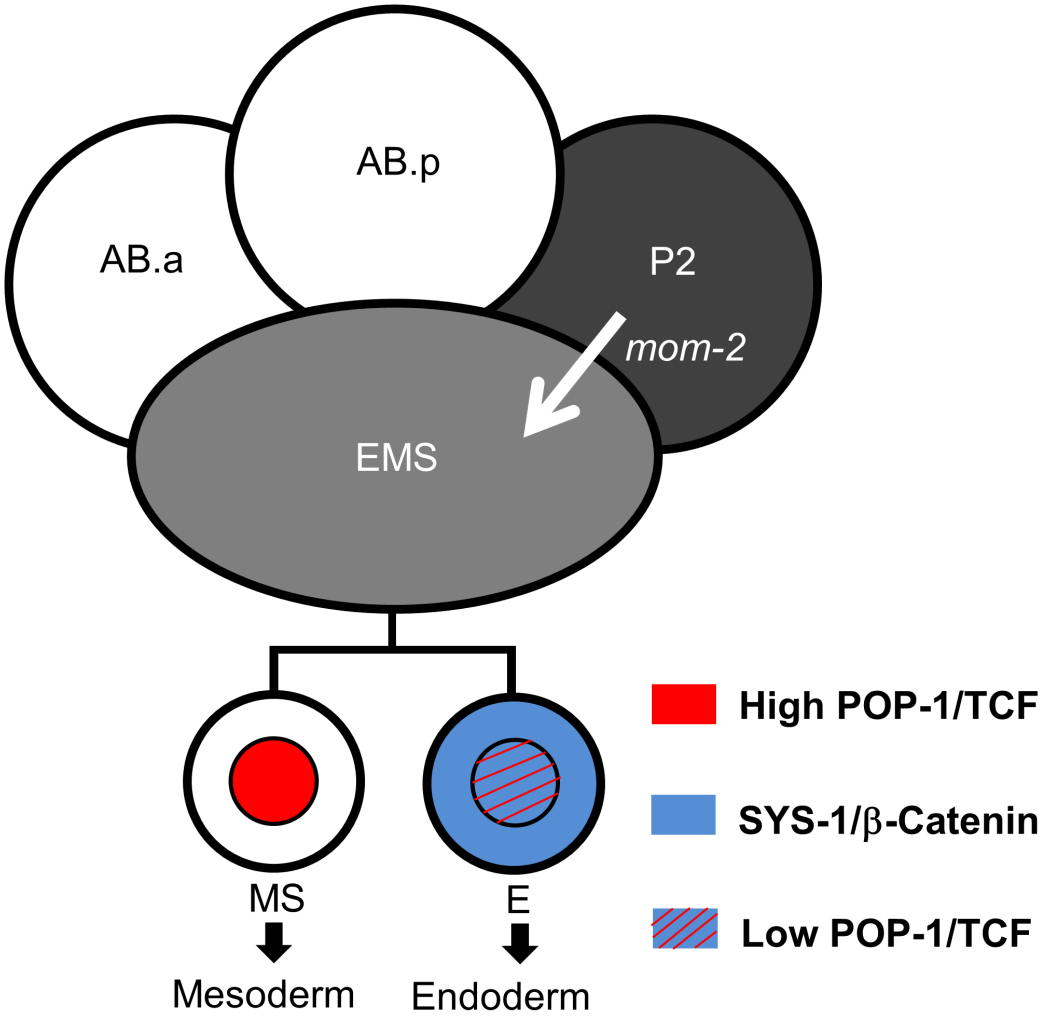

Figure 1.4 Wnt signalling regulates asymmetric division of the EMS blastomere.

The EMS blastomere receives a Wnt signal (MOM-2) from the neighbouring P2 cell. This signal polarizes EMS to divide along its anterior-posterior axis to generate a mesoderm precursor cell (MS) and an endoderm precursor cell (E) (Korswagen, 2002). POP-1/TCF levels are high in the MS daughter cell while POP-1/TCF levels are low in the E daughter cell. SYS-1/β-catenin levels are low in the MS daughter cell and high in the E daughter cell. The asymmetry and ratio of POP-1 and SYS-1 protein levels drives cell fate specification in MS and E daughter cells (Bertrand and Hobert, 2009; Huang et al., 2007).

Thus, the asymmetric division of the EMS cell is dependent on extrinsic signals such as Wnt and MAPK signals from the neighbouring P2 cell.

1.3.2 Intrinsic mechanisms regulate asymmetric division of the zygote

In *C. elegans*, asymmetric cell division has been studied extensively during division of the one-cell zygote and studies done on this division have demonstrated how intrinsic mechanisms contribute to the regulation of asymmetric division. The zygote (P0) divides asymmetrically along the anterior-posterior axis generating a larger anterior daughter (AB) which will divide to give rise to most of the ectoderm and a smaller posterior daughter (P1) which will generate the endoderm, mesoderm and the germ line (Sulston et al., 1983). This initial asymmetric division of the zygote is dependent on a group of PAR (partition defective) proteins (reviewed in Hoege and Hyman, 2013).

PAR-4 (a serine/threonine kinase) and PAR-5 (a 14-3-3 protein) are symmetrically distributed at the cell cortex while the other PAR proteins are asymmetrically localized to either the anterior or posterior cortex of prior to division (Morton et al., 2002; Watts et al., 2000). The PDZ domain containing PAR-3 and PAR-6 are localized along with the atypical protein kinase-like 3 (PKC-3) at the anterior cortex of the cell to form an anterior domain (Cuenca et al., 2003; Etemad-Moghadam et al., 1995; Tabuse et al., 1998; Watts et al., 1996). The PAR-1 (serine/threonine kinase), PAR-2 (RING-domain containing protein) and LGL-1 (lethal giant larvae-like 1) proteins form a posterior domain (Figure 1.5) (Beatty et al., 2010; Boyd et al., 1996; Guo and Kemphues, 1995; Hoege et al., 2010).

The establishment of these two domains help maintain polarity of the cell. The kinase PKC-3 at the anterior domain and PAR-1 at the posterior domain inhibits specific proteins from associating to the wrong domain (reviewed in Hoege and Hyman, 2013). PKC-3 phosphorylates PAR-2 to prevent its cortical association at the anterior domain (Hao et al., 2006).

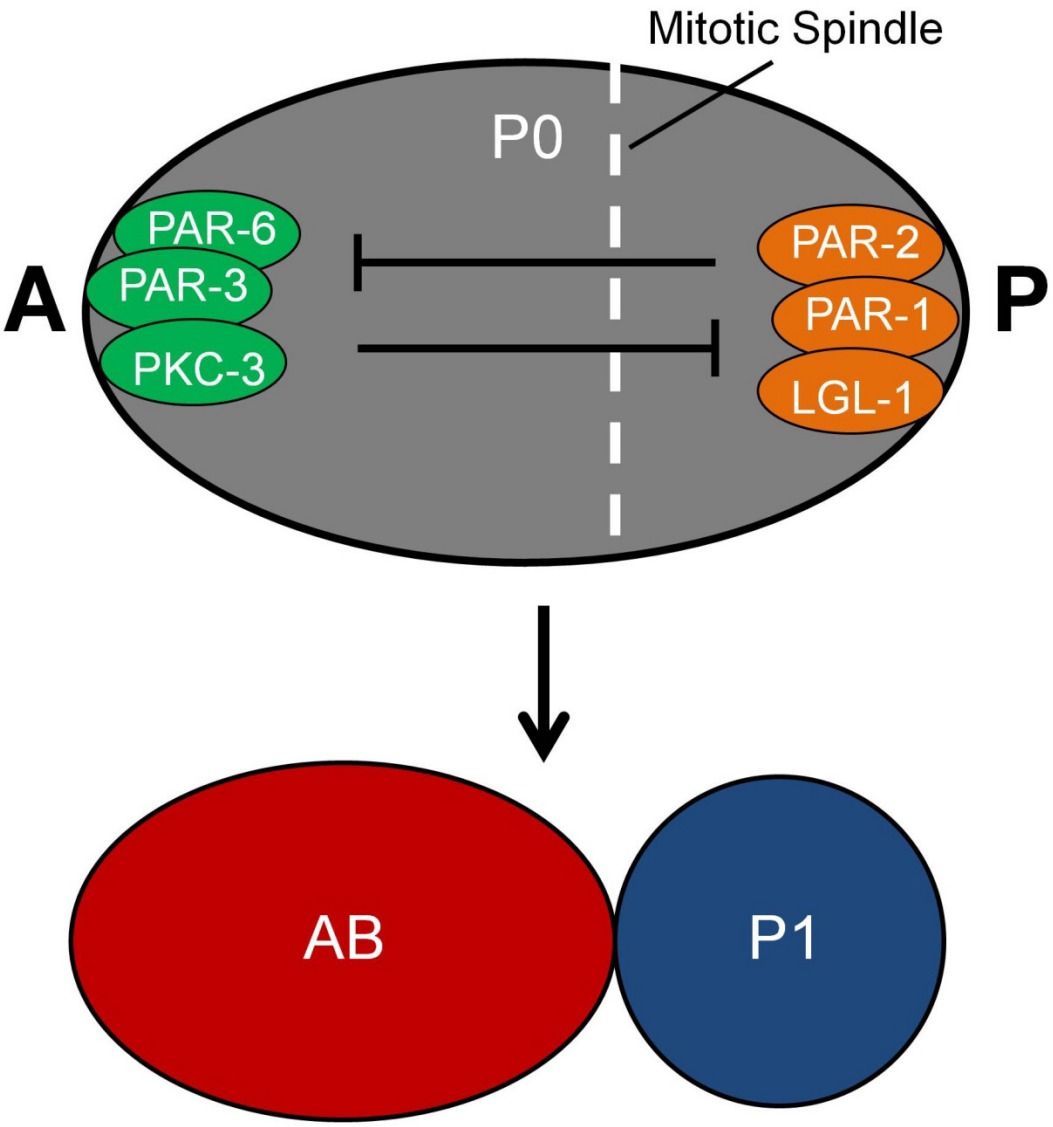

Figure 1.5 Asymmetric division of the *C. elegans* one cell zygote.

The one cell zygote (P0) divides asymmetrically to produce a larger anterior daughter (AB) and a smaller posterior daughter (P1). One group of PAR proteins, PAR-6, PAR-3 and PKC-3 are localized to the anterior cortex to form an anterior domain. Another group of PAR proteins, PAR-2, PAR-1 and LGL-1 are localized to the posterior cortex to form a posterior domain. The components of the anterior domain inhibit components of the posterior domain from localizing to the anterior cortex and vice versa. The establishments of these domains maintain the polarity of the cell (reviewed in Hoege and Hyman 2013)

At the posterior domain, PAR-2 helps promote the accumulation of PAR-1 which prevents cortical association of anterior PAR proteins (Cuenca et al., 2003). The role of the PAR domains is to direct the asymmetric localization of the zinc finger proteins MEX-5 and MEX-6. These proteins are restricted to the anterior cortex which promotes the enrichment of P granules and PIE-1 to the posterior cortex (Cuenca et al., 2003; Schubert et al., 2000). The PAR proteins also control the positioning of the mitotic spindle by determining the asymmetric localization of regulators of G protein signalling (GPR-1/2) and the DEP domain containing protein LET-99. These proteins bias the mitotic spindle posteriorly to ensure that the cleavage will be unequal (Colombo et al., 2003; Gotta et al., 2003; Tsou et al., 2002). Mutation in any of the *par* genes causes defect in spindle orientation, daughter cell size and cell fate (Morton et al., 2002; Tabuse et al., 1998; Watts et al., 1996). Thus, asymmetric division of the one-cell zygote requires asymmetric distribution of intrinsic factors such as the PAR proteins and effector proteins. However, the group of PAR proteins, Numb and other proteins from studies undertaken in *Drosophila* have not been implicated in later asymmetric divisions in *C. elegans*.

1.4 HAM-1 is a key regulator of asymmetric neuroblast divisions in *C. elegans*

Although the group of PAR proteins are crucial intrinsic factors in the regulation of asymmetric division of the *C. elegans* zygote and the *Drosophila* nervous system, these proteins have not been associated in later asymmetric divisions in *C. elegans*. In *C. elegans*, the HSN Abnormal Migration (HAM-1) protein is an intrinsic factor that has been implicated in regulating asymmetric division of many neuronal lineages during embryogenesis and post-embryonically. Interestingly, *ham-1* mutants affect only neuronal linages that produce neurons and apoptotic daughter cells (Frank et al., 2005).

HAM-1 encodes a 414 amino acid protein (Figure 1.6) with a predicted molecular weight of 46.2 kDa that is asymmetrically localized in dividing cells. Through immunostaining of fixed embryos it was observed that HAM-1 is expressed in a ring-shaped pattern around the cell periphery of a subset of cells during embryogenesis (Figure 1.7A). In dividing cells however, HAM-1 is localized asymmetrically, forming crescents at the posterior cortex of the cell (Figure 1.7B) (Frank et al., 2005). Bioinformatics analysis of HAM-1 through the Eukaryotic Linear Motif program (http://elm.eu.org/) did not reveal any obvious sequences responsible for mediating cortical localization such as a Pleckstrin Homology (PH) domain or N-myristylation sequences. Although HAM-1 is a predicted 46.2 kDa protein, it appears as a closely migrating doublet at approximately 55 kDa on a Western blot (Frank et al., 2005). The closely migrating doublet observed suggests that there are two isoforms of HAM-1, however, HAM-1 has only one transcript and there is no supporting evidence for alternative splicing of HAM-1 according to RNAseq data available from wormbase (http://www.wormbase.org/). Thus, the shift in size and the appearance of a closely migrating doublet could be due to post-translational modification of HAM-1.

HAM-1 has been extensively studied in the lineage that generates the Hermaphrodite Specific Neuron (HSN) and the PHB sensory neuron during embryonic development (Frank et al., 2005; Guenther and Garriga, 1996). In wild-type, the HSN/PHB neuroblast divides asymmetrically to produce a smaller anterior daughter cell that undergoes apoptosis and a larger posterior daughter cell, the HSN/PHB precursor (Figure 1.8A) (Sulston et al., 1983). Loss of *ham-1* function results in the size reversal of the anterior and posterior daughter cells; however, the cell fates were not reversed. Instead the anterior daughter cell often inappropriately survives resulting in the duplication of the HSN and PHB neurons (Figure 1.8B). The penetrance of HSN and PHB duplication are 24% and 33% respectively in a *ham-1(gm279)* null allele (Frank et al., 2005).

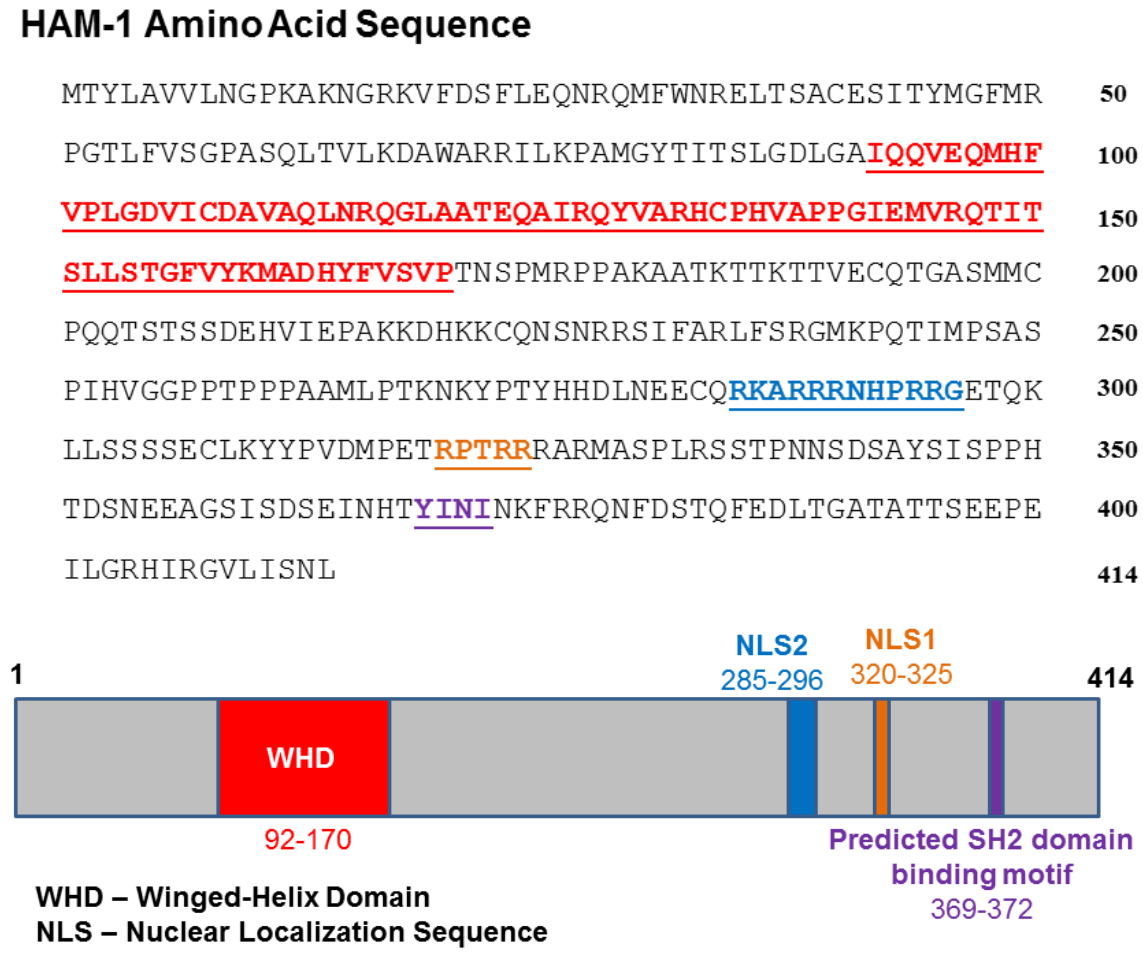

Figure 1.6 Amino acid sequence and schematic of domains within HAM-1.

The top panel shows the full amino acid sequence of HAM-1. The Winged-Helix Domain (WHD) is represented in red, Nuclear Localization Sequence 1 (NLS1) is represented in orange, NLS2 is represented in blue and a predicted SH2 domain binding motif is represented in purple. The bottom panel is a schematic diagram of HAM-1 illustrating the WHD, NLS1, NLS2 and the predicted SH2 domain binding motif.

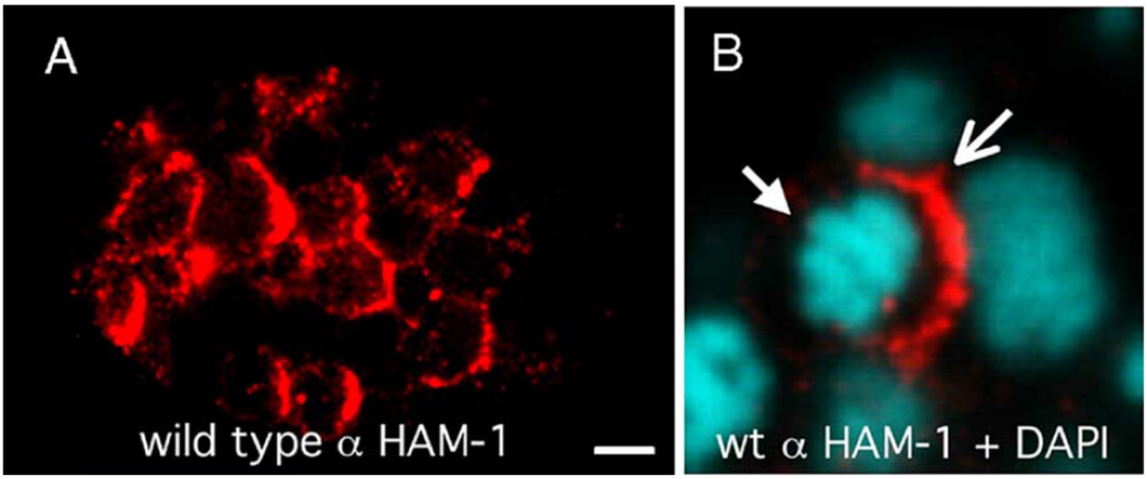

Figure 1.7 Immunostaining of HAM-1 in wild-type embryos.

Wild-type embryos were fixed and stained with α-HAM-1 antibodies (red) and DAPI (blue) to indicate the nuclei. (A) Shows the expression of HAM-1 at the cell cortex of many cells during embryogenesis. (B) HAM-1 forms an asymmetric cresent at the posterior cortex (open arrow) of mitotic cells, as indicated by the condensed chromosomes (closed arrow). Scale bar is 5 μm. Reprinted from Frank et al. 2005, with permission from Elsevier.

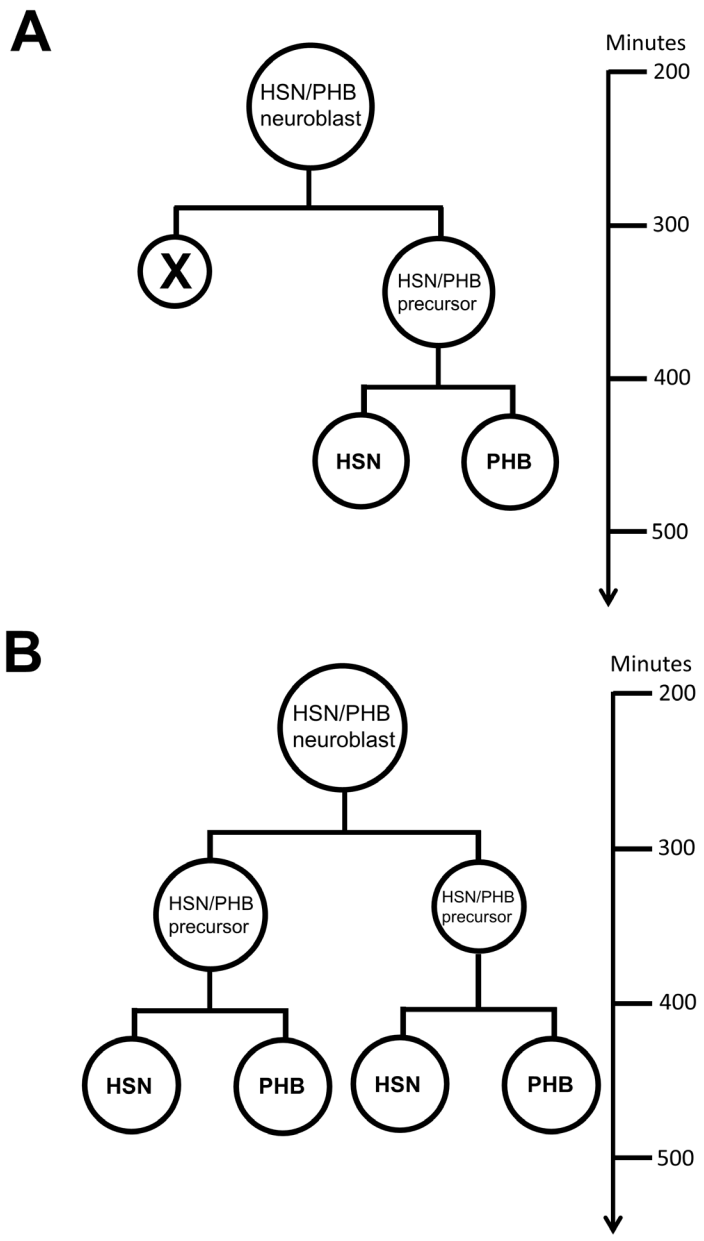

Figure 1.8 Divisions of the HSN/PHB neuroblast.

(A) Illustration of normal HSN/PHB neuroblast division at 270 minutes which generates a smaller anterior daughter that undergoes apoptosis and a larger posterior daughter, the HSN/PHB precursor. The HSN/PHB precursor divides to generate the HSN and PHB neurons (Sulston et al., 1983). **(B)** Illustration of HSN/PHB neuroblast division defect at 270 minutes in *ham-1* mutants which results in a reversal in cell size and an anterior-posterior cell fate transformation. The consequence of this is a duplication of HSN and PHB neurons (Frank et al., 2005).

Another neuronal lineage that is affected by loss of *ham-1* function is the lineage that generates the PLM mechanosensory neurons and the ALN sensory neurons during embryonic development. In wild-type, the final three divisions in this lineage are asymmetric divisions. At 295 minutes of embryonic development, the neuroblast divides to produce an anterior daughter cell that undergoes apoptosis and a posterior neuroblast. At 395 minutes, this neuroblast then divides asymmetrically to produce an anterior daughter, the PLM/ALN precursor cell, and a posterior daughter that undergoes apoptosis. The PLM/ALN precursor cell then divides to give rise to the PLM and ALN neurons (Figure 1.9A) (Sulston et al., 1983). In *ham-1* mutants, there is an 80% loss of PLM neurons with a similar loss for the ALN neurons (Leung et al., 2014). Through lineage analysis it was determined that the division at 295 minutes appeared normal in the null mutant *ham-1(gm279)* (Leung et al., 2014). Thus, it is hypothesized that there is an asymmetric division defect at 395 minutes resulting in the transformation of the anterior daughter into the posterior daughter cell. The consequence of this would be the production of two posterior daughter cells which both undergo apoptosis and a subsequent loss of both PLM and ALN neurons (Figure 1.9B). To examine whether the inhibition of programmed cell death would rescue the *ham-1* loss of PLM neurons, all programmed cell death was inhibited by using a *ced-4* mutant. CED-4 encodes the *C. elegans* APF-1 homolog which is required to initiate programmed cell death. Thus, loss of *ced-4* function in *C. elegans* results in survival of cells that normally undergo apoptosis during development (Ellis and Horvitz, 1986). In *ced-4* mutants, PLM neurons are duplicated at a low penetrance due to the inappropriate survival of the daughter cells that normally die in this lineage. In a *ham-1(gm279); ced-4* double mutant, the PLM neuronal loss is completely suppressed which indicates that HAM-1 does not directly specify the fate of the PLM/ALN neurons (Leung et al., 2014).

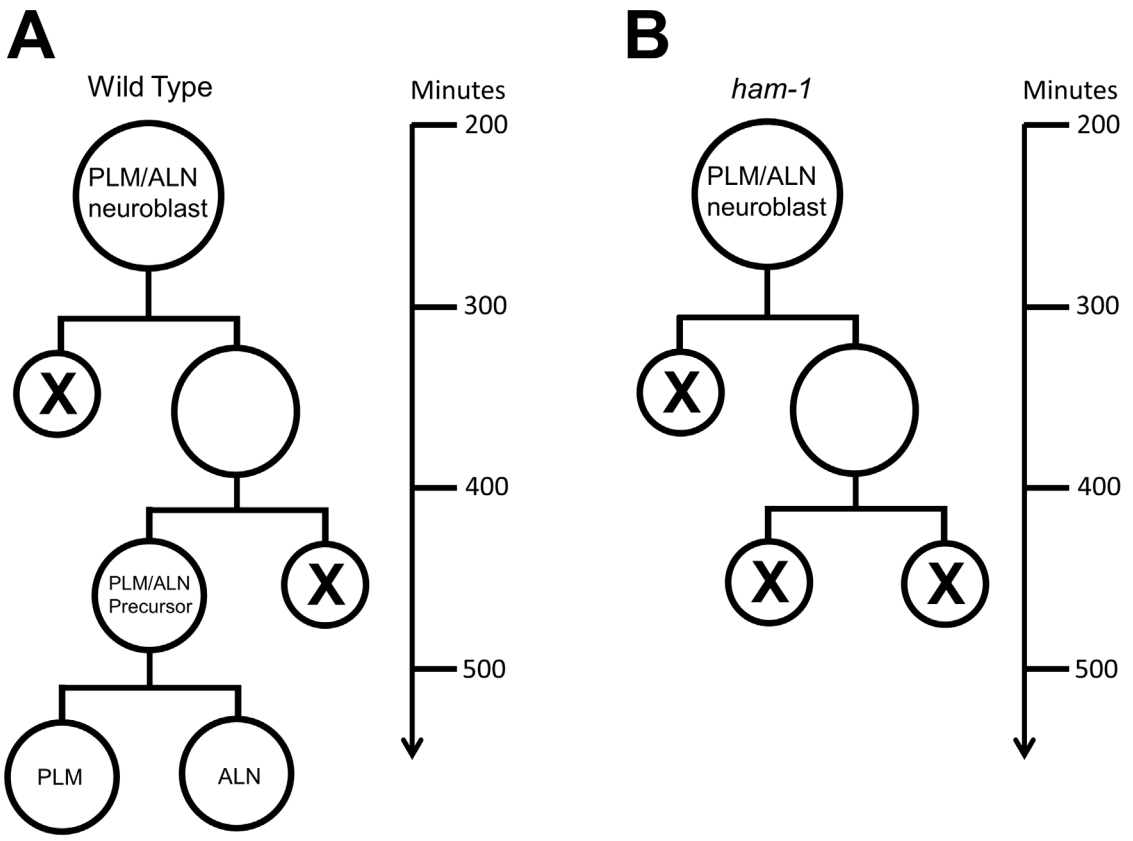

Figure 1.9 Divisions of PLM/ALN neuroblast during embryonic development.

(A) Illustration of the last three asymmetric divisions in the PLM/ALN lineage in wild-type worms. At 295 minutes the PLM/ALN neuroblast divides to produce an anterior daughter which undergoes apoptosis and a posterior daughter. The posterior daughter divides at 395 minutes to give rise to an anterior daughter the PLM/ALN precursor and a posterior daughter which undergoes apoptosis. The PLM/ALN precursor will then give rise to the PLM and ALN neurons (Sulston et al., 1983). **(B)** Predicted lineage defect in a *ham-1* mutant. An anterior to posterior cell fate transformation at 395 minutes would result in two apoptotic daughter cells and a loss of PLM and ALN neurons (Leung et al., 2014).

HAM-1 has also been shown to regulate asymmetric division of larval neuroblasts, specifically in the Q cell lineage. In L1 larvae, the Q neuroblast lineage undergoes three asymmetric divisions to give rise to three types of neurons (A/PQR oxygen sensory neurons, A/PVM mechanosensory neurons and SDQL/R interneurons) and two apoptotic daughter cells (Sulston and Horvitz, 1977). The first division of the Q neuroblasts results in an anterior Q.a daughter and a posterior Q.p daughter cell. Q.a goes on to divide once to generate a smaller anterior daughter cell which undergoes apoptosis and a larger posterior daughter (A/PQR neuron) while Q.p divides twice to generate a larger anterior daughter which is the A/PVM and SDQL/R precursor and a smaller posterior daughter that undergo apoptosis (Figure 1.10A) (Sulston and Horvitz, 1977).

In the Q.a division, the mitotic spindle is positioned in the middle of the Q.a cell and there is an accumulation of myosin II (NMY-2) at the anterior end of the cell during cytokinesis. This unequal distribution of myosin results in asymmetric cortical tension where the anterior pole is more contracted and the posterior pole is more relaxed and expanded. The division will result in a smaller anterior daughter and a larger posterior daughter. However, the asymmetric Q.p division is NMY-2 independent. In this division, the mitotic spindle is displaced posteriorly which results in the generation of a larger anterior daughter and a smaller posterior daughter following cytokinesis. Thus, the mechanisms in which Q.a and Q.p generate daughter cell size asymmetry are different from each other (Ou and Vale, 2009).

In *ham-1* mutants, there is a duplication of A/PQR neurons (Figure 1.10B) but no defects were observed for A/PVM or SDQL/R neurons (Feng et al., 2013). This suggests that HAM-1 specifically regulates Q.a division while Q.p development is independent of HAM-1. When the centrosome and myosin dynamics were examined, it was observed that some Q.a cells were able to position the mitotic spindle correctly in the middle of the cell but failed to asymmetrically distribute myosin. In other Q.a cells, the mitotic spindle was displaced posteriorly along with symmetric myosin distribution.

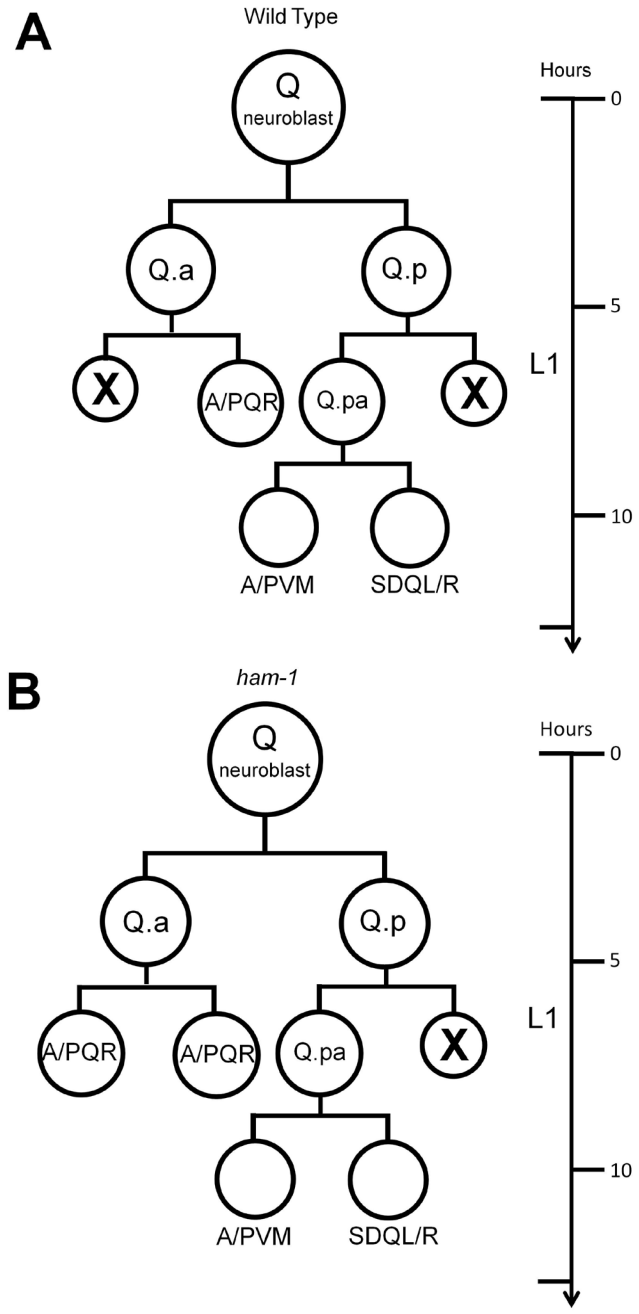

Figure 1.10 Divisions of the Q neuroblast during L1 larval development.

The Q neuroblast lineage undergoes three asymmetric divisions to give rise to three types of neurons (A/PQR oxygen sensory neurons, A/PVM mechanosensory neurons and SDQL/R interneurons) and two apoptotic daughter cells (Sulston and Horvitz, 1977). **(A)** Illustration of normal Q neuroblast divisions in wild-type larva. **(B)** Illustration of Q.a division defect in *ham-1* mutants resulting in a duplication of the A/PQR neurons (Feng et al., 2013).

The consequence of this is the production two equal daughter cells with the same cell fate. Thus, it appears that HAM-1 is responsible for the regulation of spindle positioning and myosin polarization in the Q.a neuroblast (Feng et al., 2013).

1.5 HAM-1 sequence homology

To gain insight into how HAM-1 could function in the regulation of neuroblast asymmetric division, sequence homology of the 414 amino acid protein was analyzed bioinformatically using BLASTP (protein-protein BLAST). This analysis showed that HAM-1 has homologs in *Caenorhabditis* species *(C. briggsae*, *C. brenneri* and *C. remanei*) and a limited number of other species within the nematoda phylum (*Ancylostoma ceylanicum*, *Haemonchus contortus*, *Necator americanus*, *Ascaris suum*, *Brugia malayi* and *Loa loa*) (Figure A.3). These proteins all contain a storkhead box domain at their N-terminus. Outside nematodes, sequence homology is restricted to the storkhead box domain. The N-terminal half of HAM-1 has 33% identity to the human transcription factor STOX1 and 31% to Knockout in *Drosophila* (Figure A.4). *knockout* is a target gene of the transcription factor Kruppel (Hartmann et al., 1997), but not much is known about this particular gene. Sequence analysis of the protein Knockout by Interpro (http://www.ebi.ac.uk/interpro/) reveals that it is a winged-helix domain containing stork-head box protein. Although our knowledge of Knockout function and regulation is very limited, proteins containing winged-helix domains have generally been shown to participate in establishing protein-DNA interactions (Teichmann et al., 2012). This then suggests that Knockout is a potential transcription factor.

Also showing homology to HAM-1, the human transcription factor STOX1 is a key player in trophoblast dysfunction underlying preeclampsia and is functionally involved in late onset Alzheimer's disease (Berends et al., 2007; van Dijk et al., 2010a). STOX1 contains a winged-helix domain with sequence

similarity to the DNA binding domain found in the family of FOX transcription factors (van Dijk et al., 2005). Through chromatin immunoprecipitation (ChIP) experiments, it was determined that STOX1 is a known transcription factor which modulates the expression of transcription factors in trophoblast cells (Rigourd et al., 2009). STOX1 also downregulates the expression of Contactin-Associated Protein-like 2 (*CNTNAP2*) which is associated with late onset Alzheimer's disease (van Abel et al., 2012). STOX1 is localized to both the nucleus as well as the cytoplasm but it is not cortically localized. The localization of STOX1 is regulated by the PI3K-Akt pathway where phosphorylation of STOX1 by Akt prevents entry into the nucleus resulting in degradation by ubiquitination (van Dijk et al., 2010b). Similar to STOX1, HAM-1 also contains a winged-helix domain which would suggest a putative DNA binding role for HAM-1. However, the C-terminus of HAM-1 is completely divergent from that of STOX1 which makes it difficult to draw conclusions of HAM-1 function from STOX1. Despite the presence of a conserved winged helix domain, the sequence homology of HAM-1 is inconsistent with the previously described localization of the protein. The question of why an asymmetrically localized protein would have homology with a transcription factor and contain a winged-helix domain could provide further clues into the role of HAM-1 during development.

1.6 Regions of HAM-1 required for function and localization

A study done by Leung et al., 2014 dissected regions of HAM-1 that were essential for its function and localization. A *gfp::ham-1* fusion construct was created by expressing a full length *ham-1* cDNA driven by a *unc-119* promoter sequence due to a lack of endogenous *ham-1* promoter sequence being available. The full length GFP::HAM-1 fusion protein was assayed for proper localization and function. This fusion protein was functional as it was able to rescue the loss of PLM neurons in *ham-1(gm279)* and by immunostaining with an α-GFP antibody, GFP::HAM-1 was asymmetrically localized at the cortex in

dividing cells like wild-type HAM-1 (Figure 1.10A). However, when this GFP::HAM-1 fusion protein was observed under direct fluorescence, it was localized to both the cell cortex and the nucleus (Figure 1.10B). Although GFP::HAM-1 was detected in the nucleus under direct fluorescence, nuclear localization of this fusion protein was not observed by immunostaining of transgenic embryos with either anti-GFP or anti-HAM-1 antibodies. This suggests that endogenous HAM-1 may also localize to the nucleus but is undetectable by immunohistochemistry. Nuclear localization of endogenous HAM-1 would be consistent with the presence of a putative DNA binding domain within the protein.

Following analysis of the full length GFP::HAM-1 fusion protein, a structure function analysis was performed by truncating the full length GFP::HAM-1 from the C-terminal end and the N-terminal ends followed by localization and function assays. Truncation of GFP::HAM-1 from either the C-terminus or the N-terminus completely abolished the function of the protein (Leung et al., 2014). It was determined that deletion of either the C-terminus or the N-terminus also decreased membrane localization of GFP::HAM-1 suggesting that there are sequences within these regions responsible for proper membrane localization (Leung et al., 2014). The structure function analysis also revealed a region of HAM-1 between amino acid 268 and 364 that is required for nuclear localization as the nuclear localization was completely abolished when this region was deleted. It was determined bioinformatically that this region of HAM-1 contains two potential nuclear localization sequences (NLSs), a conserved NLS and a less conserved bipartite NLS. While mutation of either sequence individually had little effect on nuclear localization, mutation of both sequences eliminated nuclear localization of the protein (Leung et al., 2014).

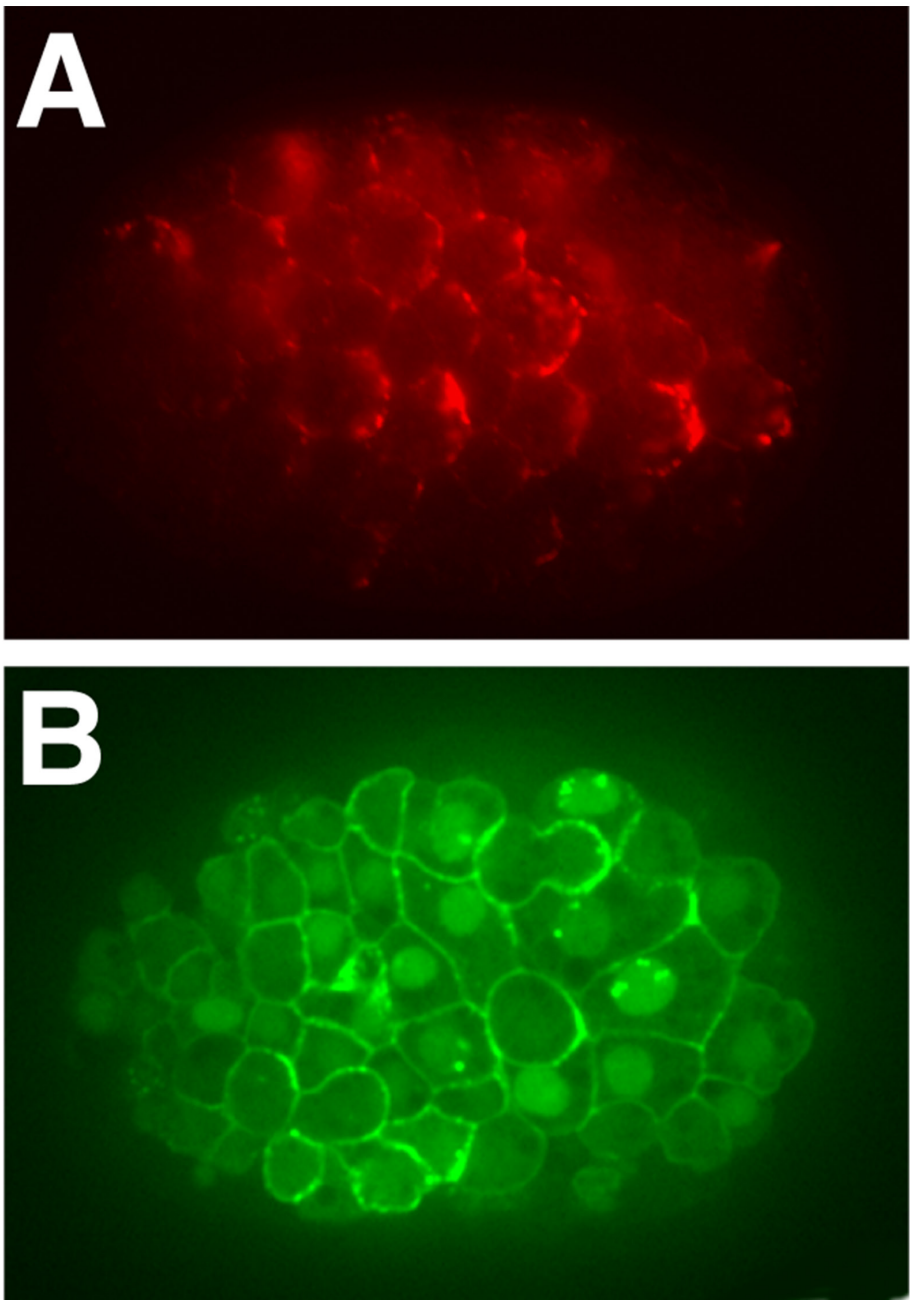

Figure 1.11 GFP::HAM-1 localization.

(A) A transgenic embryo expressing GFP::HAM-1 stained with anti-GFP antibodies. GFP::HAM-1 is localized to the cell cortex (Leung et al., 2014). **(B)** A transgenic embryo expressing GFP::HAM-1 examined directly for GFP fluorescence. HAM-1 is localized to both the membrane and the nucleus (Leung et al., 2014).

1.7 Models of HAM-1 function

While HAM-1 plays a key role in the asymmetric division of many neuronal lineages, the mechanism in which HAM-1 regulates the divisions in these lineages is largely unknown. One feature in common between the HSN/PHB, PLM and Q.a lineage is the anterior-posterior cell fate transformation observed in a *ham-1* mutant. Since HAM-1 is asymmetrically localized at the cell cortex, it could function as a cell fate determinant within one of the daughter cell following division. However, evidence thus far indicates that HAM-1 does not behave as a cell fate determinant. In the HSN/PHB lineage, it is the anterior daughter cell which does not inherit HAM-1 that is transformed in *ham-1* mutants in the HSN/PHB lineage (Guenther and Garriga, 1996). In the PLM lineage, the loss of PLM neurons in a *ham-1* mutant is suppressed by a *ced-4* mutation. Thus, HAM-1 is not required to specify the PLM neuron fate. Instead, *ham-1* may function as a negative regulator of cell death in this lineage (Leung et al., 2014).

Although HAM-1 does not function as a cell fate determinant, a model proposed by Guenther and Garriga 1996 suggest it may tether factors required for cell fate to the posterior cortex of the mitotic neuroblast which would ensure that these factors are only inherited by the HSN/PHB precursor cell. In *ham-1* mutants, these factors might be inappropriately inherited by the anterior daughter leading to the duplication of HSN and PHB neurons. Although the proposed tethering function is consistent with the *ham-1* mutant defects in the HSN/PHB lineage, direct evidence for this model has not thus far been obtained (Frank et al., 2005). Furthermore, the fact that HAM-1 lacks the protein-protein interaction domains suggestive of a tethering protein is also inconsistent with the above model.

Studies done by Frank et al., 2005 revealed a role for HAM-1 in the positioning of the mitotic spindle. In wild-type, the mitotic spindle is biased anteriorly in the HSN/PHB neuroblast which results in a smaller anterior daughter and a larger posterior daughter. In *ham-1* mutants the cell size of the daughters

are reversed. Thus, the defects in cell fate could be a secondary consequence resulting from the posterior bias of the cleavage plane position. The anterior daughter could then inherit neuronal determinants which allow it to escape programmed cell death and produce HSN/PHB neurons. However, the reversal in cell size does not completely affect the cell fate of the anterior daughter as the penetrance of HSN and PHB duplication are 24% and 33% respectively. While the positioning of the mitotic spindle may contribute to differential inheritance of molecular determinants, cell size alone is not sufficient to dictate developmental fates. This is due to a competing cell death program which directs the daughter cells to die. When cell death is eliminated the cell fate transformation becomes increasingly penetrant (Frank et al., 2005). The role of HAM-1 in the positioning of the mitotic spindle is also evident in the Q neuroblast lineage and in this lineage HAM-1 has an additional role in myosin polarization (Feng et al., 2013).

1.8 Research objectives

1) Determine if endogenous HAM-1 is localized to the nucleus.

The nuclear localization of the GFP::HAM-1 fusion protein and the discovery of the NLSs indicate that endogenous HAM-1 could potentially be localized to the nucleus (Leung et al., 2014). Although GFP::HAM-1 is localized in the nucleus, the expression is from an integrated extrachromosomal array and the level of expression is substantially higher than endogenous HAM-1. Thus, the nuclear localization could be an artifact of the overexpression. Since we cannot detect endogenous HAM-1 through antibody staining we performed a subcellular fractionation followed by Western blotting to determine if endogenous HAM-1 localizes to the nucleus.

2) Identify residues within the C-terminus required for HAM-1 function.

The study done by Leung et al., 2014 was able to determine that both the N-terminus and C-terminus of HAM-1 was crucial for function and localization via

a truncation analysis. However, this analysis was only able to analyze segments of the protein rather than specific sequences. In this study we aim to narrow down specific sequences within a particular segment that is responsible for the function and localization of the protein. The focus was on the C-terminal 50 amino acids of the protein which contains a potentially phosphorylated Tyrosine residue at position 369 (Tyr 369), which is within a predicted SH2 domain binding motif, **YINI**. The approach was to mutate this particular residue with respect to GFP::HAM-1 and analyze the function and localization of this fusion protein.

3) Identify sequences responsible for cortical localization of HAM-1.

Although HAM-1 runs as a closely migrating doublet on a Western blot, the nature of the doublet observed is currently unknown. It is possible that the doublet observed is a result of post-translational modifications and these modifications could contribute to the cortical localization of HAM-1. However, HAM-1 does not contain any obvious sequences that would mediate cortical localization such as a PH domain or N-myristylation sequence. To identify sequences responsible for cortical localization and the closely migrating doublet observed on a Western blot, we analyzed existing point mutation and deletion mutant alleles of *ham-1* available by whole mount immunostaining and Western blotting.

Chapter 2.

Material and Methods

2.1 Strains

Methods for growth and culture of *C. elegans* were previously described (Brenner, 1974). Strains were maintained at 20°C on Nematode Growth Media (NGM) agar, with *Escherichia coli* OP50 or HB101 as the food source. The wild-type strain used was N2 Bristol. The following mutations and GFP arrays were used for this study:

LG I: *zdIs5[mec-4::gfp]* (Clark and Chiu, 2003)

LG II: *ptp-2(op194)* (Gutch et al., 1998), *mIn1[dpy-10(e128) mIs14(myo-2::GFP)]* (Edgley and Riddle, 2001), *rrf-3(pk1426)* (Simmer et al., 2002)

LG IV: *ham-1(n1811)* (Guenther and Garriga, 1996)*, ham-1(gm214), ham-1(gm267), ham-1(gm279)* (Frank et al., 2005), *ham-1(cas27), ham-1(cas46), ham-1(cas137)* (Feng et al., 2013)*, ham-1(ot361)* (Doitsidou et al., 2008), *dpy20(e1282ts)* (Hosono et al., 1982)*, unc30(e191)* (Brenner, 1974).

2.2 Generation of transgenic animals

Transgenic animals were generated by microinjection, as previously described (Mello et al., 1991). Each construct was co-injected with *dpy-*

30p::dsRed (Cordes et al., 2006), which is detected throughout the body. The introduced DNA forms extrachromosomal concatemers that are inherited mosaically by a fraction of the offspring. Both the *unc-119p*::*gfp::ham-1(Y369F) and unc-119p::gfp::ham-1(Y369E)* constructs were injected at 50 ng/μL along with *dpy-30p::dsRed* (Cordes et al., 2006) at 40 ng/μL into a strain containing *zdIs5(mec-4::gfp)* (Clark and Chiu, 2003). Three arrays containing *gfp::ham-1(Y369F)* were generated (*hkEx234, 235 and 236*) and two arrays containing *gfp::ham-1(Y369E)* were generated (*hkEx296, and 297*).

2.3 Genetic crosses

To introduce *hkEx234, 235, 236, 296 and 297* into a *ham-1(gm279)* (Frank et al., 2005) background, crosses were done following the same scheme for each extra chromosomal arrays (Figure A.1). N2 males were crossed with *zdIs5(mec-4::gfp)* hermaphrodites containing the extra chromosomal array (*hkEx#*). Male progeny carrying the extra chromosomal array and *zdIs5(mec-4::gfp)* were crossed with *zdIs5(mec-4::gfp); dpy20(e1282ts) unc30(e191)* hermaphrodites. *dpy20(e1282ts) unc30(e191)* was used to balance *ham-1*. *hkEx#*; *zdIs5(mec-4::gfp)/zdIs5(mec-4::gfp) or +; dpy20(e1282ts) unc30(e191)/+* males were crossed with *zdIs5(mec-4::gfp); ham-1(gm279)* hermaphrodites. Hermaphrodites carrying the extrachromosomal array, *hkEx#*; z*dIs5(mec-4::gfp); ham-1(gm279)/dpy20(e1282ts) unc30(e191)* or + were cloned. From plates segregating DpyUnc animals, non-DpyUnc animals carrying the extrachromosomal array were cloned to homozygous *ham-1(gm279)*. If necessary, animals were further cloned to homozygous *zdIs5(mec-4::gfp)*.

zdIs5(mec-4::gfp) was introduced into a *ptp-2(op194)* strain to visualize and score PLM neurons following the crossing scheme in Figure A.2. To generate a *zdIs5; ptp-2(op194)* strain, N2 males were crossed with *zdIs5(mec-4::gfp)* hermaphrodites. F1 male progeny were then crossed with a strain heterozygous for the balancer *mIn1[dpy-10(e128) mIs14(myo-2::GFP)]*. This

balancer is a large chromosomal inversion for the middle of chromosome II (Edgley and Riddle, 2001) and balances *ptp-2(op194). zdIs5/+; mIn1/+* male progeny were crossed with *ptp-2(op194)* hermaphrodites. *zdIs5*/+; *ptp-2(op194)/mIn1* hermaphrodite progeny were cloned. Following this, worms lacking the *mIn1* balancer were cloned to homozygous *zdIs5(mec-4::gfp)* and generate the final strain; *zdIs5(mec-4::gfp)*; *ptp-2(op194).*

2.4 Worm lysis for PCR reaction

Ten adult worms were placed in 20 μL of worm lysis solution (60 μg/mL proteinase K, 10 mM Tris pH 8.2, 50 mM KCl, 2.5 mM $MgCl_2$, 0.5% Tween-20, 0.05% gelatin) in the cap of a PCR tube. The tube was then spun at 13,000 rpm for 2 minutes and then frozen at -80°C for 30 minutes. The tube was then thawed and incubated in a PCR machine at 60°C for 1 hour and then 95°C for 15 minutes. 1 μL of worm lysate was then used as template in PCR reactions.

2.5 Subcloning of *src-1* into L4440 RNAi vector

The largest exon of *src-1* (exon 5) was amplified by nested PCR. The outer primers used were Src-1 outer left (5'-CAGGCAAGACCCATCGAGAG-3') and Src-1 outer right (5'-GGACGGTGAGATTTGGTTCA-3'). The inner primers used were Src-1 inner left (5'-CAGTAGATCTCGCTGAGTTAAATTTTGTTAAACC-3') and Src-1 inner right (5'-CAGTCTCGAGTCAATTTTGTTTCAATTTTCACG-3'). The inner forward primer contains a BglII restriction site and the inner reverse primer contains an XhoI restriction site. PCR reactions were performed in a final volume of 25 μL consisting of 2.5 μL 10X Pfu reaction buffer (200 mM Tris-HCl pH 8.8, 100 mM $(NH_4)_2SO_4$, 100 mM KCl, 1 mg/mL BSA, 1% (v/v) Triton X-100, 2 mM $MgSO_4$), 0.2 mM dinucleotide triphosphates, 0.5 μM of each primer, and 1 unit of Pfu DNA

polymerase (Addgene plasmid 12509). 1 μL of genomic DNA was used for the outer PCR reaction. 1 μL of diluted (1:100) PCR product from the outer PCR reaction was used for the inner PCR reaction. For both the outer primers and inner primers the cycling condition was: 95°C for 3 minutes, 35 cycles of 95°C for 30 seconds, 65.5°C for 30 seconds, 72°C for 6 minutes, and then 72°C for 10 minutes with the exception of the annealing temperature. The annealing temperature for the outer primers was 65.5°C while the annealing temperature for the inner primer was 53°C.

PCR products were purified using the Fermentas GeneJET™ PCR purification kit. The purified PCR product was quantified using the Nanodrop ND-1000 spectrophotometer. 1 μg of DNA was digested in a 40 μL reaction volume with 1X NEBbuffer 3.1 (100 mM NaCl, 50 mM Tris-HCl, 10mM $MgCl_2$, 100 μg/mL BSA, pH 7.9 @ 25°C), 10 units BglII (New England Biolabs R0144S) and 10 units XhoI (Life Technologies 15231-012) restriction enzymes at 37°C overnight. 100 μL of ddH_2O was added to the reaction to dilute the sample which was then phenol/chloroform extracted and ethanol precipitated. The pellet was resuspended in 10 μL of ddH_2O.

An L4440 vector containing two IPTG-inducible T7 promoter was prepared for ligation by digestion. 1 μg of DNA was digested in a 40 μL reaction volume with 1X NEBbuffer 3.1 (100 mM NaCl, 50 mM Tris-HCl, 10 mM $MgCl_2$, 100 μg/mL BSA, pH 7.9 @ 25°C), 10 units BglII (New England Biolabs R0144S) and 10 units XhoI (Life Technologies 15231-012) restriction enzymes at 37°C overnight. Calf intestinal alkaline phosphatase (Roche 10713023001) was diluted 1:20 in 1X NEBbuffer 3.1 and 1 μL was added to the digestion mixture. The vector was phosphatase treated for 30 minutes. The phosphatase treatment was inactivated by adding 1 μL of 0.5M EDTA and heated at 65°C. The digested vector was purified by phenol/chloroform extraction followed by ethanol precipitation. The pellet was resuspended in 10 μL of ddH_2O.

The purified digested *src-1* PCR product and digested L4440 vector was ligated together in a 10 μL reaction. The reaction consisted of 3 μL digested vector and 3 μL digested *src-1* PCR product in 1X reaction buffer (30 mM Tris-HCl (pH 7.8), 10 mM $MgCl_2$, 10 mM DTT and 1 mM ATP) with 1 unit of T4 DNA ligase (Promega M1801). The reaction was incubated at room temperature for 1 hour.

1 μL of the ligation reaction was used to electroporate into *E. coli (DH5α)* and spread onto Luria Broth (LB) agar plates containing 100 μg/mL ampicillin. The plates were grown overnight at 37°C. The next day 10 individual colonies were innoculated in ten different culture tubes containing 5 mL of LB with 100 μg/mL ampicillin. Plasmid was extracted from each bacterial culture using the GeneJET plasmid miniprep kit (Thermo Scientific K0503). Plasmid isolated from each colony was digested with 1X NEBbuffer 3.1, 10 units BglII (New England Biolabs R0144S) and 10 units XhoI (Life Technologies 15231-012) restriction enzymes at 37°C overnight to test whether the plasmid contains the *src-1* insert. Correct subclones produced a 1 kb insert band and a 2.7 kb vector band.

2.6 RNAi knockdown of *src-1* by feeding

The purified *src-1* L4440 construct was electroporated into *E. coli (HT115)* which is an RNase III-deficient *E. coli* strain. After electroporation the cells were streaked out onto Luria Broth (LB) agar plates containing 50 μg/mL carbenicillin and 12.5 μg/mL tetracyclin and grown overnight at 37°C. The following RNAi feeding protocol is adapted from (Kamath et al., 2001). An individual colony was inoculated into 5 mL of LB with 50 μg/mL carbenicillin and 12.5 μg/mL tetracycline and grown overnight at 37°C. The next day, bacteria from the liquid culture was spread onto NGM agar plates containing 50 μg/mL carbenicillin, 12.5 μg/mL tetracycline and 1 mM Isopropyl β-D-1-thiogalactopyranoside (IPTG). The IPTG was used to induce T7 polymerase production in bacteria. Plates were left

to dry and induce overnight. The following day, L4 worms were transferred onto the RNAi plates and grown at 20°C for 24 hours. The next day, the worms were transferred onto fresh RNAi plates and grown at 20°C for 24 hours. Progeny from the previous plates were scored for the number of PLM neurons. This was repeated for a total feeding time of 72 hours.

2.7 RNAi knockdown of *src-1* by microinjection

2 μg of purified *src-1* L4440 construct was digested with 1X NEBbuffer 3.1 and 10 units Bgl II (New England Biolabs R0144S) overnight at 37°C. 2 μg of purified *src-1* L4440 construct was also digested with 1X REact4 Buffer (20 mM Tris-HCl (pH 7.4), 5 mM $MgCl_2$, 50 mM KCl) and 10 units of Apa I (Invitrogen 15440-019) overnight at 25°C. After incubation each digest was treated with 200 μg/mL proteinase K and 0.5% SDS followed by incubation at 50 degrees for 30 minutes to degrade any RNAase. Following RNAase degradation, each linearized construct was purified by phenol/chloroform extraction and ethanol precipitation in preparation for *in vitro* transcription. After ethanol precipitation, both pellets from the Bgl II digest and Apa I digest were resuspended in 10 μL of ddH_2O. Linearized construct from the Bgl II digest and Apa I digest were each *in vitro* transcribed using the Invitrogen MegaScript T7 kit in a 20 μL reaction: 8 μL of dinucleotide triphosphates, ~1 μg of linearized construct, 2 μL of 10X reaction buffer, 2 μL of enzyme mix. The reaction was carried out at 37°C for 4 hours. Following *in vitro* transcription, the construct linearized with Apa I generated the sense RNA while the construct linearized with Bgl II generated the anti-sense RNA. Equal molar amounts of the sense RNA and anti-sense RNA strands were combined, incubated at 70°C for 15 minutes then allowed to cool to room temperature. The double stranded RNA was then stored at -20°C.

2.8 Embryo isolation by hypochlorite treatment

To isolate embryos, gravid hermaphrodites were washed off of plates into 15 mL Falcon tubes with ddH_2O containing 0.05% Triton X-100. The gravid hermaphrodites were then washed three times with ddH_2O containing 0.05% Triton X-100. A hypochlorite solution (0.8 M NaOH, 0.125% sodium hypochlorite) was added to dissolve adult tissues and leave the embryos intact. The intact embryos were then washed three times with ddH_2O containing 0.05% Triton X-100.

2.9 Preparation of embryonic protein extracts

Embryos were isolated by hypochlorite treatment as described above. After washing, 50 μL of packed embryos were transferred into a 1.5 mL eppendorf tube and the supernatant was removed leaving 100 μL of liquid. 20 μL of 100% of Trichloroacetic acid (TCA) was added ($1/5^{th}$ volume). 0.5 mm glass beads (Soda Lime) were added to the embryos up until the meniscus. The tube was then vortexed in five 1 minute intervals with icing in between. 1 mL of 5% TCA was then added and the tube was centrifuged at 13,000 rpm at 4°C for 20 minutes. The supernatant was removed, 1 mL of 90% acetone was added and the tube was then spun at 13,000 rpm at 4°C for 5 minutes. The supernatant was then removed and the pellet was left to air dry. 2X SDS sample buffer (10% SDS, 80 mM Tris pH 6.8, 12.5% Glycerol, 4% β-mercaptoethanol, 0.1% Bromophenol blue) was added to the pellet. 2 M Tris base was added to a final concentration of 0.2 M to neutralize the pH. The sample was then boiled for 10 minutes and stored at -20°C.

2.10 Immunohistological Methods

Embryos were isolated by hypochlorite treatment as described above. Embryos for antibody staining were fixed using the modified fixation protocol from Guenther and Garriga, 1996. The embryos were then fixed in a 1% paraformaldehyde solution containing 80 mM KCl, 20 mM NaCl, 2 mM EGTA, 0.5 mM spermidine HCl, 0.2 mM spermine, 0.5% β-mercaptoethanol, 15 mM PIPES pH 7.4, with 1/5 volume of 90% MeOH; 10% 0.05 M EGTA for 15 minutes. After fixation, the embryos were immediately frozen in liquid nitrogen for 1 minute and then stored at -80°C.

Embryos were then thawed in room temperature water and rocked for 15 minutes at room temperature. 500 μL of Tris-Triton buffer (100 mM Tris-Cl pH 7.4, 1% Triton X-100, 1 mM EDTA) was added to stop the fixation. The embryos were spun down at 2000 x g for 10 seconds and the supernatant was removed. The embryos were then washed with 1 mL of Tris-Triton buffer. Followed by two washes with 1 mL of PBST-B buffer (1X PBS, 0.1% BSA, 0.5% Triton X-100, 0.05% NaN_3). Embryos were transferred into 0.5 mL eppendorf tubes and blocked at room temperature in PBST-A buffer (1X PBS, 1% BSA, 0.5% Triton X-100, 0.05% NaN_3). The embryos were then incubated overnight at room temperature in 50 μL of rabbit α-HAM-1 antibody (Guenther and Garriga, 1996) (1:250 in PBST-A). Three washes were done in 500 μL of PBST-B for 15 minutes each wash. The embryos were incubated overnight at room temperature in 50 μL of Alexa Fluor® 488 Goat Anti-Rabbit (Molecular Probe A-11004) (1:2500 in PBST-A). Three washes were done in 500 μL of PBST-B for 15 minutes each wash. For the last wash 1 μL of 1 mg/mL 4'6-diamidino-2-phenylindole (DAPI) dilactate was added to 500 μL of PBST-B making a working concentration of 2 μg/mL. Then the supernatant was removed leaving approximately 50 μL of liquid. 5 μL of embryos were mounted on a slide with 2% agarose pad and immersed in 5 μL of Slowfade® Gold antifade reagent (Molecular Probes S369367) to prevent photobleaching.

2.11 Microscopy

Live larvae were immobilized in 100 mM sodium azide to score for number of PLM neurons using a Leica DMRA2 upright microscope. Stained embryos were mounted in Slowfade® Gold antifade reagent (Molecular Probes S369367) while live embryos were mounted in M9 on 2% agarose pads and examined on a WaveFX Spinning Disc Confocal Microscope system (Quorum Technologies, Guelph ON). Images were captured with a Hammamatsu 9100-13 EMCCD digital camera. All sample analysis done on the WaveFX Spinning Disc Confocal Microscope system (Quorum Technologies, Guelph ON) used the following settings: GFP Confocal (Set "Exposure" to "500 ms". Set "Sensitivity" to "150". Set "LMM5 Laser Changer" to "GFP/YFP Laser". Set "LMM5 Transmission 2" to "70").

2.12 Nuclear-cytoplasmic fractionation and Western blotting

The following protocol was adapted and modified from Lichtsteinerl and Tjian, 1995. Embryos were isolated from gravid hermaphrodites by hypochlorite treatment and washed three times with water and 0.05% Triton X-100. 500 μL of packed embryos were resuspended in 3 mL of Sucrose Buffer 0 (0.176 M sucrose, 3 mM $CaCl_2$, 2 mM magnesium acetate, 0.1 mM EDTA, 10 mM Tris-Cl pH 8.0, 0.5% NP-40, 1 mM DTT, protease inhibitor) and homogenized for 30 strokes in a pre-cooled 7 mL Wheaton stainless steel homogenizer with a stainless steel pestle until approximately 80% of the embryos were broken. The embryo breakage and nuclei integrity was monitored by DAPI staining under the Leica DMRA2 upright microscope. 500 μL of the homogenate (total fraction) was removed and kept on ice. The remaining 2.5 mL of homogenate was transferred to a 7 mL glass dounce homogenizer and homogenized with a tight pestle for five

strokes. The homogenate was transferred to a 15 mL falcon tube and centrifuged at 200 x g for 30 sec in a table top centrifuge to pellet unbroken embryos. The supernatant was transferred to a fresh tube and this step was repeated twice to ensure there were no unbroken embryos remaining in the homogenate. 2 mL of Sucrose buffer 2 (2 M sucrose, 3 mM $CaCl_2$, 2 mM magnesium acetate, 0.1 mM EDTA, 10 mM Tris-Cl pH 8.0, 1 mM DTT, protease inhibitor) was added to 2 mL of the homogenate and 1 mL aliquots were layered over 550 μL of Sucrose buffer 2 in 2.2 mL ultracentrifuge tubes (Thermo Fisher Polyclear tubes 45315) for a total of four tubes. Finally, 100 μL of Sucrose Buffer 1 (0.32 M Sucrose, 3 mM $CaCl_2$, 2 mM magnesium acetate, 0.1 mM EDTA, 10 mM Tris-Cl pH 8.0, 0.5% NP-40, 1 mM DTT, protease inhibitor) was layered on top of each tube and the tubes were centrifuged at 30,000 x g at 4˚C for 45 minutes in a Beckman TLS-55 rotor. The supernatant (fraction containing all non-nuclear proteins) was removed and each pellet (nuclear fraction) was resuspended in 1 mL of Sucrose buffer 1 and combined in a 15 mL falcon tube. The nuclear fraction was centrifuged at 800 x g using a swinging bucket rotor in a table top centrifuge. The pellet was then gently washed three times with 10 mL of Sucrose Buffer 1. After the last wash the pellet was resuspended in 250 μL of Sucrose 1 buffer. The protein in the nuclear and cytosolic fractions, as well as the total cell extract, was concentrated by TCA precipitation, and the protein was re-suspended in 2X SDS sample buffer (10% SDS, 80 mM Tris pH 6.8, 12.5% Glycerol, 4% β-mercaptoethanol) without Bromophenol blue. Protein was quantified using the RC DC Protein assay kit (BioRad). For gel electrophoresis and Western blotting equivalent amounts of protein were loaded for all fractions. Primary antibodies used: anti-GAPDH antibody (1:1000) (Sigma G8795), anti-Nuclear Pore Complex antibody (1:500) (Abcam ab24609) and mouse anti-HAM-1 (1:25) (Guenther and Garriga, 1996). Secondary antibody used: goat anti-mouse IgG (H+L) HRP (1:20,000) (Life Technologies 62-6520).

2.12 Large SDS-PAGE and Western blotting

Protein extract from each different *ham-1* mutant strain, *ham-1(n1811), ham-1(gm214), ham-1(gm267), ham-1(gm279)*, *ham-1(cas27), ham-1(cas46), ham-1(cas137)* and *ham-1(ot361)* was extracted as described above. An equal amount of each protein extract was heated at 65°C for 30 minutes prior to loading on a gradient (6%-15%) 18 × 16 cm discontinuous polyacrylamide gel. The gel was run using the Hoeffer SE600 electrophoresis system at constant amperage of 25 mA for 10 hours at 4°C. Following electrophoresis, the gel is incubated in 1X transfer buffer (25 mM Tris, 192 mM glycine) with 20% (v/v) methanol for 30 minutes prior to transfer. The transfer was done using the Amersham Biosciences Transphor unit at constant amperage of 1 A for 1.5 hours at 4°C. After transfer, the membrane was blocked with 5% (w/v) Blotto (skim milk powder in 19 mM Tris, 137 mM NaCl and 0.05% Tween-20) followed by probing of primary antibody overnight at 4°C. Primary antibodies used: rabbit anti-HAM-1 3807 TB (1:100) (Guenther and Garriga, 1996), mouse anti-Actin (1:2500) (EMD Millipore MAB1501). Secondary antibodies used: goat anti-mouse IgG (H+L) HRP (1:20,000) (Life Technologies 62-6520), goat anti-rabbit IgG (whole molecule) HRP (1:20,000) (Sigma Aldrich A0545).

2.13 Bioinformatics analyses

To identify HAM-1 sequence homology, a BLASTP (protein-protein BLAST) (http://blast.ncbi.nlm.nih.gov/Blast.cgi) search was done against the NCBI non-redundant protein database (Altschul et al., 1997). To generate multiple sequence alignments sequences were inputted into Clustal Omega (http://www.ebi.ac.uk/Tools/msa/clustalo/) (Thompson et al., 1994). To detect potential protein domains, HAM-1 amino acid sequence was used as query against the InterPro database (Mulder et al., 2005). HAM-1 amino acid

sequence was inputted into the Eukaryotic Linear Motif server (http://elm.eu.org/) (Puntervoll et al., 2003) to predict short linear motifs.

2.14 Quantification of GFP::HAM-1, GFP::HAM-1(Y369F) and GFP::HAM-1(Y369E).

ImageJ (Abràmoff et al., 2004) program was used to quantify the nuclear, cytoplasmic and membrane signal of GFP::HAM-1, GFP::HAM-1(Y369F) and GFP::HAM-1(Y369E). A 5 pixel by 5 pixel sample area was used to sample the mean grey value of the nucleus and cytoplasm of each cell within an embryo for each strain (n=6 embryos per strain). The nuclear to cytoplasmic ratio was then calculated for cells with a GFP signal in the nucleus in each embryo. To test for differences in the mean nuclear to cytoplasmic ratio among the different strains, a one-way analysis of variance (ANOVA) was done using PAST, a statistical software package (Hammer et al., 2001). PAST was also used to perform a *post hoc* (Tukey test) analysis which compares the mean nuclear to cytoplasmic ratio in each embryo between all strains.

Chapter 3.

Results

3.1 Function and localization analysis of the phospho-null GFP::HAM-1(Y369F)

We wanted to further define regions of HAM-1 that were essential for function. It was previously shown that deletion of the last 50 amino acids of GFP::HAM-1 completely abolished its ability to rescue the loss of PLM neurons in a *ham-1* mutant background (Leung et al., 2014). When the HAM-1 amino acid sequence was inputted into the Eukaryotic Linear Motif bioinformatics program (http://elm.eu.org/), it was predicted that the last 50 amino acids of HAM-1 contains a potentially phosphorylated Tyrosine residue at position 369 (Tyr 369), that is within a predicted SH2 domain binding motif, **YINI** (Figure 1.6). A strong loss of function allele, *ham-1(gm214),* is an in-frame 21 amino acid deletion that also removes Tyr 369. This mutant allele has a penetrance comparable to that of the null allele *ham-1(gm279)* in the HSN/PHB lineage (Frank et al., 2005). This led to the hypothesis that phosphorylation of Tyr 369 is important for the function of HAM-1. To address the biological relevance of Tyr 369, this residue was mutated into phenylalanine in context of a rescuing full length GFP::HAM-1 fusion protein to generate GFP::HAM-1(Y369F). Since phenylalanine has the same structure as tyrosine but lacks a free hydroxyl group, this amino acid substitution will mimic a non-phosphorylated state. The *gfp::ham-1(Y369F)* construct was generated by Tyler Daniels. This construct was then injected into worms containing *zdIs5 (mec-4::GFP)* which expresses GFP in the six touch sensory neurons including the PLM neurons in the tail of the animal. In *zdIs5*

animals, there is a single GFP expressing PLM neuron on each side of the animal while *zdIs5; ham-1(gm279)* animals will lack either one or both PLM neurons (Figure 3.1). Three independent extrachromosomal arrays containing the *gfp::ham-1(Y369F)* construct were generated (*hkEx234*, *235* and *236*). Each array was then crossed into *zdIs5*; *ham-1(gm279)* and scored for the number of PLM neurons.

All three extrachromosomal arrays caused a low penetrance loss of PLMs in a wild type background; *hkEx234* had 2.5% PLM loss (n=120), *hkEx235* had 7.7% PLM loss (n=116) and *hkEx236* had 8% PLM loss (n=124) in a *zdIs5* background. These arrays failed to rescue the 80% loss of PLM neurons observed in *ham-1(gm279)* (n=141); *hkEx234* had 86.7% missing PLMs (n=120), *hkEx235* had 88.4% missing PLMs (n=130), *hkEx236* had 90.0% missing PLMs (n=110) (Figure 3.2). By mutating a single tyrosine residue to phenylalanine, we completely abolished the protein's ability to rescue the loss of PLMs phenotype in *ham-1 (gm279)* mutants. This suggests that phosphorylation of Tyrosine 369 is crucial for the function of HAM-1.

To determine the localization of the GFP::HAM-1(Y369F) fusion, live embryos from transgenic animals were mounted on 2% agarose pad and observed under direct fluorescence using the Leica DMRA2 upright microscope. These embryos were compared to age matched embryos expressing GFP::HAM-1 using the same fluorescence intensity and exposure settings. Following observation, high quality images were taken using a WaveFX Spinning Disc Confocal Microscope system (Quorum Technologies, Guelph ON) and captured with a Hammamatsu 9100-13 EMCCD digital camera. Quantification of the nuclear and cytoplasmic signal of GFP::HAM-1 and GFP::HAM-1(Y369F) was done as described in the material and methods section. We could not directly compare the nuclear, cytoplasmic and membrane signal between GFP::HAM-1, GFP::HAM-1(Y369F) and GFP::HAM-1(Y369E) due to variability in the expression of extrachromosomal arrays.

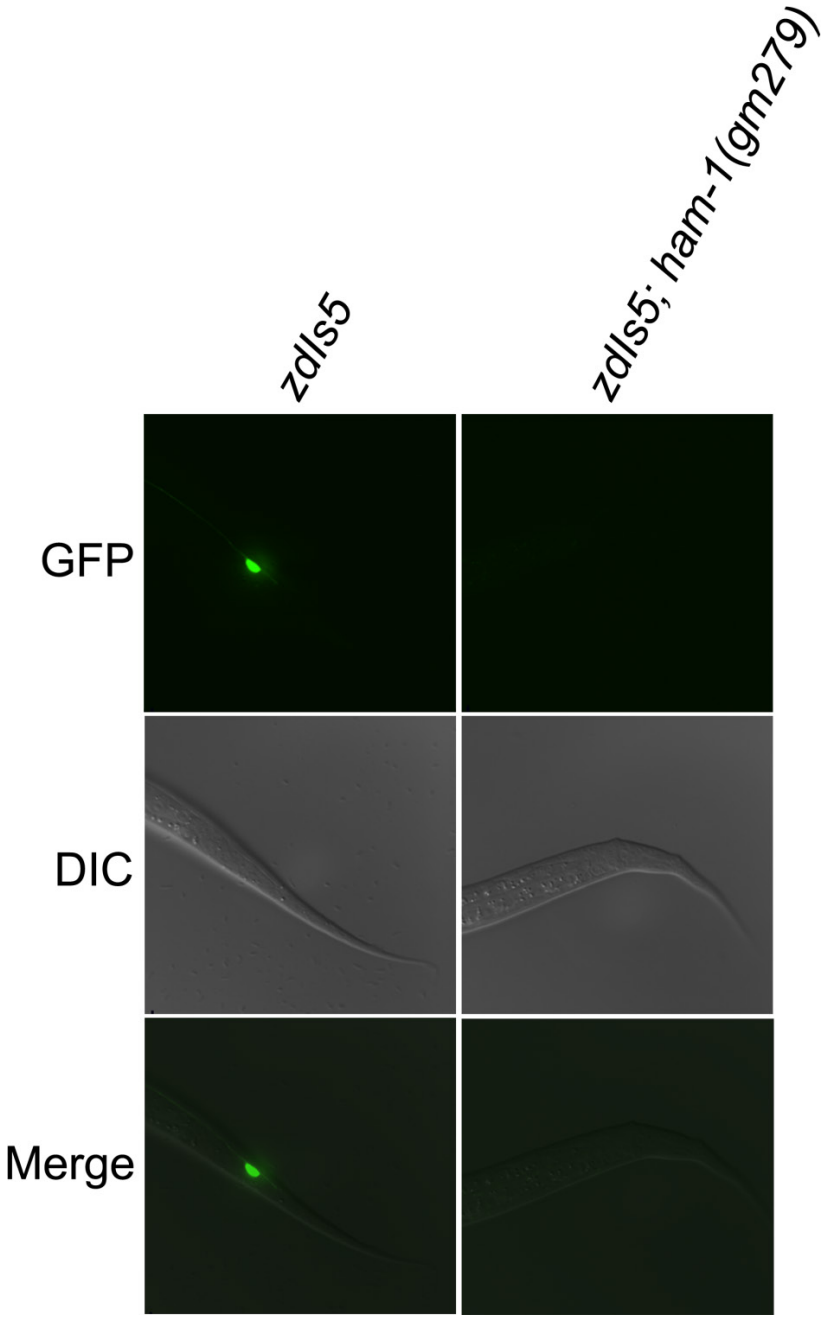

Figure 3.1 Visualization of PLM neurons using the *zdIs5(mec-4::GFP)* reporter.

The integrated *zdIs5(mec-4::GFP) reporter* is expressed in the six touch sensory neurons including the PLM neurons in the tail of the animal. (Left) display a PLM neuron expressing GFP on one side of the animal. (Right) show a loss of PLM neuron in a *ham-1(gm279)* null mutant.

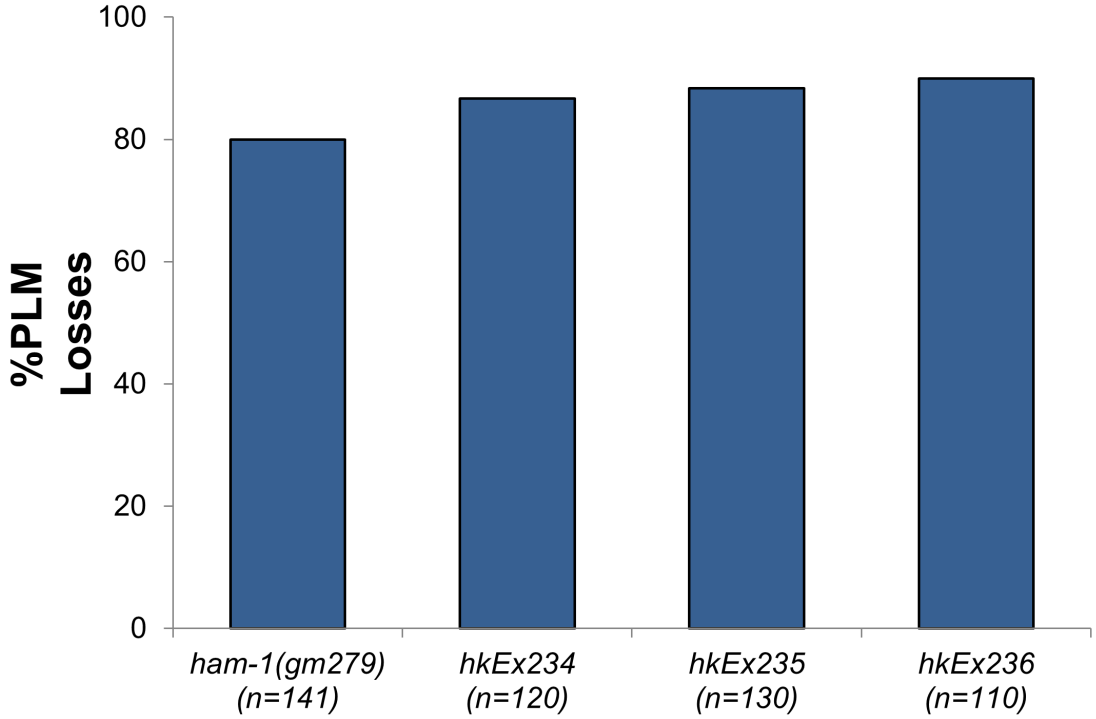

Figure 3.2 GFP::HAM-1(Y369F) is unable to rescue *ham-1(gm279)* PLM defects.

Generated extrachromosomal arrays (*hkEx234*, *235* and *236*) were crossed into *zdIs5*; *ham-1(gm279)* background and scored for the number of PLM neurons. All three arrays were unable to rescue the loss of PLM neurons observed in a *zdIs5*; *ham-1(gm279)* background.

We calculated the nuclear to cytoplasmic ratio in each cell for each strain to normalize the variable expression level. The nuclear to cytoplasmic ratio was able to determine the relative nuclear signal in each cell. Only cells expressing a GFP signal in the nucleus was used to calculate the mean nuclear to cytoplasmic ratio for each embryo in GFP::HAM-1, GFP::HAM-1(Y369F) and GFP::HAM-1(Y369E). Since we could not accurately normalize the membrane signal in each strain, we did not compare the membrane signal between each strain. A one-way ANOVA revealed significant differences among the mean nuclear to cytoplasmic ratio of GFP::HAM-1, GFP::HAM-1(Y369F) and GFP::HAM-1(Y369E) ($F_{2,15}$ = 4.672, P<0.05). A subsequent *post hoc* test showed that there was a significant pairwise difference in the mean nuclear to cytoplasmic ratio between GFP::HAM-1(Y369F) and GFP::HAM-1 (P<0.05, mean Q = 3.683) and between GFP::HAM-1(Y369F) and GFP::HAM-1(Y369E) (P<0.05, mean Q = 3.801). The nuclear signal in GFP::HAM-1(Y369F) was also qualitatively observed to be greater than that of GFP::HAM-1 and GFP::HAM-1(Y369E) (Figure 3.3). The nuclear localization is similar to what was observed in the GFP::HAM-1 C-terminal truncation (GFP::HAM-1_{1-364}) which removes Tyr 369. GFP::HAM-1_{1-364} showed a clear enhancement in nuclear signal as compared to full length GFP::HAM-1 (Leung et al., 2014). Deletion of GFP::HAM-1 further from the C-terminus resulted in complete membrane localization suggesting that the region containing Tyr 369 is responsible for nuclear export rather than membrane localization (Leung et al., 2014). Since the membrane localization appears to be unaffected by this mutation, the increase in nuclear signal suggests a potential role for phosphorylation of Tyr 369 in nuclear export of the protein out of the nucleus.

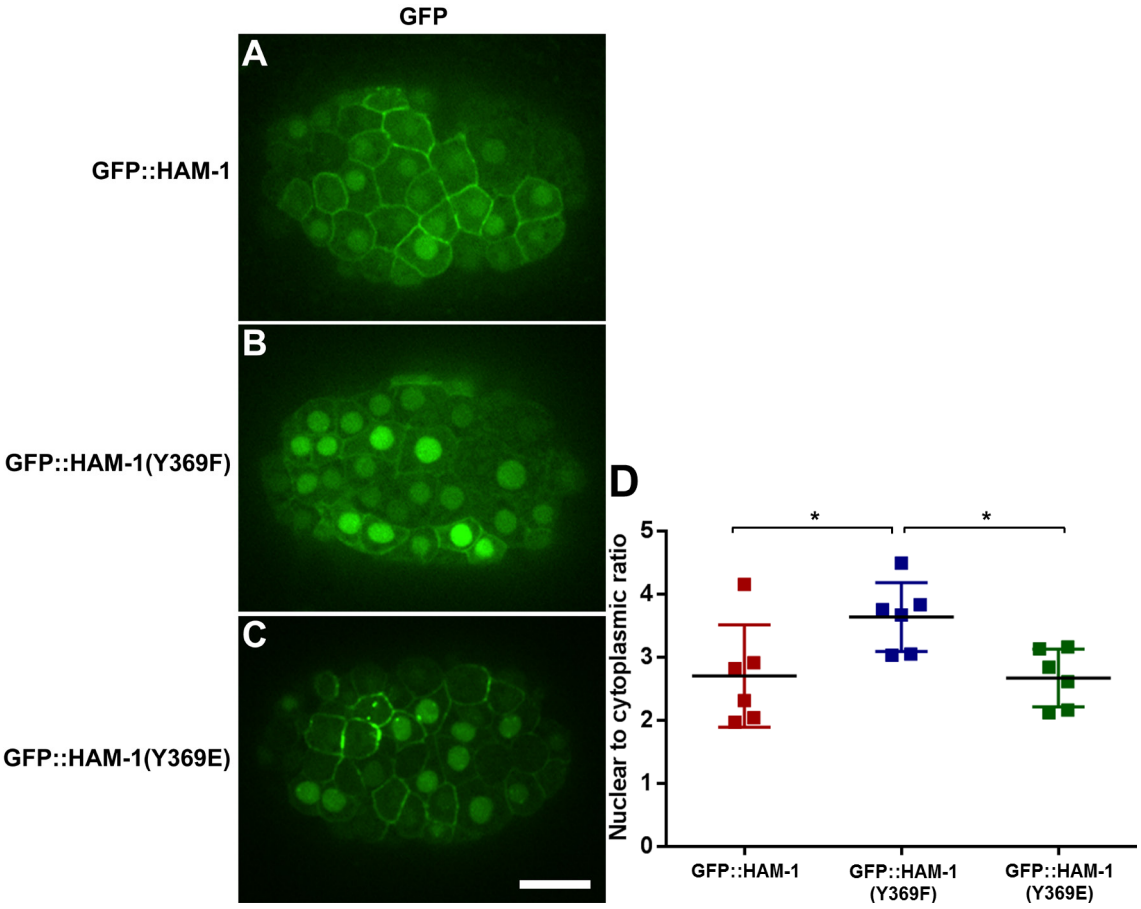

Figure 3.3 Localization of GFP::HAM-1, GFP::HAM-1(Y369F) and GFP::HAM-1(Y369E).

(A) A transgenic embryo expressing GFP::HAM-1 examined directly for GFP fluorescence. **(B)** A transgenic embryo expressing GFP::HAM-1(Y369F) examined directly for GFP fluorescence. **(C)** A transgenic embryo expressing GFP::HAM-1(Y369E) examined directly for GFP fluorescence. Scale bar is 10 μm. **(D)** Quantification of nuclear to cytoplasmic signal ratio in GFP::HAM-1, GFP::HAM-1(Y369F) and GFP::HAM-1(Y369E) (n=6 embryos per strain). Each data point represents the mean nuclear to cytoplasmic ratio of an embryo; the black line represents the mean nuclear to cytoplasmic ratio for each strain. *P<0.05.

3.2 Function and localization analysis of the phospho-mimetic GFP::HAM-1(Y369E)

Due to the inability of GFP::HAM-1(Y369F) to rescue *ham-1(gm279)* PLM defects, we wanted to determine whether the phospho-mimetic could rescue or cause a gain-of-function phenotype. To address this, Tyr 369 was mutated into a glutamic acid in context of full length GFP::HAM-1 to generate GFP::HAM-1(Y369E). The *gfp::ham-1(Y369E)* construct was generated by Ziwei Ding. Glutamic acid is a negatively charged amino acid which should mimic the negative charge of the phosphate group. Similar to the previous experiment, this construct was injected into worms containing *zdIs5*. Two independent extrachromosomal arrays were generated, *hkEx296* and *hkEx297*. Each extrachromosomal array was crossed into a *zdIs5*; *ham-1(gm279)* and scored for the number of PLM neurons. In *zdIs5*, there were weak PLM neuronal losses observed for each of the arrays; *hkEx296* showed 4% PLM loss (n=92) and *hkEx297* showed 7% PLM loss (n=90). Thus, there was no penetrant gain of function phenotype. These arrays failed to rescue the 80% loss of PLM neurons observed in *ham-1(gm279)* (n=141); *hkEx296* showed 86% PLM loss (n=114) and *hkEx297* showed 79% PLM loss (n=128) (Figure 3.4). It was determined that the phospho-mimetic was unable to rescue the *ham-1*(gm279) PLM neuronal loss. We can conclude that Tyr 369 is an essential residue for function. However, we have not unambiguously implicated a role for phosphorylation. It is possible that the ability to undergo both phosphorylation and dephosphorylation is essential for function.

The localization of this protein was also observed through live imaging of transgenic embryos under direct fluorescence using the Leica DMRA2 upright microscope. These embryos were compared to age matched embryos expressing GFP::HAM-1 using the same fluorescence intensity and exposure settings. Following observation, high quality images were taken using a WaveFX Spinning Disc Confocal Microscope system (Quorum Technologies, Guelph ON).

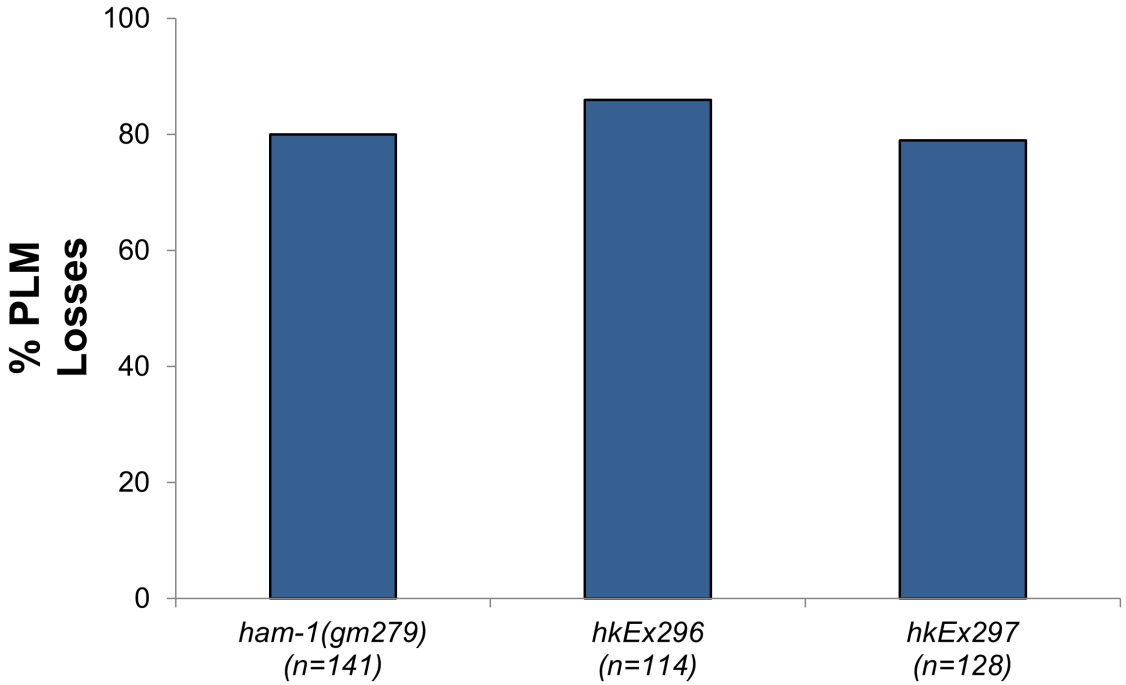

Figure 3.4 GFP::HAM-1(Y369E) is unable to rescue *ham-1(gm279)* PLM defects.

The generated extrachromosomal arrays, *hkEx296* and *297* were crossed into *zdIs5*; *ham-1(gm279)* and scored for the number of PLM neurons. Both arrays were unable to rescue the loss of PLM neurons observed in a *zdIs5; ham-1(gm279)* background.

Quantification of the nuclear and cytoplasmic signal of GFP::HAM-1 and GFP::HAM-1(Y369E) was done as described in the material and methods section. We calculated the nuclear to cytoplasmic ratio as mentioned previously due to the variability in expression levels of extrachromosomal arrays. A one-way ANOVA revealed significant differences among the mean nuclear to cytoplasmic ratio of GFP::HAM-1, GFP::HAM-1(Y369F) and GFP::HAM-1(Y369E) ($F_{2,15}$= 4.672, P<0.05). The *post hoc* test showed that was no significant difference in the mean nuclear to cytoplasmic ratio between GFP::HAM-1(Y369E) and GFP::HAM-1 (P>0.05, mean Q = 0.118). The mean nuclear to cytoplasmic ratio of GFP::HAM-1(Y369E) was significantly less than that of GFP::HAM-1(Y369F) (P<0.05, mean Q = 3.801) (Figure 3.3). It was also qualitatively observed that membrane localization of GFP::HAM-1(Y369E) was similar to that of GFP::HAM-1 (Figure 3.3) which suggests that the negative charge of glutamic acid allowed the protein to localize properly.

3.3 RNAi knockdown of *src-1* tyrosine kinase did not result in loss of PLM neurons

When the HAM-1 amino acid sequence was inputted into a Eukaryotic Linear Motif bioinformatics program, it was predicted that the consensus SH2 domain binding motif **YINI** which encompasses the critical Tyrosine residue 369 interacts with the SRC family of non-receptor tyrosine kinases. In *C. elegans*, there are two members in the SRC family of non-receptor tyrosine kinases, *src-1* and *src-2*. The role of *src-2* during embryonic development is largely unknown. However, *src-1* has been shown to function together with a Wnt signaling pathway to specify endodermal cell fate and division orientation of the EMS blastomere during early embryonic development (Bei et al., 2002). *src-1* also functions in the engulfing cell during cell corpse engulfment during embryonic development (Hsu and Wu, 2010). Due to *src-1* roles in cell fate determination during embryonic development, we hypothesized that *src-1* could be responsible

for regulating HAM-1 activity. Thus, we wanted to determine whether *src-1* mutants display a *ham-1(gm279)* like phenotype in the PLM lineage. Since loss of *src-1* function results in embryonic lethality (Hirose et al., 2003), we could not assay number of PLM neurons in a strong *src-1* mutant background. Therefore the approach was to knockdown *src-1* function in *zdIs5* using RNAi then assay for the number of PLM neurons. However, there was no *src*-1 RNAi clone available in the *C. elegans* genome wide RNAi library. Thus, I had to generate an RNAi construct.

To generate an RNAi construct, the largest exon of *src-1* (exon 5) was amplified through PCR. A 1 kb PCR fragment was subcloned into a L4440 RNAi vector. This construct was then transformed into an RNAse deficient *E. coli* strain (HT115) to knock down *src-1* function via feeding. *zdIs5* worms were then fed *E. coli* carrying the *src-1* RNAi construct for 24, 48 and 72 hours. The number of PLM neurons were scored in the progeny of animals fed with the RNAi bacteria. After 24 hours (n=82), 48 hours (n=74) and 72 hours (n=84) of feeding, there was no loss in PLM neurons (Table 3.1). There was also no lethality observed at any time point during the experiment which is expected if *src-1* function was reduced. Thus, the RNAi appeared to be ineffective at reducing *src-1* function. The experiment was repeated using *zdIs5; rrf-3* worms. *rrf-3* is an RNA-directed RNA polymerase which enhances somatic RNAi.

Table 3.1 Knock down of *src-1* using RNAi by feeding.

		# PLM's/side (%)			
Strains	Timepoint (hours)	0	1	2	N
zdIs5	24	0	100	0	72
	48	0	100	0	84
	72	0	100	0	74
zdIs5; rrf-3	24	0	100	0	76
	48	0	100	0	80
	72	0	100	0	62

Thus, loss of function of *rrf-3* results in a substantial enhancement of sensitivity to RNAi (Simmer et al., 2002). Following 24 hours (n=76), 48 hours (n=80) and 72 hours (n=62) of feeding, there was also no loss of PLM neurons and again no lethality observed (Table 3.1). The lack of lethality observed in a sensitized background, suggests that RNAi knockdown of *src-1* via feeding was ineffective. Therefore, we decided to perform RNAi knockdown of *src-1* by injection of double stranded RNA (dsRNA) because this can be a much more effective method of gene knockdown in *C. elegans*. The *src-1* RNAi construct was *in vitro* transcribed to form single stranded RNA which was then annealed together to generate dsRNA. Complete embryonic lethality was observed when the dsRNA was injected into *zdIs5* worms indicating efficient knock down of *src-1* function. To be able to score the number of PLM neurons, it is necessary to obtain L1 escapers. Therefore we needed to lower the concentration of the dsRNA. There were very few escapers at 1:5, 1:10, 1:25 and 1:50 dilution of the dsRNA. A large number of escapers were observed at a dilution of 1:75, and an even greater amount at 1:90. At 1:75, there was no loss in PLM neurons observed (n=78), and at 1:90 there was also no loss in PLM neurons observed (n=104) (Table 3.2). Therefore, we believe that *src-1* is not involved in the regulation of HAM-1 activity in the lineage that generates PLM neurons. However, it is possible that the degree of knock down was insufficient to generate a phenotype in the PLM lineage.

3.4 A *ptp-2* mutant does not cause a loss of PLM neurons

A *C. elegans* SH2 domain-containing non-receptor protein tyrosine phosphatase PTP-2 was predicted to interact with the consensus SH2 domain binding motif **YINI** of HAM-1 by a Eukaryotic Linear Motif bioinformatics program. *ptp-2* activity is required during development to regulate activity of several signaling pathways (Gutch et al., 1998), and its activity is essential during oogenesis (Yang et al., 2010).

Table 3.2 ***src-1*** **RNAi by microinjection.**

		# PLM's/side (%)			
Strains	dsRNA dilution	0	1	2	N
zdIs5	1:75	0	100	0	78
	1:90	0	100	0	104

We wanted to determine whether *ptp-2* mutants display a *ham-1* mutant phenotype in the PLM lineage. The approach was to cross a *ptp-2*(op194) allele, which is a large deletion allele, into a *zdIs5* background to assay for the number of PLM neurons. While *zdIs5; ham-1(gm279)* have an 80% loss of PLM neurons (n=138) no defects were observed in the *ptp-2*(op194) mutant worms (n=94) (Table 3.3). Thus, mutation in *ptp-2* does not result in a loss of PLM neurons phenotype which suggests that *ptp-2* is not involved in the regulation of HAM-1 activity in the lineage that generates PLM neurons.

3.5 Endogenous HAM-1 is primarily localized to the nucleus

It has been shown that HAM-1 is an asymmetrically localized protein. When embryos are fixed and immunostained with α-HAM-1 antibody, it was observed that HAM-1 is localized to the posterior cortex in dividing cells (Frank et al., 2005). Surprisingly, HAM-1 contains a winged-helix domain and two nuclear localization sequences (Leung et al., 2014). The winged-helix domain is found in core components of transcription systems of eukaryotes and this domain has been shown to participate in establishing protein-DNA interactions (Teichmann et al., 2012). This suggests a putative DNA binding role for HAM-1. Consistent with this, it was observed that under direct fluorescence a GFP::HAM-1 fusion protein was localized to both the cell cortex and the nucleus (Leung et al., 2014). This indicates that endogenous HAM-1 could potentially be localized in the nucleus. However, we have never been able to detect HAM-1 within the nucleus through antibody staining of fixed embryos. Thus, we wanted to determine whether endogenous HAM-1 is indeed localized in the nucleus. The approach was to perform a subcellular fractionation experiment to isolate a nuclear and cytoplasmic fraction. Protein isolated from each fraction could then be analyzed by Western blotting. If endogenous HAM-1 is located in the nucleus, we would detect HAM-1 in the nuclear fraction through Western blotting analysis.

Table 3.3 PLM neuron in *ptp-2(op194)* mutants.

	# PLM's/side (%)			
Strains	0	1	2	N
zdIs5	0	100	0	126
zdIs5; ham-1(gm279)	80	20	0	138
zdIs5; ptp-2(op194)	0	100	0	94

To isolate nuclei, a subcellular fractionation was done using a sucrose gradient. Synchronized worm cultures were collected for large scale embryo isolation. Approximately 500 μL of embryos was isolated and homogenized. A metal dounce homogenizer was critical in breaking open the chitinous egg shell of *C. elegans* embryos without damaging the nuclei. The effectiveness of the metal dounce homogenizer in the mechanical breakage of the embryos was demonstrated by Lichtsteinerl and Tjian, 1995. The embryo breakage and nuclei integrity was monitored by DAPI staining under the microscope. Homogenization was stopped once approximately 80% of the embryos were broken. The lysate was layered over a 2 M sucrose cushion and centrifuged. The supernatant containing everything that is not the nuclei was removed from the nuclei pellet and kept as cytoplasmic fraction. The nuclei pellet was washed five times to remove cytoplasmic contamination. Then the total, cytoplasmic and nuclear fractions were concentrated by Trichloroacetic acid (TCA) precipitation. The total extract will contain all proteins, the nuclear extract will contain only nuclear proteins and the cytoplasmic extract will contain all non-nuclear proteins including cortical proteins. To insure equal loading, each fraction was quantified. Initially for protein quantification, the BioRad DC compatible protein quantification kit used was compatible with detergents but not compatible with β-mercaptoethanol (BME) in the 2X SDS sample buffer. Thus, we had to leave BME out of the SDS sample buffer prior to quantification. However, without BME the protein sample would not fully resuspend in the sample buffer. This led to improper quantification and uneven loading of samples from each fraction. To overcome this issue, we switched to the BioRad RC DC quantification kit which is compatible with both detergents and reducing agents. This allowed us to fully resuspend our protein sample prior to quantification and insure equal loading. 50 μg of protein from the total extract, nuclear extract and cytoplasmic extract was ran on a 10% SDS-PAGE gel followed by Western blot analysis.

From the Western blot analysis we were able to determine that the nuclear fractionation was successful as there was no cytoplasmic contamination in the

nuclear fraction. The cytoplasmic control GAPDH was present in the total extract and the cytoplasmic fraction as a single band at 37 kDa on the Western blot, but not in the nuclear fraction. The nuclear control Nuclear Pore Complex (NPC) was present in the total extract and nuclear fraction as two bands at 95 kDa and 110 kDa. There was a very small amount of nuclear contamination of NPC in the cytoplasmic fraction as can be seen by a faint band at 95 kDa for NPC in the cytoplasmic fraction. At a short exposure, HAM-1 was observed only in the total extract and the nuclear fraction as a band at 55 kDa on the Western blot, but HAM-1 was observed in the cytoplasmic fraction after a longer exposure of the blot (Figure 3.5). HAM-1 was much more abundant in the nuclear than the cytoplasmic fraction which is consistent with the intense nuclear GFP::HAM-1 signal observed by direct fluorescence microscopy of transgenic embryos. This suggests that HAM-1 is primarily a nuclear protein. Since HAM-1 contains a putative DNA binding domain and two nuclear localization sequences (Leung et al., 2014), it could potentially have a role within the nucleus for the regulation of asymmetric neuroblast division. However, the role of HAM-1 in the nucleus remains unknown.

3.6 Further identifying residues required for membrane localization

To further investigate regions of HAM-1 responsible for proper localization, we decided to examine HAM-1 localization by immunostaining fixed embryos from different *ham-1* mutant strains. *ham-1(n1811)*, a point mutant at the N-terminus which mutates Glycine 47 to Aspartic acid (Figure 3.6), has been shown to disrupt the cortical localization of HAM-1. The protein was observed to be distributed throughout the cytoplasm rather than localizing to the cell cortex (Frank et al., 2005). However, *ham-1(gm214)* an internal 21 amino acid deletion, and *ham-1(gm267)* which mutates Glycine 58 to Arginine (Figure 3.6), does not affect the cortical localization of HAM-1 (Frank et al., 2005).

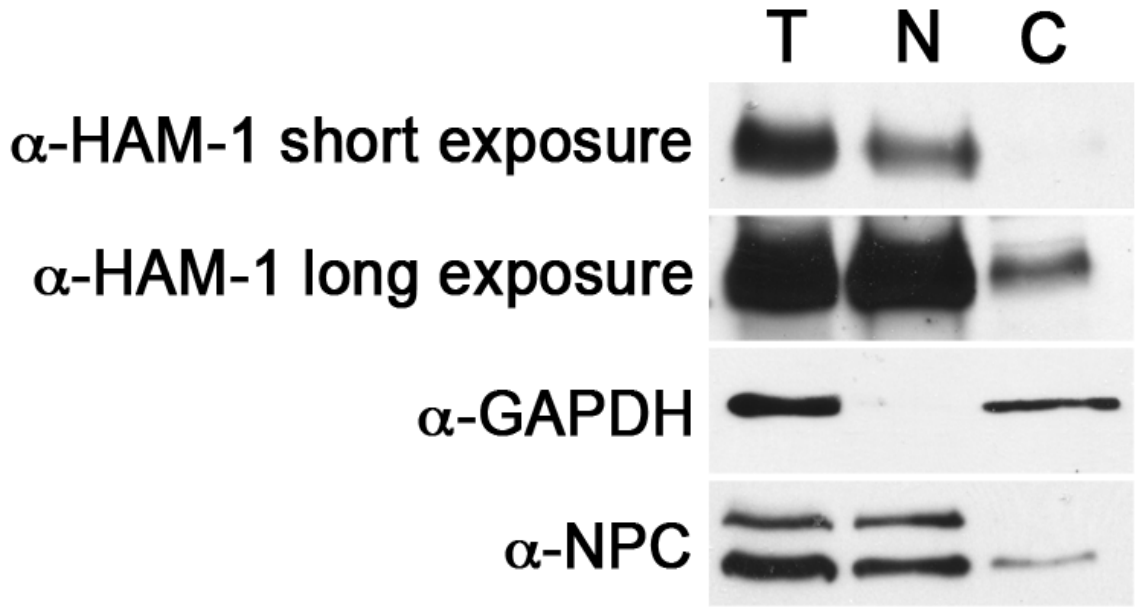

Figure 3.5 Western blot analysis of HAM-1 subcellular distribution.

Total extract (T), nuclear extract (N) and cytoplasmic extract (C) were obtained from wild-type embryos via glucose gradient subcellular fractionation. Western blot analysis was performed using 50 μg of protein from total, nuclear and cytoplasmic extracts. As shown, blots were probed for HAM-1, the cytoplasmic marker GAPDH and the nuclear marker NPC. Blots were exposed to film for a short exposure and a long exposure.

However, there are several mutants isolated subsequently that had not been analyzed by whole mount immunostaining.

ham-1(cas27), ham-1(cas46) and ham-1(cas137) (Figure 3.6) are *ham-1* alleles recently isolated from an ethyl methanesulfonate (EMS) mutagenesis screen done looking for defects in the Q cell lineage (Feng et al., 2013). These mutant alleles cause an extra AQR or PQR mutant phenotype due to an asymmetric division defect of Q.a. *ham-1(ot361)* (Figure 3.6) is a point mutant which was isolated in an EMS screen for defects in dopaminergic neuron specification (Doitsidou et al., 2008). Embryos from each of these mutants were fixed and stained with α-HAM-1 antibodies followed by examination under the Leica DMRA2 upright microscope. Mutant embryos (n=40) were examined and compared with age matched wild-type embryos (n=40). Representative high quality images were taken of immunostained embryos from each mutant (n=15) using a WaveFX Spinning Disc Confocal Microscope system (Quorum Technologies, Guelph ON).

In *ham-1(cas27),* which mutates Glycine 10 to Arginine, HAM-1 was completely delocalized from the membrane and distributed throughout the cytoplasm (Figure 3.7D). The same Glycine residue is changed in *ham-1(cas137)*, but it is mutated to Glutamic acid instead. It was observed that the levels of HAM-1 were greatly decreased as compared to wild type, but HAM-1 was still able to form asymmetric crescents at the cell cortex (Figure 3.7J). In *ham-1(cas46)*, the C-terminus of HAM-1 is truncated by 33 amino acids which caused partial delocalization from the cortex. HAM-1 signal could be observed at the membrane and throughout the cytoplasm (Figure 3.7G). In *ham-1(ot361)* which mutates Glycine 58 to Alanine, HAM-1 is cytoplasmic with membrane localization detected in only a subset of cells (Figure 3.7M). This data suggests that there are sequences within the N-terminus and C-terminus of HAM-1 which is responsible for proper localization of the protein during embryogenesis.

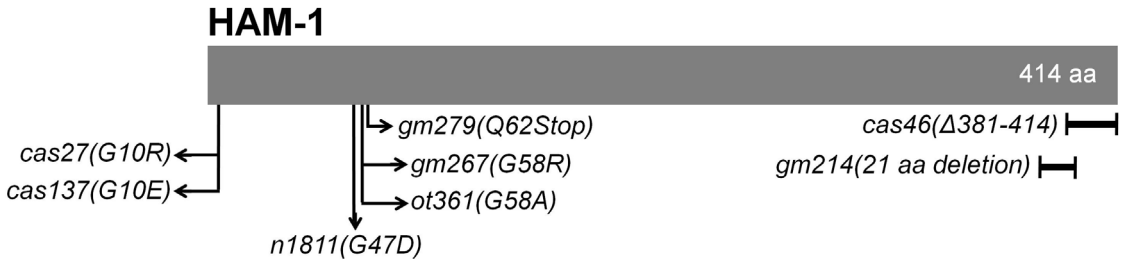

Figure 3.6 Schematic of various *ham-1* mutant alleles.

The grey bar represents the full length 414 amino acid (aa) protein. The position of point mutation alleles with the corresponding amino acid change is shown by the arrows. The location of the deletion alleles are shown by the black bars.

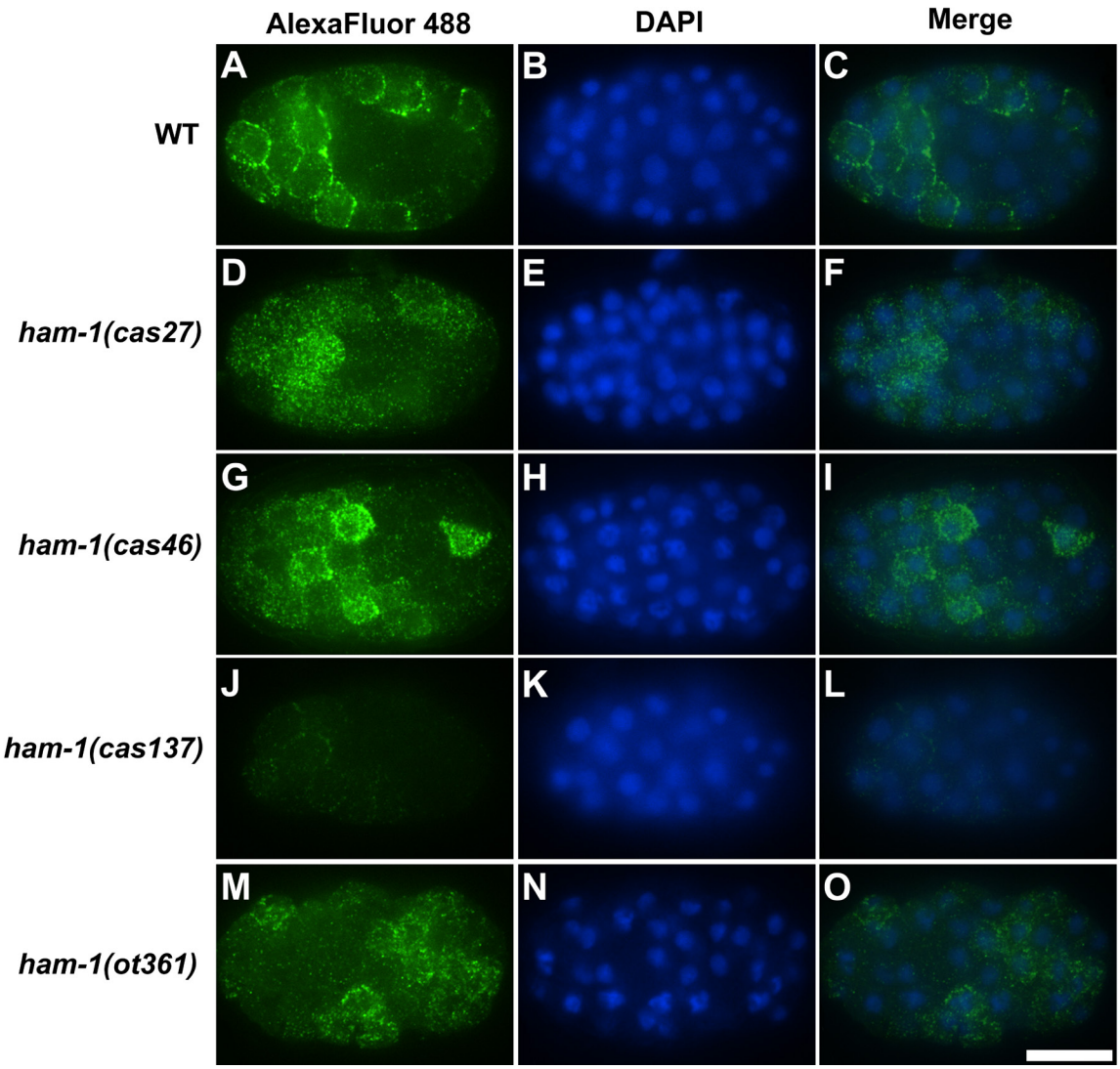

Figure 3.7 Localization of HAM-1 in wild type and *ham-1* mutant embryos.

Images of embryos stained with anti-HAM-1 antibodies (A,D,G,J,M), the corresponding DAPI staining to detect DNA (B,E,H,K,N) and the HAM-1/DAPI merge (C,F,I,L,O). (A) In wild type embryos, HAM-1 is at the cell cortex of many cells and forms an asymmetric cresent in mitotic cells. (D) In *ham-1(cas27),* HAM-1 is delocalized from the cell cortex and is distributed throughout the cytoplasm. (G) *In ham-1(cas46),* HAM-1 is partially delocalized from the membrane. (J) In *ham-1(cas137),* the signal of HAM-1 is very weak compared to wild type. However, HAM-1 was still able to form the asymmetric crescent at the cell cortex similar to wild type. (M*)* In *ham-1(ot361),* HAM-1 is cytoplasmic with membrane localization in only a subset of cells. Scale bar is 10 µm.

3.7 Identifying residues required for the closely migrating doublet observed on Western blot

HAM-1 encodes a 414 amino acid protein with a predicted molecular weight of 46.2 kDa but by Western blot analysis gel HAM-1 runs as a closely migrating doublet at 55 kDa (Figure 3.8A) (Frank et al., 2005). Since HAM-1 does not have alternate splice forms, the shift in size and the closely migrating doublet could be due to post translational modifications. To identify sequences responsible the closely migrating doublet observed on a Western blot, we analyzed existing point mutation and deletion mutant alleles of *ham-1* available by Western blotting.

The HAM-1 doublet is difficult to resolve as two distinct bands on a mini SDS-PAGE gel. Thus, to be able to separate the closely migrating doublet, samples need to be run on a large 18 × 16 cm discontinuous polyacrylamide gel using the Hoeffer SE600 electrophoresis system. However, it was very difficult to detect a sharp doublet on a Western blot. Initially samples were run on a 10% polyacrylamide gel followed by Western blot analysis and the resulting bands detected were extremely diffuse. To address this issue, troubleshooting was done on many parameters such as electrophoresis conditions, transfer conditions, protein preparation and amount of protein loaded. To reduce diffusion of protein and increase the separation between bands, we switched from a 10% polyacrylamide gel to a 6%-15% gradient gel with 2 M Urea. To ensure complete denaturation of the proteins, 4 M Urea was also added to each sample prior to heating. Heating of sample in boiling water for 10 minutes prior to gel electrophoresis did not yield a doublet that we were looking for. We tried different sample heating conditions by altering the temperature and the length of heating. It was determined that heating each protein sample at 65°C for 30 minutes prior to electrophoresis allowed us to detect the closely migrating doublet. The use of a gradient gel sharpened the bands and increased separation between bands but did not completely eliminate the diffusion problem.

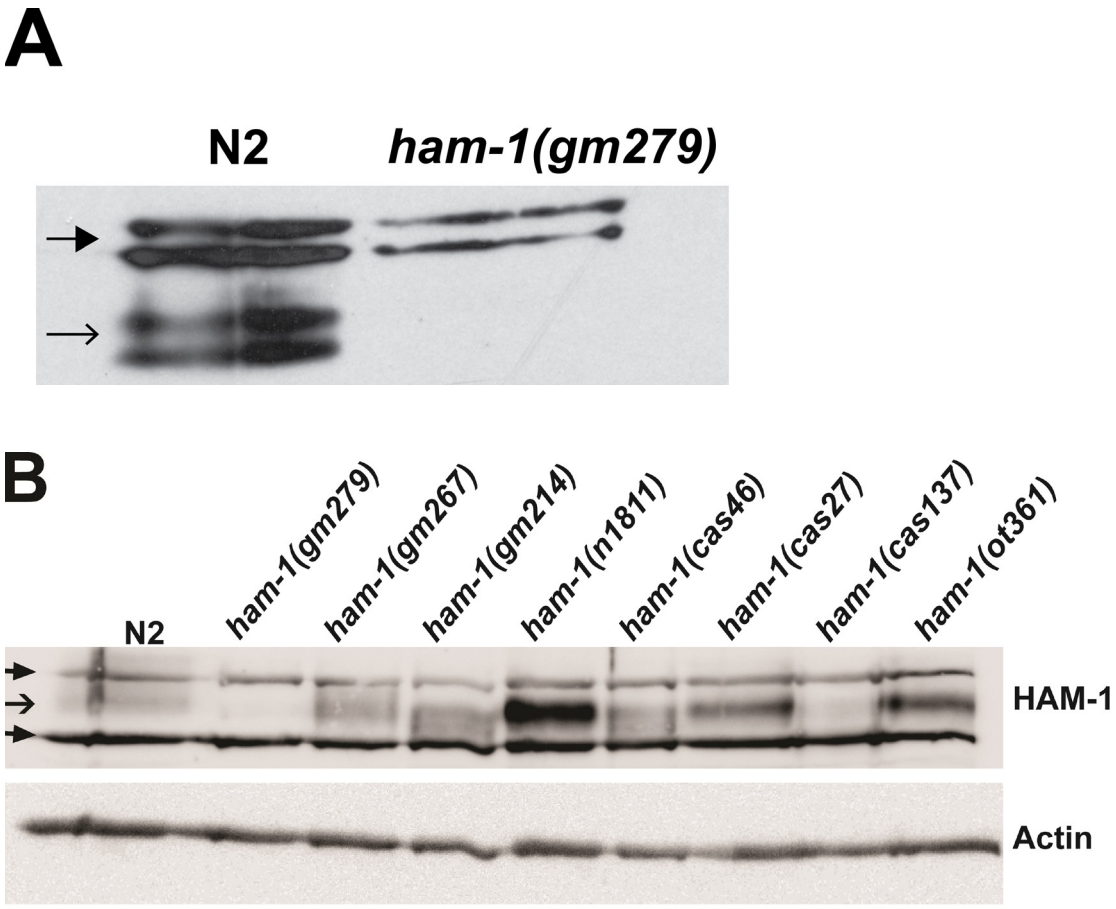

Figure 3.8 Western blot analysis of various *ham-1* mutant alleles.

(A) Western blot of N2 and *ham-1(gm279)* protein extract probed with anti-HAM-1 antibody obtained from Nancy Hawkins. The bands corresponding to HAM-1 are indicated by the open arrow and the closed arrows indicate the non-specific cross reacting bands. **(B)** Equal amount of protein extract isolated from wild-type N2 and each *ham-1* mutant strain was loaded on a 6%-15% gradient gel with 2 M Urea. Following gel electrophoresis and transfer, the blot was probed for HAM-1 and actin as a loading control. The bands corresponding to HAM-1 are indicated by the open arrow and the closed arrows indicate the non-specific cross reacting bands.

Incubation of the gel in 1X transfer buffer with 20% (v/v) methanol for 30 minutes allowed the gel to preshrink prior to transfer which helps prevent the appearance of diffused protein bands.

Protein extract was isolated from wild-type N2 and each *ham-1* mutant strain, *ham-1(n1811), ham-1(gm214), ham-1(gm267), ham-1(gm279)*, *ham-1(cas27), ham-1(cas46), ham-1(cas137)* and *ham1(ot361)* in the presence of 4 M Urea. Equal amount of each protein extract was loaded on a 6%-15% gradient gel with 2 M Urea and ran at constant amperage. Following gel electrophoresis, the gel was incubated in 1X transfer buffer with 20% (v/v) methanol for 30 minutes prior to transfer. After transfer and blocking, the blot was probed with anti-HAM-1 antibodies and anti-actin antibodies as a loading control.

The bands corresponding to HAM-1 in each lane are indicated by the open arrow, while the closed arrows indicate non-specific cross reacting bands of the anti-HAM-1 antibody. The closely migrating cross reacting and actin loading control bands are very sharp but the bands corresponding to HAM-1 appear to be more diffuse. The HAM-1 bands in the wild-type N2 lane are diffuse and are extremely close to each other, however, the closely migrating doublet could be better observed in the *ham-1(gm267)*, *ham-1(gm214)* and *ham-1(cas46)* lanes (Figure 3.8B). In *ham-1(gm214)* and *ham-1(cas46),* the HAM-1 doublet bands are shifted downwards which corresponds with a smaller size since both these mutations are 21 amino acids and 33 amino acids respectively. In *ham-1(gm267)* which mutates Glycine 58 to Arginine, the closely migrating doublet was present at the expected size of wild-type HAM-1 at 55 kDa (Figure 3.8B).

The point mutation of Glycine 47 to Aspartic acid in *ham-1(n1811)* however resulted in only a single band with much higher intensity than all of the other samples (Figure 3.8B) even though the amount of protein loaded was the same for each sample. Point mutations in other mutant alleles such as *ham-1(cas27)* and *ham-1(ot361)* also results in the collapse of the doublet into a single band (Figure 3.8B). This suggests that these particular residues could be part of a recognition sequence for post translational modification that would lead

to a doublet observed on a Western blot. Post translational modifications such as phosphorylation, acetylation, palmitoylation, N-myristylation or glycation would cause proteins to run as a doublet on a Western blot. Alternatively, cleavage of HAM-1 would result in two forms of HAM-1 and appear as a doublet on a Western blot. In *ham-1(cas137),* the HAM-1 protein is extremely low as compared to all the other lanes which suggest that the mutation of Glycine 10 to Glutamic acid results in destabilization of the protein consistent with the observed immunostaining data (Figure 3.7J). It was observed that point mutations which affect the closely migrating doublet are clustered within the N-terminus of HAM-1.

Chapter 4.

Discussion

4.1 A potential nuclear role for HAM-1

HAM-1 was initially characterized as an asymmetrically distributed intrinsic factor required for asymmetric division of neuroblasts. Through immunostaining of fixed wild type embryos, HAM-1 was asymmetrically localized as crescents at the posterior cortex of dividing cells (Figure 1.9) (Frank et al., 2005; Guenther and Garriga, 1996). However, the mechanism of how HAM-1 functions in the regulation of asymmetric cell division remains unknown. Work done by Leung et al., 2014 has shown that HAM-1 contains a putative DNA binding winged-helix domain as well as two nuclear localization sequences which was inconsistent with the original immunostaining data. In embryos expressing GFP::HAM-1, this fusion protein was localized to the cell cortex by antibody staining with either α-HAM-1 or α-GFP antibodies (Figure 1.10A) and no nuclear localization was detected. However, when live embryos expressing GFP::HAM-1 were directly visualized by fluorescence microscopy the fusion protein was observed within the nucleus and at the cell cortex (Figure 1.10B). This suggests that endogenous HAM-1 could also be localized within the nucleus. The inability to detect endogenous HAM-1 within the nucleus by antibody staining suggests that the epitopes are masked. Potentially, the protein is inaccessible to antibodies due to its association with chromatin.

Although GFP::HAM-1 is localized in the nucleus, the expression is from an integrated extrachromosomal array and the level of expression is substantially higher than endogenous HAM-1. Therefore the nuclear localization observed

could be an artifact of overexpression. However, this does not explain why GFP::HAM-1 cannot be detected in the nucleus by antibody staining. To determine whether endogenous HAM-1 is localized to the nucleus, we performed a subcellular fractionation followed Western blotting. A key step which required optimization was the breaking of the chitinous egg shell of *C. elegans* embryos while maintaining the integrity of nuclei. The second key step was ensuring accurate quantification of extracts from each subcellular fraction. Following various troubleshooting parameters, we had to switch from a BioRad DC compatible protein quantification kit to a BioRad RC DC quantification kit which is compatible with both detergents and reducing agents to obtain an accurate quantification of extracts from each subcellular fraction. I have confirmed that endogenous HAM-1 is localized within the nucleus and the protein level of endogenous HAM-1 was also much greater within the nuclear than the cytoplasmic fraction. The Western data is consistent with the GFP::HAM-1 fluorescence intensities observed under direct fluorescence. The presence of HAM-1 within the nucleus suggests that HAM-1 could have a functional role within the nucleus.

The C-terminus of HAM-1 contains two functional nuclear localization sequences (NLS). While mutation of either sequence individually has little effect on nuclear localization of GFP::HAM-1, mutation of both sequences abolished its nuclear localization. It was recently discovered that the GFP::HAM-1 double NLS mutant was able to completely rescue the *ham-1* PLM neuronal losses (Leung et al., 2014). There are two interpretations for this result: either nuclear HAM-1 has no role in the asymmetric cell division in the PLM lineage or there are still low undetectable levels of nuclear GFP::HAM-1 that is sufficient for function.

The requirement for the putative DNA binding winged-helix domain was also examined. A GFP::HAM-1 fusion protein lacking the winged-helix domain (Δ90-180) was still able to weakly rescue the *ham-1* PLM neuronal losses (Leung et al., 2014). Together, these data suggests that DNA binding is at least partially dispensable for HAM-1 function in the PLM lineage. Although it appears that a

DNA binding function for HAM-1 is not required for regulating the PLM lineage, we cannot rule out the importance of a nuclear role and potential DNA binding role in other lineages.

The asymmetric membrane localization of HAM-1 could be a mechanism to distribute HAM-1 between the two daughter cells. In the daughter cell HAM-1 could translocate to the nucleus to activate transcription of target genes. Time-lapsed direct fluorescence data of a C-terminal HAM-1::GFP fusion protein from Feng et al. 2013 showed that HAM-1::GFP was restricted to interphase nuclei and evenly distributed in dividing Q.a. and Q.p. cells. The dynamic distribution of HAM-1::GFP suggests that HAM-1 could function as a transcription factor in Q cell divisions (Feng et al., 2013). A potential target of HAM-1 is a member of the conserved PAR- 1/Kin1/SAD-1 family of serine/threonine kinases that regulate polarity and asymmetric cell division, PIG-1 (Cordes et al., 2006; Feng et al., 2013). ChIP-seq data from the modENCODE constortium (www.modencode.org) provided evidence that HAM-1::GFP may bind to the promoter of a ser/thr kinase *pig-1* (-266 to -42 bp) (Feng et al., 2013). The inhibition of *pig-1* phenocopied the *ham-1* extra neuron phenotype in the Q.a cell (Feng et al., 2013). It is possible that HAM-1 is regulating the asymmetric division of Q cells by regulating the expression of PIG-1.

A protein with similar localization pattern to HAM-1 is the *Drosophila* transcription factor Prospero. As mentioned previously, Prospero is a key cell fate determinant that is tethered to the basal cortex of the mitotic neuroblast by Miranda. Following division, Prospero is inherited by the basal daughter cell. In the basal daughter cell, Prospero dissociates from Miranda and translocate into the nucleus where it can specify the ganglion mother cell fate (reviewed in Knoblich, 2008). Unlike Prospero however, HAM-1 does not function as a direct cell fate determinant in the HSN/PHB lineage (Guenther and Garriga, 1996). It is the daughter anterior daughter which does not inherit HAM-1 that is affected (Frank et al., 2005).

Another example of a protein with both membrane localization as well as nuclear localization is Notch. Notch is a single-pass transmembrane receptor which is responsible for regulating many cellular processes such as cell fate specification, differentiation and proliferation (Artavanis-Tsakonas, 1999). Studies have shown that there is a duality in the function of Notch. It seems that Notch could function as a ligand-binding receptor as well as a modulator of gene expression (Lieber et al., 1993). Notch signalling is regulated by a proteolytic cascade. The initial proteolytic cleavage is done by Furin to generate a receptor capable of binding ligand (Logeat et al., 1998). The binding of Notch with its ligands Delta and Jagged/Serrate proteins induce a series of proteolytic events leading to the cleavage of the intracellular domain of Notch. This releases the cytoplasmic domain of Notch from the plasma membrane. The cytoplasmic domain could then translocate into the nucleus to act as a transcriptional activator of Notch-responsive genes (reviewed in Weinmaster, 2000). Similar to Notch, HAM-1 could potentially carry a dual role. Non-nuclear HAM-1 could function to position the cleavage plane as observed in the HSN/PHB lineage (Frank et al., 2005). In addition, HAM-1 could also be post-translationally modified to allow for its nuclear translocation like Notch where it could then activate transcription of responsive genes.

4.2 The N-terminus and the C-terminus of HAM-1 are required for membrane localization

Leung et al., 2014 previously identified regions of HAM-1 required for cortical localization through a series of N- and C- terminal deletions of GFP::HAM-1. Examination of the N-terminal truncations revealed that the N-terminus is required for cortical localization. Deletion of the first 32 amino acids (GFP::HAM-$1_{32\text{-}414}$) or 114 amino acids (GFP::HAM-$1_{114\text{-}414}$) almost completely eliminated membrane association. These fusion proteins were detected in both the cytoplasm and nucleus with weak membrane association in only a few cells

(Leung et al., 2014). This suggests that the N-terminus of HAM-1 contain sequences that are required for proper cortical localization.

Deletion of the C-terminus also revealed regions of the protein necessary for cortical association. Deletion of the last 50 amino acids from the C-terminus (GFP::HAM-1_{1-364}) resulted in a clear reduction of cortically localized protein and an enhancement in nuclear expression (Leung et al., 2014). However, deletion of GFP::HAM-1 further by 96 amino acids (HAM-1_{1-268}) eliminated nuclear localization and the protein was exclusively at the membrane (Leung et al., 2014). Together, the data suggest that the last 50 amino acids of HAM-1 contain sequences responsible for nuclear export rather than membrane association. Further analysis of the C-terminus revealed a region between amino acids 190 and 268 required for membrane association. This region contains a putative proline rich SH3 binding motifs located between amino acids 251 and 261 which could be responsible for the membrane association. In addition to the N-terminus, a region between amino acids 190 and 268 is also required for cortical localization of HAM-1 (Leung et al., 2014).

To further assess sequences of HAM-1 required for membrane localization, embryos from several *ham-1* mutants (*ham-1(cas27)*, *ham-1(cas46), ham-1(cas137) and ham-1(ot361)*) were fixed and stained with α-HAM-1 antibodies. HAM-1 was observed to be delocalized from the membrane in several of the *ham-1* mutants. Consistent with the importance of the N-terminus shown by Leung et al., 2014, our analysis showed that amino acid 10 is a key residue in cortical localization. There was complete delocalization of HAM-1 from the cell cortex caused by the mutation of Glycine 10 to Arginine in *ham-1(cas27)* which could be due to a change in the tertiary structure of the protein. The change from a small neutral amino acid to a larger positively charged amino acid is a drastic change which may alter the folding of the protein. However, the result is different if Glycine 10 was mutated to Glutamic acid, a negatively charged amino acid. In *ham-1(cas137)*, the mutation of Glycine 10 to Glutamic acid had minor effects on the cortical localization of HAM-1. HAM-1 was

observed to be at the cortex but the level of HAM-1 detected was significantly reduced compared to *ham-1(cas27)* and wild type. The very low signal observed could be due to the mutation causing an accumulation of HAM-1 within the nucleus which we cannot detect through immunostaining of embryos. Alternatively, the low levels of HAM-1 detected could be due to the mutation affecting the stability of the protein leading to degradation. The stability of HAM-1 was affected as indicated by the low undetectable protein levels by Western blot analysis (Figure 3.8). Although HAM-1 was able to localize to the cell cortex, the Q cell defect caused by *ham-1(cas137)* could be due to the extremely low amount of protein.

In *ham-1(ot361)* which mutates Glycine 58 to Alanine, HAM-1 is cytoplasmic with membrane localization in only a subset of cells. Although the change from Glycine to Alanine is a conservative change, the folding of the protein might be affected or this mutation could disrupt a potential post translational modification recognition sequence. Through domain prediction programs such as Interpro (http://www.ebi.ac.uk/interpro/) or Eukaryotic Linear Motifs (http://elm.eu.org/), HAM-1 does not contain any recognizable post translational recognition sequences required for membrane association at the N-terminus such as Pleckstrin Homology (PH) domain or N-myristylation sequences. However, we cannot rule out the possibility that HAM-1 might contain a less conserved recognition sequence for lipidation within the N-terminus which would allow for membrane association.

In *ham-1(cas46)*, a 33 amino acid truncation at the C-terminus of HAM-1 caused partial delocalization of the protein from the membrane. HAM-1 was localized to the cytoplasm with some membrane association in a subset of cells. This is consistent with the decrease in membrane localization observed in a 50 amino acids truncation of GFP::HAM-1 (Leung et al., 2014). However, there is evidence which suggests that the last 50 amino acids of HAM-1 contain sequences responsible for nuclear export rather than membrane association (Leung et al., 2014). The delocalization observed could be due to HAM-1 being

confined within the nucleus. Alternatively, the delocalization observed could be due to a change the structure of HAM-1 which decreases membrane association. It is uncertain at this point which type of post-translational modifications if there is any at the N-terminus and C-terminus that contributes to the membrane localization of HAM-1.

4.3 Residues within the N-terminus of HAM-1 contribute to the closely migrating doublet observed on a Western blot

Previous studies have shown that HAM-1 runs as a closely migrating doublet at a larger molecular weight than its predicted molecular weight on a Western blot (Figure 3.8A) (Frank et al., 2005). It is possible that the doublet is the result of multiple isoforms of HAM-1, but there has been no evidence for multiple splice forms of HAM-1 from RNAseq data available from wormbase (www.wormbase.org). The doublet and shift in molecular weight could be due to post translational modifications of HAM-1. Post translational modifications such as phosphorylation, acetylation, palmitoylation, N-myristylation or glycation could increase the size of proteins and cause proteins to run as a doublet on a Western blot. Alternatively, cleavage of HAM-1 would result in two forms of HAM-1 and appear as a doublet on a Western blot. There could be post translational modifications which contribute to membrane association that cause the doublet observed on a Western blot. Thus, we hypothesized that there is a correlation between the closely migrating doublet and proper membrane localization.

The approach was to extract protein from existing point mutation and deletion *ham-1* deletion alleles followed by Western blot analysis to identify residues required for the closely migrating doublet. To resolve the closely migrating doublet, samples need to be run on a large 18 × 16 cm discontinuous polyacrylamide gel. A great deal of optimization and troubleshooting was required for this experiment because HAM-1 appears to be very diffuse on a Western blot as compared to controls such as actin. Thus, it was very difficult to

clearly resolve the closely migrating doublet. It was necessary to treat samples with Urea to fully denature proteins and use a gradient polyacrylamide gel to increase the separation of protein bands. Although HAM-1 did not appear as clear sharp bands, a closely migrating double could still be detected in several samples (Figure 3.8B). The point mutation in *ham-1(gm267),* the deletions in *ham-1(gm214)* and *ham-1(cas46)* did not affect the closely migrating doublet. *ham-1(gm267)* and *ham-1(gm214)* also do not cause a change in the localization of HAM-1 (Frank et al., 2005), while *ham-1(cas46)* only caused partial delocalization of HAM-1 from the cell cortex.

N-terminal point mutations in *ham-1(n1811), ham-1(cas27)* and *ham-1(ot361)* all resulted in a collapse of the doublet into a single band. HAM-1 protein in *ham-1(n1811)* appears to be significantly greater than that of wild-type and other mutant alleles. The increase in protein level could be due to an increase in protein stability from the Glycine to Aspartic acid change at 47. These N-terminal point mutations also cause HAM-1 to be delocalized from the cell cortex. It is possible that it is part of a recognition sequence required for post translational modifications mediating membrane localization. The same modification could be the factor contributing to the closely migrating doublet observed on a Western blot. Alternatively, these mutations could be part of sequences required for cortical localization where the protein then becomes post-translationally modified.

In *ham-1(cas137)*, the mutation of Glycine 10 to Glutamic acid drastically reduced the protein level of HAM-1 as it was undetectable by Western blot. The large decrease in protein level could be due to a decrease in protein stability. The low level of HAM-1 on a Western blot in *ham-1(cas137)* is also consistent with the low HAM-1 level detected by antibody staining of fixed embryos. In *ham-1(cas137)*, HAM-1 was able to localize properly to the cell cortex which suggests that this mutation does not affect localization but rather protein levels. If the exposure was longer for the Western blot, we might be able to detect HAM-1 in *ham-1(cas137)* and HAM-1 could appear as a doublet.

4.4 Tyrosine residue 369 is crucial for the function and localization of HAM-1

To identify regions of HAM-1 required for the function of HAM-1, various truncations were examined. It was determined that truncations of HAM-1 from either the C-terminus or the N-terminus abolished its ability to rescue the loss of PLM neurons in *ham-1(gm279)* mutants (Leung et al., 2014). To further identify regions within the last 50 amino acids of HAM-1 that contributes to its function, the protein sequence of HAM-1 was examined bioinformatically. The last four amino acids of HAM-1 encodes a predicted PDZ domain binding motif **ISNL** which is not required for the function of HAM-1 (N. Hawkins unpublished). The Tyrosine residue 369 (Tyr 369) within the predicted SH2 domain binding motif **YINI** was crucial for the function of HAM-1. The phospho-null GFP::HAM-1(Y369F) which mutates Tyr 369 to phenylalanine abolished the proteins ability to rescue the loss of neurons in *ham-1(gm279)* mutants. This fusion protein also caused a weak PLM neuronal loss phenotype in a wild-type background. This phenotype could be due to the fusion protein competing with endogenous HAM-1 in the pathway controlling asymmetric division of the PLM/ALN neuroblast. Due to the non-functional nature of the protein, it may antagonize the normal function of endogenous HAM-1 which would result in a defect of the pathway and ultimately a loss of PLM neurons. Mutation of Tyr 369 to Phenylalanine also resulted an increase in nuclear localization of GFP::HAM-1 but did not affect membrane localization. This result might indicate that Tyr 369 has a role in nuclear export rather than membrane localization. Regardless, my results indicate that Tyr 369 is required for the proper function and localization of HAM-1.

The phospho-mimetic GFP::HAM-1(Y369E) which mutates Tyr 369 to Glutamic acid was also unable to rescue the loss of PLM neurons and caused a weak PLM neuronal loss in a *zdIs5* alone background. The loss of PLM neurons in a *zdIs5* background could once again be due to competition with endogenous HAM-1. The phosphomimetic will mimic the charge of a phosphoryl group but it

is not part of a functional SH2 domain binding motif. Thus, the phosphomimetic would not be able to interact with SH2 domain containing proteins. This could explain the inability to rescue the loss of PLM neurons. Dephosphorylation of this residue could also be a contributing factor to the function of the protein. The phospho-mimetic showed normal localization similar to that of GFP::HAM-1 through qualitative observation while the phospho-null had an increase in nuclear signal and a decrease in cortical signal. This suggests that having a negative charge at this particular residue does not affect the localization of GFP::HAM-1. Since this protein was able to localize properly but still unable to function, it is possible that both phosphorylation and dephosphorylation of Tyr 369 is responsible for regulating HAM-1 function. However, we have no direct evidence that Tyr 369 is phosphorylated. To detect protein phosphorylation, we can immunoprecipitate HAM-1 and perform a Western blot, probing with an anti-phosphorylated Tyrosine antibody. We can then immunoprecipitate the phospho-null fusion protein or a *ham-1* mutant lacking Tyr 369 to determine whether the phosphorylation signal would be present. Although there is a lack in direct evidence of phosphorylation, we can conclude that Tyr 369 is a crucial residue of HAM-1.

The function and localization of the STOX1 human transcription factor which has homology to HAM-1 is regulated by phosphorylation. The localization of STOX1 in particular is regulated by the PI3K-Akt pathway where phosphorylation of STOX1 by Akt prevents entry into the nucleus resulting in degradation by ubiquitination (van Dijk et al., 2010b). The regulation of HAM-1 localization could function in a similar manner in which phosphorylation of Tyr 369 would allow HAM-1 to be exported out of the nucleus. A GFP::HAM-1 truncation which removes the last 50 amino acids of HAM-1 and subsequently Tyr 369 also results in decreased membrane localization and an increased in nuclear localization (Leung et al., 2014). Altogether, this suggests that Tyr 369 could be part of a nuclear export signal required for export of HAM-1 so it could localize to the cell cortex and get distributed to daughter cells.

4.5 SRC-1 kinase knockdown by RNAi does not affect PLM/ALN production

It was bioinformatically predicted that HAM-1 could interact with the SRC family of tyrosine kinases through its consensus SH2 domain binding motif, **YINI**. SRC-1 contributes to the spindle orientation of the EMS blastomere and cell fate specification of the endoderm in conjunction with the Wnt signalling pathway during early embryonic development (Bei et al., 2002). Due to SRC-1 involvement in cell fate determination, it was hypothesized that SRC-1 could interact with HAM-1 to regulate asymmetric neuroblast division. If SRC-1 functions in the same pathway as HAM-1 to regulate asymmetric neuroblast division, loss of SRC-1 function would result in loss of PLM neurons. However, RNAi knockdown of *src-1* through microinjection of dsRNA did not result in a loss of PLM neurons. This suggests that although SRC-1 is required for cell fate determination during early embryonic development, we have determined that SRC-1 is not required for the generation of PLM/ALN neurons. However, SRC-1 levels were only knocked down and not completely knocked out, it is possible that the protein levels of SRC-1 was not reduced enough to have an effect in the PLM lineage.

SRC-2 is another member of the SRC family of tyrosine kinases that could interact with the SH2 domain binding motif of HAM-1 according to the Eukaryotic Linear Motif program (http://elm.eu.org/). However, the role of *src-2* during embryonic development is largely unknown. Introduction of a *src-2* cDNA into wild-type worms greatly reduced viability in the early stages of development and escapers exhibit defects in the structure of the pharynx (Hirose et al., 2003). In contrast, RNAi knockdown of *src-2* in wild-type worms did not show any overt phenotype (Hirose et al., 2003). RNAi knockdown of *src-2* only has an effect in the background of retinoblastoma pathway mutants which results in embryonic and larval lethality, as well as sterility (Ceron et al., 2007). Although there is no evidence for *src-2* function in asymmetric cell division, we cannot rule out a

potential role for *src-2* in this pathway. To test this we can analyze *src-2* mutants in a *zdIs5* background to look for *ham-1* like phenotypes in the PLM lineage.

SRC-1 was only one predicted tyrosine kinase to interact with the potential SH2 domain binding motif of HAM-1 out of 66 tyrosine kinases in the *C. elegans* genome (Shaye and Greenwald, 2011). Tyrosine kinase mutants can be crossed into *zdIs5* to look for a *ham-1* like phenotype in the PLM lineage. However, lethality is a potential issue in mutant tyrosine kinases involved in early embryonic development. An alternative approach would be an RNAi screen to knockdown expression of these tyrosine kinases in *zdIs5*. I have adapted a tyrosine kinase list from (Shaye and Greenwald, 2011) which prioritizes tyrosine specific kinases based on time of expression and whether an RNAi clone is available in the *C. elegans* genome wide RNAi library (Table A.1). For tyrosine kinases without an available RNAi clone, an RNAi construct needs to be made for those tyrosine kinases.

A potential candidate with high priority is the receptor tyrosine kinase CAM-1 which regulates multiple processes such as cell migration and asymmetric cell division. *cam-1* is broadly expressed from the 200 cell stage of embryogenesis through to larval development. During larval development, *cam-1* mutants cause defects in the asymmetric division of the V1 cell. The cell division becomes reversed, with the anterior daughter adopting the fate of the posterior daughter (Forrester et al., 1999). *cam-1* mutants also cause defects in the migration of ALM, BDU, HSN and CA neurons. The common feature between cell motility and asymmetric division is polarity. Thus, it has been proposed that *cam-1* function to regulate the polarity involved in cell motility and asymmetric division (Forrester et al., 1999). Similar to *cam-1*, *ham-1* mutants cause defects in asymmetric divisions as well as abnormal migration of the HSN. It is possible that *cam-1* could function in the same pathway as *ham-1* to control asymmetric division and cell motility. With the availability of *cam-1* mutants as well as an RNAi clone in the *C. elegans* genome wide RNAi library we will be

able to analyze the role of *cam-1* in the regulation of asymmetric PLM neuroblast division.

4.6 PTP-2 tyrosine phosphatase is not required for PLM/ALN neuroblast asymmetric division

The PTP-2 tyrosine phosphatase was predicted to interact with the putative SH2 domain binding motif of HAM-1. Since, the phospho-mimetic GFP::HAM-1 was unable to rescue the loss of PLM neurons, it was hypothesized that a phosphatase was required to regulate the function of HAM-1. However, *ptp-2(op194)* mutants did not display a loss of PLM neurons phenotype. Although *ptp-2* activity is required during development to regulate activity of several signaling pathways, it appears that *ptp-2* is not involved in the asymmetric division of the PLM neuroblast.

ptp-2 has been ruled out as a potential candidate for regulating HAM-1 activity in the lineage which generates PLM neurons but there is a large list of 83 conventional protein-tyrosine-phosphatases (Plowman et al., 1999) which could act as a regulator of HAM-1. An RNAi screen could be done in a *zdIs5* strain to identify protein-tyrosine-phosphatases that cause defects in the PLM lineage. This would aid in the determination of phosphatases regulating HAM-1 activity or perhaps identify phosphatases that function in a parallel pathway regulating asymmetric division of the PLM neuroblast.

4.7 Future Directions

There is very little knowledge about the functional role of HAM-1 in the regulation of asymmetric neuroblast division therefore additional work needs to be done to elucidate the function of HAM-1. To gain knowledge of the role of HAM-1 in the regulation of asymmetric neuroblast division and the potential pathway which regulates this process, we need to identify interacting partners of

HAM-1. There are biochemical and genetic approaches that can be taken to identify these interacting partners. To identify proteins which physically interact with HAM-1, we can take a biochemical approach by co-immunoprecipitating HAM-1 along with any closely associated proteins followed by mass spectrometry. This will provide us with a list of proteins that interact with HAM-1; however, these proteins might not be biologically relevant in the regulation asymmetric cell division as there is a high rate of false positive hits. Each potential candidate would have to be tested genetically to see its effect on neuronal lineages that HAM-1 has a role in.

In conjunction with the biochemical approach, we can perform an EMS genetic screen of *zdIs5* to look for additional genes that phenocopy the loss of PLM neurons in *ham-1*. Following backcross and sequencing we can identify genes that could interact with *ham-1* genetically in the same pathway or discover other genes in a parallel pathway that regulate asymmetric cell division.

HAM-1 is protein that is larger than its predicted molecular weight and appears as a doublet as observed on a Western blot which is indicative of potential post-translation modifications. It is possible that these modifications are required for the membrane association as well as the function of HAM-1. However, the amino acid sequences of HAM-1 provide little insight into the potential post-translational modifications as there are no obvious post-translational modification sites. To identify potential post-translational modifications associated with HAM-1 we need to take a biochemical approach such as immunoprecipitation to isolate HAM-1 followed by tandem mass spectrometry (MS/MS) to determine post-translational modifications. Mass spectrometry provide several advantages for the characterization of post-translational modifications, such as very high sensitivity, ability to discover novel modifications, ability to identify the specific site of modification, capability to identify post-translational modifications in complex mixtures of proteins; and the ability to quantify the relative changes in post-translational modifications occupancy at distinct sites (reviewed in Larsen et al. 2006). This method will

provide information on what type of post-translational modifications are attached to HAM-1 and the specific regions of HAM-1 that is modified allowing us to understand how HAM-1 is functioning in the regulation of asymmetric cell division.

Chapter 5.

Conclusion

This study builds on previous work done to characterize regions of HAM-1 responsible for both function and localization. We now have strong evidence for the nuclear localization of endogenous HAM-1 but the role of HAM-1 within the nucleus remains unknown. With recent data suggesting that the nuclear localization and the potential DNA binding role of HAM-1 is not required for function in the PLM lineage and the cortical localization appears to be more crucial for the function of HAM-1 (Leung et al., 2014). With the analysis of multiple *ham-1* point mutants (*cas27*, *cas37* and *ot361*) and a deletion mutant (*cas46*) by immunostaining of embryos, we identified two point mutations at the N-terminus (*cas27* and *ot361*) and the last 33 amino acids of HAM-1 as important regions required for membrane association. The *ham-1(cas137)* mutant however, was able localize to the cell cortex but the stability of HAM-1 was greatly affected. There is a potential connection between membrane localization and the closely migrating doublet observed by Western blot analysis suggesting that there are regions of HAM-1 that is attached with post-translation modifications responsible for membrane association. We have not only identified residues required for localization of HAM-1 but we have also identified a critical Tyrosine residue at position 369 which is essential for the function of HAM-1 because mutation of this residue to either a phospho-null or a phospho-mimetic completely abolished the function of HAM-1. In conclusion, my thesis provided further analysis of HAM-1 localization as well as identification of specific residues important for the localization and function of HAM-1.

References

Van Abel, D., Michel, O., Veerhuis, R., Jacobs, M., van Dijk, M., and Oudejans, C.B.M. (2012). Direct downregulation of CNTNAP2 by STOX1A is associated with Alzheimer's disease. J. Alzheimers. Dis. *31*, 793–800.

Abràmoff, M.D., Magalhães, P.J., and Ram, S.J. (2004). Image processing with ImageJ. Biophotonics Int. *11*, 36–42.

Altschul, S.F., Madden, T.L., Schäffer, A.A., Zhang, J., Zhang, Z., Miller, W., and Lipman, D.J. (1997). Gapped BLAST and PSI-BLAST : a new generation of protein database search programs. *25*, 3389–3402.

Artavanis-Tsakonas, S. (1999). Notch signaling: cell fate control and signal integration in development. Science (80-.). *284*, 770–776.

Beatty, A., Morton, D., and Kemphues, K. (2010). The *C. elegans* homolog of *Drosophila* Lethal giant larvae functions redundantly with PAR-2 to maintain polarity in the early embryo. Development *137*, 3995–4004.

Bei, Y., Hogan, J., Berkowitz, L.A., Soto, M., Rocheleau, C.E., Pang, K.M., Collins, J., and Mello, C.C. (2002). SRC-1 and Wnt signaling act together to specify endoderm and to control cleavage orientation in early *C. elegans* embryos. Dev. Cell *3*, 113–125.

Berdnik, D., Török, T., González-Gaitán, M., and Knoblich, J.A. (2002). The endocytic protein alpha-Adaptin is required for Numb-mediated asymmetric cell division in *Drosophila*. Dev. Cell *3*, 221–231.

Berends, A.L., Bertoli-Avella, A.M., de Groot, C.J.M., van Duijn, C.M., Oostra, B.A., and Steegers, E.A.P. (2007). STOX1 gene in pre-eclampsia and intrauterine growth restriction. BJOG *114*, 1163–1167.

Bertrand, V., and Hobert, O. (2009). Linking asymmetric cell division to the terminal differentiation program of postmitotic neurons in *C. elegans*. Dev. Cell *16*, 563–575.

Betschinger, J., and Knoblich, J.A. (2004). Dare to be different: asymmetric cell division in *Drosophila*, *C. elegans* and vertebrates. Curr. Biol. *14*, R674–R685.

Boyd, L., Guo, S., Levitan, D., Stinchcomb, D.T., and Kemphues, K.J. (1996). PAR-2 is asymmetrically distributed and promotes association of P granules and PAR-1 with the cortex in *C. elegans* embryos. Development *122*, 3075–3084.

Brenner, S. (1974). The genetics of *Caenorhabditis elegans*. Genetics *77*, 71–94.

Calvo, D., Victor, M., Gay, F., Sui, G., Luke, M.P.-S., Dufourcq, P., Wen, G., Maduro, M., Rothman, J., and Shi, Y. (2001). A POP-1 repressor complex restricts inappropriate cell type-specific gene transcription during *Caenorhabditis elegans* embryogenesis. EMBO J. *20*, 7197–7208.

Ceron, J., Rual, J.-F., Chandra, A., Dupuy, D., Vidal, M., and van den Heuvel, S. (2007). Large-scale RNAi screens identify novel genes that interact with the *C. elegans* retinoblastoma pathway as well as splicing-related components with synMuv B activity. BMC Dev. Biol. *7*, 30.

Clark, S.G., and Chiu, C. (2003). *C. elegans* ZAG-1, a Zn-finger-homeodomain protein, regulates axonal development and neuronal differentiation. Development *130*, 3781–3794.

Colombo, K., Grill, S.W., Kimple, R.J., Willard, F.S., David, P., and Gönczy, P. (2003). Translation of polarity cues into asymmetric spindle positioning in *Caenorhabditis elegans* embryos. Science (80-.). *300*, 1957–1961.

Cordes, S., Frank, C.A., and Garriga, G. (2006). The *C. elegans* MELK ortholog PIG-1 regulates cell size asymmetry and daughter cell fate in asymmetric neuroblast divisions. Development *133*, 2747–2756.

Cuenca, A.A., Schetter, A., Aceto, D., Kemphues, K., and Seydoux, G. (2003). Polarization of the *C. elegans* zygote proceeds via distinct establishment and maintenance phases. Development *130*, 1255–1265.

Van Dijk, M., Mulders, J., Poutsma, A., Könst, A.A.M., Lachmeijer, A.M.A., Dekker, G.A., Blankenstein, M.A., and Oudejans, C.B.M. (2005). Maternal segregation of the Dutch preeclampsia locus at 10q22 with a new member of the winged helix gene family. Nat. Genet. *37*, 514–519.

Van Dijk, M., van Bezu, J., Poutsma, A., Veerhuis, R., Rozemuller, A.J., Scheper, W., Blankenstein, M.A., and Oudejans, C.B. (2010a). The pre-eclampsia gene STOX1 controls a conserved pathway in placenta and brain upregulated in late-onset Alzheimer's disease. J. Alzheimer's Dis. *19*, 673–679.

Van Dijk, M., van Bezu, J., van Abel, D., Dunk, C., Blankenstein, M.A., Oudejans, C.B.M., and Lye, S.J. (2010b). The STOX1 genotype associated with pre-eclampsia leads to a reduction of trophoblast invasion by alpha-T-catenin upregulation. Hum. Mol. Genet. *19*, 2658–2667.

Doe, C.Q., Chu-LaGraff, Q., Wright, D.M., and Scott, M.P. (1991). The *prospero* gene specifies cell fates in the *Drosophila* central nervous system. Cell *65*, 451–464.

Doitsidou, M., Flames, N., Lee, A.C., Boyanov, A., and Hobert, O. (2008). Automated screening for mutants affecting dopaminergic-neuron specification in *C. elegans*. Nat. Methods *5*, 869–872.

Edgley, M., and Riddle, D. (2001). LG II balancer chromosomes in *Caenorhabditis elegans*: *mT1(II;III)* and the *mIn1* set of dominantly and recessively marked inversions. Mol. Genet. Genomics *266*, 385–395.

Ellis, H.M., and Horvitz, H.R. (1986). Genetic control of programmed cell death in the nematode *C. elegans*. Cell *44*, 817–829.

Etemad-Moghadam, B., Guo, S., and Kemphues, K.J. (1995). Asymmetrically distributed PAR-3 protein contributes to cell polarity and spindle alignment in early *C. elegans* embryos. Cell *83*, 743–752.

Feng, G., Yi, P., Yang, Y., Chai, Y., Tian, D., Zhu, Z., Liu, J., Zhou, F., Cheng, Z., Wang, X., et al. (2013). Developmental stage-dependent transcriptional regulatory pathways control neuroblast lineage progression. Development *140*, 3838–3847.

Forrester, W.C., Dell, M., Perens, E., and Garriga, G. (1999). A *C. elegans* Ror receptor tyrosine kinase regulates cell motility and asymmetric cell division. Nature *400*, 717–721.

Frank, C.A., Hawkins, N.C., Guenther, C., Horvitz, H.R., and Garriga, G. (2005). *C. elegans* HAM-1 positions the cleavage plane and regulates apoptosis in asymmetric neuroblast divisions. Dev. Biol. *284*, 301–310.

Goldstein, B., and Macara, I.G. (2007). The PAR proteins: fundamental players in animal cell polarization. Dev. Cell *13*, 609–622.

Gotta, M., Dong, Y., Peterson, Y.K., Lanier, S.M., and Ahringer, J. (2003). Asymmetrically distributed *C . elegans* homologs of AGS3/PINS control spindle position in the early embryo. Curr. Biol. *13*, 1029–1037.

Guenther, C., and Garriga, G. (1996). Asymmetric distribution of the *C. elegans* HAM-1 protein in neuroblasts enables daughter cells to adopt distinct fates. Development *122*, 3509–3518.

Guo, S., and Kemphues, K.J. (1995). *par-1*, a gene required for establishing polarity in *C. elegans* embryos, encodes a putative Ser/Thr kinase that is asymmetrically distributed. Cell *81*, 611–620.

Guo, M., Jan, L.Y., and Jan, Y.N. (1996). Control of daughter cell fates during asymmetric division: interaction of Numb and Notch. Neuron *17*, 27–41.

Gutch, M.J., Flint, A.J., Keller, J., Tonks, N.K., and Hengartner, M.O. (1998). The *Caenorhabditis elegans* SH2 domain-containing protein tyrosine phosphatase PTP-2 participates in signal transduction during oogenesis and vulval development. Genes Dev. *12*, 571–585.

Hammer, Ø., Harper, D.A.T., and Ryan, P.D. (2001). Paleontological statistics software package for education and data analysis. Palaeontol. Electron. *4*, 9–18.

Hao, Y., Boyd, L., and Seydoux, G. (2006). Stabilization of cell polarity by the *C. elegans* RING protein PAR-2. Dev. Cell *10*, 199–208.

Hartmann, C., Landgraf, M., Bate, M., and Jäckle, H. (1997). *Krüppel* target gene *knockout* participates in the proper innervation of a specific set of Drosophila larval muscles. EMBO J. *16*, 5299–5309.

Hawkins, N., and Garriga, G. (1998). Asymmetric cell division: from A to Z. Genes Dev. *12*, 3625–3638.

Hirata, J., Nakagoshi, H., Nabeshima, Y., and Matsuzaki, F. (1995). Asymmetric segregation of the homeodomain protein Prospero during *Drosophila* development. Nature *377*, 627–630.

Hirose, T., Koga, M., Ohshima, Y., and Okada, M. (2003). Distinct roles of the Src family kinases, SRC-1 and KIN-22, that are negatively regulated by CSK-1 in *C. elegans*. FEBS Lett. *534*, 133–138.

Hoege, C., and Hyman, A.A. (2013). Principles of PAR polarity in *Caenorhabditis elegans* embryos. Nat. Rev. Mol. Cell Biol. *14*, 315–322.

Hoege, C., Constantinescu, A.-T., Schwager, A., Goehring, N.W., Kumar, P., and Hyman, A.A. (2010). LGL can partition the cortex of one-cell *Caenorhabditis elegans* embryos into two domains. Curr. Biol. *20*, 1296–1303.

Horvitz, H.R., and Herskowitz, I. (1992). Mechanisms of asymmetric cell division: two Bs or not two Bs, that is the question. Cell *68*, 237–255.

Hosono, R., Hirahara, K., Kuno, S., and Kurihara, T. (1982). Mutants of *Caenorhabditis elegans* with Dumpy and Rounded Head phenotype. J. Exp. Zool. *224*, 135–144.

Hsu, T.-Y., and Wu, Y.-C. (2010). Engulfment of apoptotic cells in *C. elegans* is mediated by Integrin Alpha/SRC Signaling. Curr. Biol. *20*, 477–486.

Huang, S., Shetty, P., Robertson, S.M., and Lin, R. (2007). Binary cell fate specification during *C. elegans* embryogenesis driven by reiterated reciprocal asymmetry of TCF POP-1 and its coactivator beta-catenin SYS-1. Development *134*, 2685–2695.

Hutterer, A., and Knoblich, J.A. (2005). Numb and alpha-Adaptin regulate Sanpodo endocytosis to specify cell fate in *Drosophila* external sensory organs. EMBO Rep. *6*, 836–842.

Kidd, A.R., Miskowski, J.A., Siegfried, K.R., Sawa, H., and Kimble, J. (2005). A beta-Catenin identified by functional rather than sequence criteria and its role in Wnt/MAPK signaling. Cell *121*, 761–772.

Knoblich, J.A. (2008). Mechanisms of asymmetric stem cell division. Cell *132*, 583–597.

Knoblich, J.A. (2010). Asymmetric cell division: recent developments and their implications for tumour biology. Nat. Rev. Mol. Cell Biol. *11*, 849–860.

Korswagen, H.C. (2002). Canonical and non-canonical Wnt signaling pathways in *Caenorhabditis elegans*: variations on a common signaling theme. BioEssays *24*, 801–810.

Larsen, M., Trelle, M., Thingholm, T., and Jensen, O. (2006). Analysis of posttranslational modifications of proteins by tandem mass spectrometry. Biotechniques *40*, 790–798.

Leung, A., Hua, K., Narasimha, P., Hingwing, K., Wu, M., Hilton, L., and Hawkins, N.C. (2014). *C. elegans* HAM-1 functions in the nucleus to regulate asymmetric neuroblast division. Dev. Biol. *In revisio*.

Li, P., Yang, X., Wasser, M., Cai, Y., and Chia, W. (1997). Inscuteable and Staufen mediate asymmetric localization and segregation of *prospero* RNA during *Drosophila* neuroblast cell divisions. Cell *90*, 437–447.

Lichtsteinerl, S., and Tjian, R. (1995). Synergistic activation of transcription by UNC-86 and MEC-3 in *Caenorhabditis elegans* embryo extracts. *14*, 3937–3945.

Lieber, T., Kidd, S., Alcamo, E., Corbin, V., and Young, M.W. (1993). Antineurogenic phenotypes induced by truncated Notch proteins indicate a role in signal transduction and may point to a novel function for Notch in nuclei. Genes Dev. *7*, 1949–1965.

Lin, R., Thompson, S., and Priess, J.R. (1995). *pop-1* encodes an HMG box protein required for the specification of a mesoderm precursor in early *C. elegans* embryos. Cell *83*, 599–609.

Lin, R., Hill, R.J., and Priess, J.R. (1998). POP-1 and anterior-posterior fate decisions in *C. elegans* embryos. Cell *92*, 229–239.

Logeat, F., Bessia, C., Brou, C., LeBail, O., Jarriault, S., Seidah, N.G., and Israël, A. (1998). The Notch1 receptor is cleaved constitutively by a furin-like convertase. Proc. Natl. Acad. Sci. U. S. A. *95*, 8108–8112.

MacDonald, B.T., Tamai, K., and He, X. (2009). Wnt/Beta-Catenin signaling: components, mechanisms, and diseases. Dev. Cell *17*, 9–26.

Matsuzaki, F., Ohshiro, T., Ikeshima-Kataoka, H., and Izumi, H. (1998). Miranda localizes Staufen and Prospero asymmetrically in mitotic neuroblasts and epithelial cells in early *Drosophila* embryogenesis. Development *125*, 4089–4098.

McGill, M.A., Dho, S.E., Weinmaster, G., and McGlade, C.J. (2009). Numb regulates post-endocytic trafficking and degradation of Notch1. J. Biol. Chem. *284*, 26427–26438.

Mello, C.C., Kramer, J.M., Stinchcomb, D., and Ambros, V. (1991). Efficient gene transfer in *C.elegans*: extrachromosomal maintenance and integration of transforming sequences. EMBO J. *10*, 3959–3970.

Morton, D.G., Shakes, D.C., Nugent, S., Dichoso, D., Wang, W., Golden, A., and Kemphues, K.J. (2002). The *Caenorhabditis elegans par-5* gene encodes a 14-3-3 protein required for cellular asymmetry in the early embryo. Dev. Biol. *241*, 47–58.

Mulder, N.J., Apweiler, R., Attwood, T.K., Bairoch, A., Bateman, A., Binns, D., Bradley, P., Bork, P., Bucher, P., Cerutti, L., et al. (2005). InterPro, progress and status in 2005. Nucleic Acids Res. *33*, D201–D205.

Neumüller, R.A., and Knoblich, J.A. (2009). Dividing cellular asymmetry: asymmetric cell division and its implications for stem cells and cancer. Genes Dev. *23*, 2675–2699.

O'Connor-Giles, K.M., and Skeath, J.B. (2003). Numb inhibits membrane localization of Sanpodo, a four-pass transmembrane protein, to promote asymmetric divisions in Drosophila. Dev. Cell *5*, 231–243.

Ou, G., and Vale, R.D. (2009). Molecular signatures of cell migration in *C. elegans* Q neuroblasts. J. Cell Biol. *185*, 77–85.

Phillips, B.T., and Kimble, J. (2009). A new look at TCF and beta-Catenin through the Lens of a divergent *C. elegans* Wnt pathway. Dev. Cell *17*, 27–34.

Phillips, B.T., Kidd, A.R., King, R., Hardin, J., and Kimble, J. (2007). Reciprocal asymmetry of SYS-1/beta-catenin and POP-1/TCF controls asymmetric divisions in *Caenorhabditis elegans*. PNAS *104*, 3231–3236.

Plowman, G.D., Sudarsanam, S., Bingham, J., Whyte, D., and Hunter, T. (1999). The protein kinases of *Caenorhabditis elegans*: a model for signal transduction in multicellular organisms. Proc. Natl. Acad. Sci. U. S. A. *96*, 13603–13610.

Puntervoll, P., Linding, R., Gemund, C., Chabanis-Davidson, S., Mattingsdal, M., Cameron, S., Martin, D.M., Ausiello, G., Brannetti, B., Costantini, A., et al. (2003). ELM server: a new resource for investigating short functional sites in modular eukaryotic proteins. Nucleic Acids Res. *31*, 3625–3630.

Rhyu, M.S., Jan, L.Y., and Jan, Y.N. (1994). Asymmetric distribution of Numb protein during division of the sensory organ precursor cell confers distinct fates to daughter cells. Cell *76*, 477–491.

Rigourd, V., Chelbi, S., Chauvet, C., Rebourcet, R., Barbaux, S., Bessières, B., Mondon, F., Mignot, T.-M., Danan, J.-L., and Vaiman, D. (2009). Re-evaluation of the role of STOX1 transcription factor in placental development and preeclampsia. J. Reprod. Immunol. *82*, 174–181.

Rocheleau, C.E., Yasuda, J., Shin, T.H., Lin, R., Sawa, H., Okano, H., Priess, J.R., Davis, R.J., and Mello, C.C. (1999). WRM-1 activates the LIT-1 protein kinase to transduce anterior/posterior polarity signals in *C. elegans*. Cell *97*, 717–726.

Rolls, M.M., Albertson, R., Shih, H.-P., Lee, C.-Y., and Doe, C.Q. (2003). *Drosophila* aPKC regulates cell polarity and cell proliferation in neuroblasts and epithelia. J. Cell Biol. *163*, 1089–1098.

Santolini, E., Puri, C., Salcini, A.E., Gagliani, M.C., Pelicci, P.G., Tacchetti, C., and Di Fiore, P.P. (2000). Numb is an endocytic protein. J. Cell Biol. *151*, 1345–1352.

Sawa, H., and Korswagen, H.C. (2013). Wnt signaling in *C. elegans*. WormBook 1–30.

Schubert, C.M., Lin, R., de Vries, C.J., Plasterk, R.H., and Priess, J.R. (2000). MEX-5 and MEX-6 function to establish soma/germline asymmetry in early *C. elegans* embryos. Mol. Cell *5*, 671–682.

Shaye, D.D., and Greenwald, I. (2011). OrthoList: a compendium of *C. elegans* genes with human orthologs. PLoS One *6*, e20085.

Shen, C.P., Knoblich, J.A., Chan, Y.M., Jiang, M.M., Jan, L.Y., and Jan, Y.N. (1998). Miranda as a multidomain adapter linking apically localized Inscuteable and basally localized Staufen and Prospero during asymmetric cell division in *Drosophila*. Genes Dev. *12*, 1837–1846.

Shin, T.H., Yasuda, J., Rocheleau, C.E., Lin, R., Soto, M., Bei, Y., Davis, R.J., and Mello, C.C. (1999). MOM-4, a MAP Kinase Kinase Kinase-Related protein, activates WRM-1/LIT-1 kinase to transduce anterior/posterior polarity signals in *C. elegans*. Mol. Cell *4*, 275–280.

Simmer, F., Tijsterman, M., Parrish, S., Koushika, S.P., Nonet, M.L., Fire, A., Ahringer, J., and Plasterk, R.H.A. (2002). Loss of the putative RNA-Directed RNA Polymerase RRF-3 makes *C. elegans* hypersensitive to RNAi. Curr. Biol. *12*, 1317–1319.

Smith, C.A., Lau, K.M., Rahmani, Z., Dho, S.E., Brothers, G., She, Y.M., Berry, D.M., Bonneil, E., Thibault, P., Schweisguth, F., et al. (2007). aPKC-mediated phosphorylation regulates asymmetric membrane localization of the cell fate determinant Numb. EMBO J. *26*, 468–480.

Sulston, J.E., and Horvitz, H.R. (1977). Post-embryonic cell Lineages of the nematode, *Caenorhabditis elegans*. Dev. Biol. *56*, 110–156.

Sulston, J.E., Schierenberg, E., White, J.G., and Thomson, J.N. (1983). The embryonic cell lineage of the nematode *Caenorhabditis elegans*. Dev. Biol. *100*, 64–119.

Tabuse, Y., Izumi, Y., Piano, F., Kemphues, K.J., Miwa, J., and Ohno, S. (1998). Atypical protein kinase C cooperates with PAR-3 to establish embryonic polarity in *Caenorhabditis elegans*. Development *125*, 3607–3614.

Teichmann, M., Dumay-Odelot, H., and Fribourg, S. (2012). Structural and functional aspects of winged-helix domains at the core of transcription initiation complexes. Transcription *3*, 2–7.

Thompson, J.D., Higgins, D.G., and Gibson, T.J. (1994). CLUSTAL W: improving the sensitivity of progressive multiple sequence alignment through sequence weighting, position-specific gap penalties and weight matrix choice. Nucleic Acids Res. *22*, 4673–4680.

Tsou, M.-F.B., Hayashi, A., DeBella, L.R., McGrath, G., and Rose, L.S. (2002). LET-99 determines spindle position and is asymmetrically enriched in response to PAR polarity cues in *C. elegans* embryos. Development *129*, 4469–4481.

Watts, J.L., Etemad-Moghadam, B., Guo, S., Boyd, L., Draper, B.W., Mello, C.C., Priess, J.R., and Kemphues, K.J. (1996). *par-6*, a gene involved in the establishment of asymmetry in early *C. elegans* embryos, mediates the asymmetric localization of PAR-3. Development *122*, 3133–3140.

Watts, J.L., Morton, D.G., Bestman, J., and Kemphues, K.J. (2000). The *C. elegans par-4* gene encodes a putative serine-threonine kinase required for establishing embryonic asymmetry. Development *127*, 1467–1475.

Weinmaster, G. (2000). Notch signal transduction: a real rip and more. Curr. Opin. Genet. Dev. *10*, 363–369.

Wodarz, A., Ramrath, A., Grimm, A., and Knust, E. (2000). *Drosophila* Atypical Protein Kinase C associates with Bazooka and controls polarity of epithelia and neuroblasts. J. Cell Biol. *150*, 1361–1374.

Yang, Y., Han, S.M., and Miller, M.A. (2010). MSP hormonal control of the oocyte MAP kinase cascade and reactive oxygen species signaling. Dev. Biol. *342*, 96–107.

Appendix.

Table A.1: List of *C. elegans* tyrosine kinases.

Gene Name	Sequence	Family	RNAi Phenotypes	Expression	Kamath clone
cam-1	C01G6.8	RTK	Asymmetric cell division variant, multiple other phenotypes	Early/late embryo, L1-L4	Yes
sid-3	B0302.1	CTK	Sterile, Lethal	Early/late embryo	No
ark-1	C01C7.1	CTK	Germ cell development variant	Early/late embryo, L1-L4	No
src-2	F49B2.5	CTK	Embryonic lethal, sick, larval arrest in Rb mutant background	Late embryo/L1-L4/males	No
abl-1	M79.1	CTK	Apoptosis variant, pathogen resistance	Early/late embryo, L1-L4	No
-	Y47G6A.5	CTK	Organism development variant in let-60 background	Late embryo/L1-L4/males	No
csk-1	Y48G1C.2	CTK	Sterile, Lethal, larval lethal	Early/late embryo, L1-L4, adult	No
kin-14	F22D6.1	FER	Small	Early/late embryo, L1-L4, young adult	No
lin-18	C16B8.1	RTK	Bi/multi vulva, vulva lineage variant	Early/late embryo, L1-L4	No
rol-3	C16D9.2	RTK	Roller, organism development variant, lethal and embryonic lethal	Late embryo, mid L3	No
ddr-1	C25F6.4	RTK	transgene subcellular localization variant	Early/late embryo, males	No
ddr-2	F11D5.3	RTK	Organism development variant	Early/late embryo	No
egl-15	F58A3.2	RTK	Egg laying defect, axon guidance defect	Early/late embryo, L1-L4	No
vab-1	M03A1.1	RTK	Embryonic lethal, decreased cell corpse number	Early/late embryo, L1-L4	No
scd-2	T10H9.2	RTK	Organism development variant	Late embryo, mid L1	No
daf-2	Y55D5A.5	RTK	Dauer formation variant	Early/late embryo, L1-L4	No
let-23	ZK1067.1	RTK	Cell fate transformation, early larval lethal, vulva defects	Early/late embryo, L1-L4	No
kin-32	C30F8.4	CTK	N/A	Early/late embryo, L3, males	No
-	F11E6.8	RTK	N/A	Early/late embryo, L1-L4	No
ver-3	F59F3.1	RTK	N/A	Early/late embryo, L1-L4	No
svh-2	T14E8.1	RTK	N/A	Early/late embryo, L1-L4	No
ver-1	T17A3.1	RTK	N/A	Early/late embryo, L1-L4	No
frk-1	T04B2.2	FER	Embryonic development variant, embryonic lethal, fat content increased	Mid L4/ mid L4-males	No
ver-4	F59F3.5	RTK	Organism development variant, sluggish, protein aggregation variant	L2-L4	Yes
-	ZK622.1	FER	N/A	Mid-L4 males	No

RTK = Receptor Tyrosine Kinase
CTK = Cytoplasmic Tyrosine Kinase
FER = Nontransmembrane Receptor Tyrosine Kinase

Crossing transgenic arrays *(hkEx??)* into *zdIs5(mec-4::gfp); ham-1(gm279)*

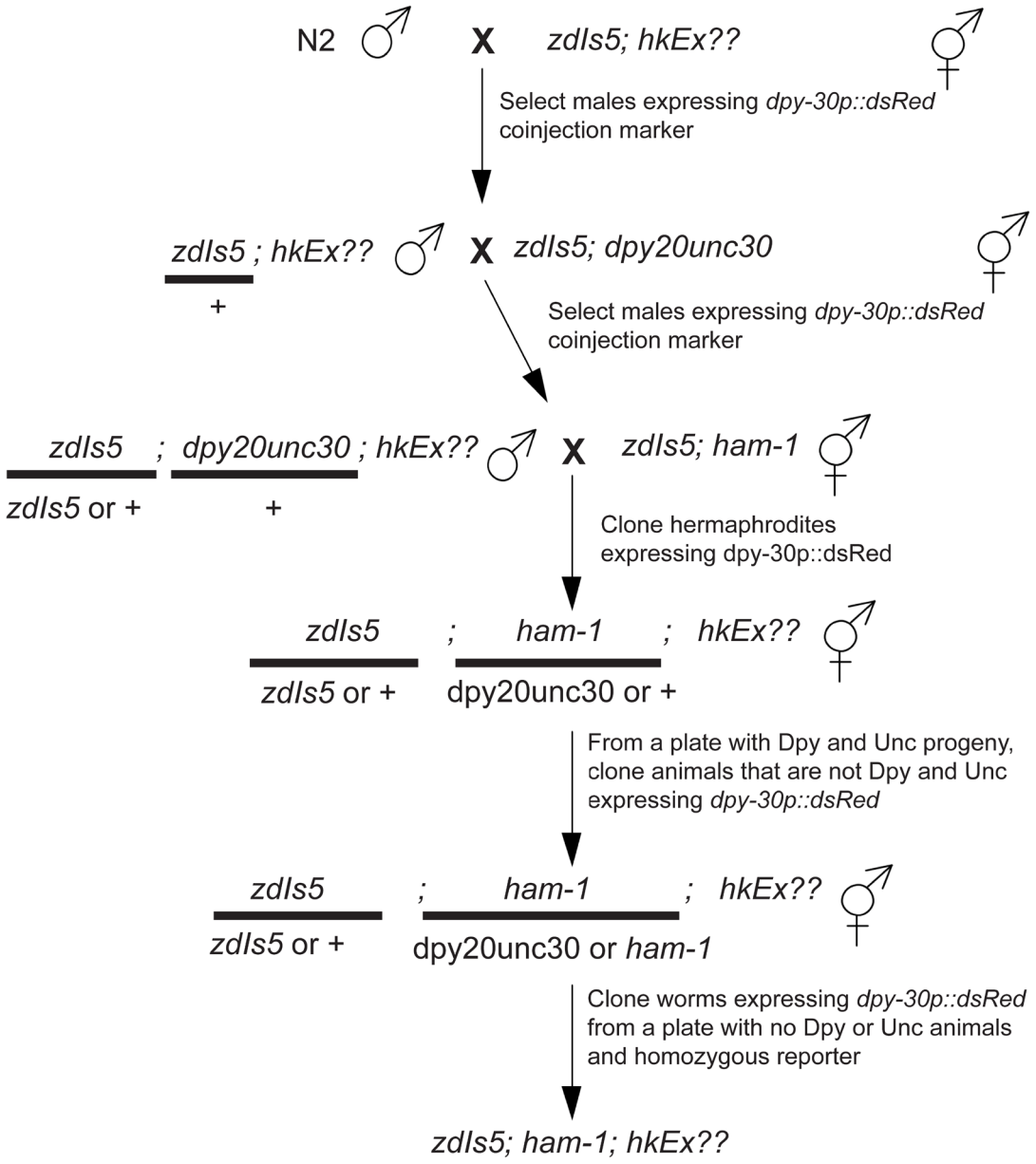

Figure A.1 Schematic of crossing transgenic arrays into *zdIs5(mec-4::gfp); ham-1(gm279).*

The crossing scheme shown above was used to introduce transgenic arrays generated in this study into a *ham-1(gm279)* background containing the PLM neurons reporter *zdIs5(mec-4::gfp)*.

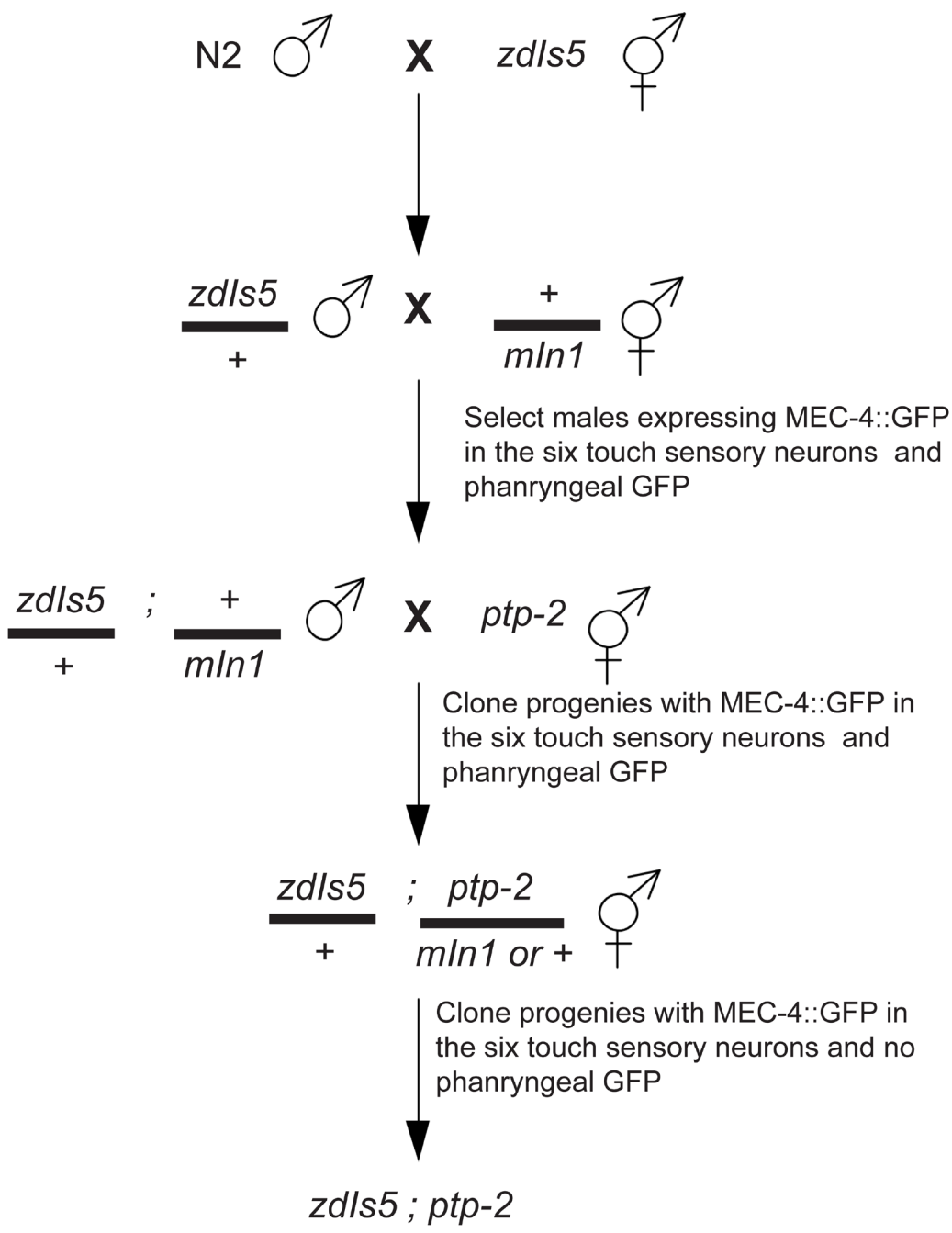

Figure A.2 Schematic of crossing *zdIs5(mec-4::gfp)* reporter into *ptp-2(op194).*

The crossing scheme shown above was used to introduce the *zdIs5(mec-4::GFP)* reporter into *ptp-2(op194)* which allowed us to score the number PLM neurons in *ptp-2(op194)* mutants.

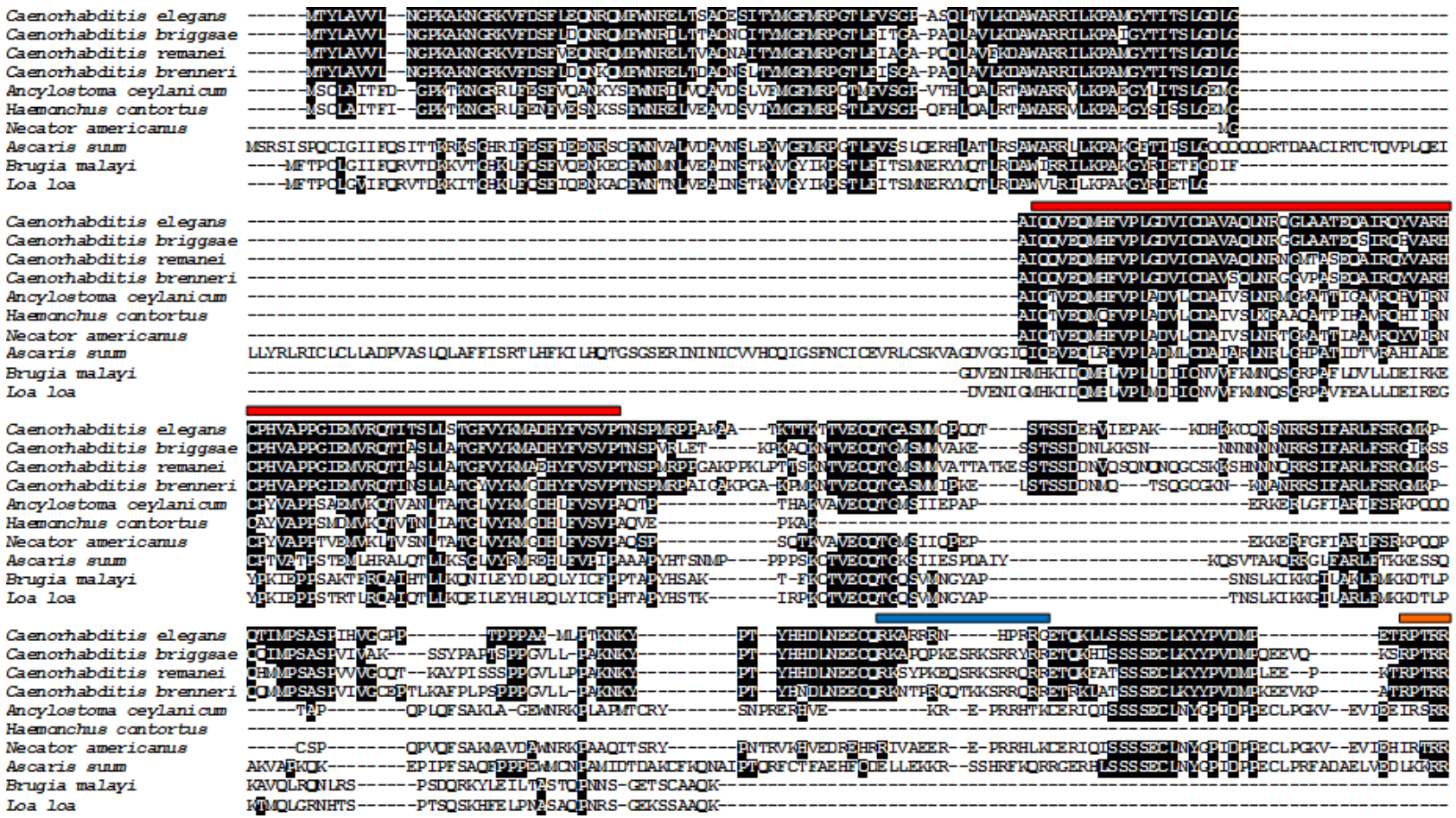
Caenorhabditis elegans
Caenorhabditis briggsae
Caenorhabditis remanei
Caenorhabditis brenneri
Ancylostoma ceylanicum
Haemonchus contortus
Necator americanus
Ascaris suum
Brugia malayi
Loa loa

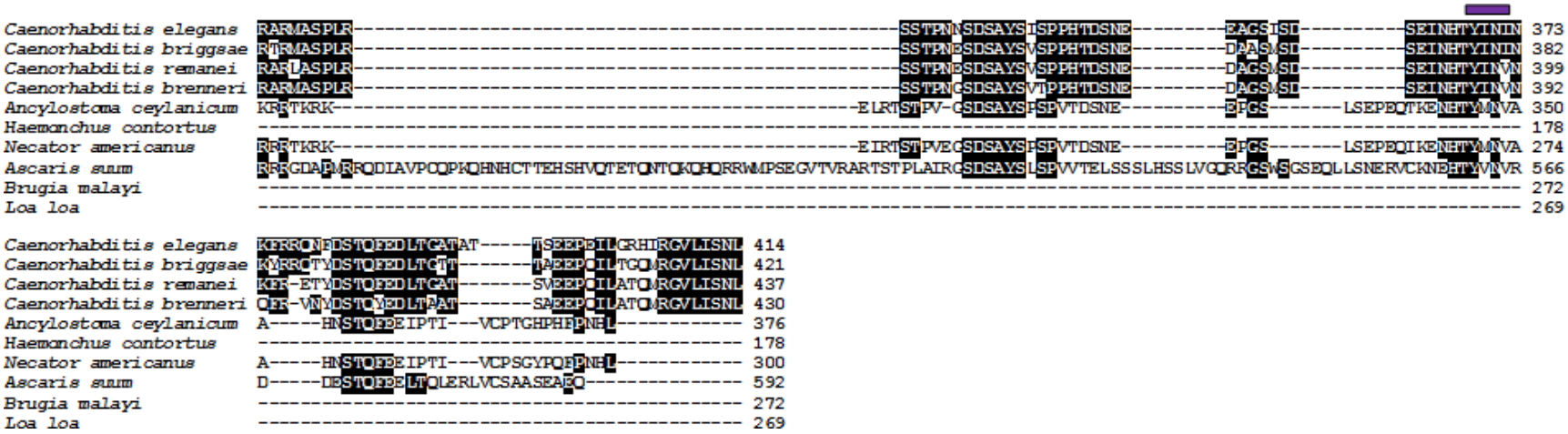

Figure A.3 Amino acid sequence alignment of full length HAM-1 and multiple nematode species.

This figure is extended from the previous page. The full length HAM-1 amino acid sequence was aligned with proteins multiple nematode species with conserved amino acids highlighted in black. The Winged-Helix Domain is represented by a red bar above the corresponding sequence. The Nuclear Localization Sequences are represented by the blue and orange bar over the corresponding sequence. The predicted SH2 domain binding motif is represented by a purple bar above the corresponding sequence.

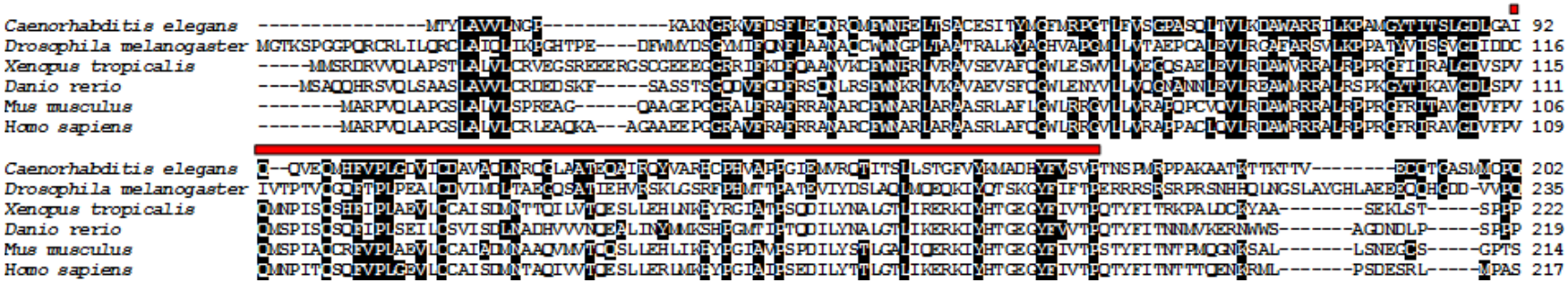

Figure A.4 Amino acid sequence alignment of the N-terminus of HAM-1.

Alignment of the N-terminus of HAM-1 with proteins from multiple divergent species. The conserved amino acids highlighted in black and the Winged-Helix Domain is represented by a red bar above the corresponding sequence.